NTNU – Trondheim
Norwegian University of
Science and Technology

Simulations of Dual Gradient Drilling

Analytical and Theoretical Studies of tripping-
and pressure trapping operations when using
Dual Gradient Drilling in deep waters

Tarald Husevåg Gaup

Earth Sciences and Petroleum Engineering
Submission date: June 2012
Supervisor: John-Morten Godhavn, IPT

Norwegian University of Science and Technology
Department of Petroleum Engineering and Applied Geophysics

Preface

This report is a Master's thesis written during the spring of 2012, in accordance with the course TPG4910 at the Norwegian University of Science and Technology (NTNU), Department of Petroleum Engineering and Applied Geophysics. The total workload is 100% of that of a full-time student.

I would like to thank my supervisor John-Morten Godhavn for his guidance and feedback on my work, and for being available for support in a time period after the original final delivery date. I would also like to thank the professors Arild Rødland, Pål Skalle and Sigbjørn Sangesland at NTNU, who have answered my questions through email correspondence and in meetings.

The MATLAB functions used for simulation in this report are programmed by me, and are included in the Appendix. The *.m-files and the Excel file with input data can be received from me on enquiry.

I hereby declare that this report has been produced solely by myself, and that I have been working in accordance with regulations passed down by NTNU. Other author's work and sources for information are referred to throughout the text and included in the Bibliography at the end of the report.

Gjøvik, Norway, 18.6.2012

Tarald Husevåg Gaup

Abstract

To cover the world's future consume of hydrocarbons, technological improvements are needed, turning currently unreachable and unprofitable reservoirs into the opposite. The main focus of this thesis, Dual Gradient Drilling (DGD), is a drilling technology that is ideal for drilling in ultra-deep waters, and could prove vital in drilling the reservoirs that are currently undrillable. This will increase the possible supply of hydrocarbons available for consumption.

DGD is not fully accepted in the drilling industry, and DGD is still considered *unconventional*. In this thesis, simulations investigating pressure control in a DGD system are done, showing possibilities and limitations when using DGD. Also, it is done a study of how the challenges faced on the Macondo prospect in the Gulf of Mexico could have been solved better by using DGD instead of the conventional drilling methods.

MATLAB was used for mathematical simulation of the control of the hydraulic pumping system. The program reads field- and equipment specific input data from an excel sheet. The different input parameters are changed separately, and simulations are run for each parameter change, showing each parameter's effect caused to the system abilities. Criteria for approved well control are set, and by trial and error with the program, requirements for pump rates, well bore design and pressure safety margins needed are found, presented and discussed.

It is here shown that the currently available pumping rates are not able to control the pressure as agile as other available drilling technology can, using the marine riser size currently developed. A subsea pump producing rates of more than 13000LPM, the double of what can be produced today, is needed. Utilizing a narrower marine drilling riser, with an inner diameter (ID) of 12¼" instead of the conventional riser with 19½" ID, can increase the speed of a pressure change with 171%; from 0.045bar/s to 0.121bar/s, when other parameters are kept constant. Because of linearity, a doubling of pumprates will result in a doubling of pressure change speed.

It is here concluded that sufficiently agile wellbore control, depends on the development of a narrower riser and higher subsea pump rates. Other unconventional drilling currently available, like Managed Pressure Drilling (MPD), is far superior to DGD when it comes to quickness and accuracy in keeping the BHP at a desired level.

Sammendrag

For å dekke verdens fremtidige energibehov er det nødvendig med teknologiske nyvinninger, som gjør utilgjengelige og ulønnsomme reservoarer til det motsatte. Hovedtemaet for denne diplomoppgaven, Dual Gradient Drilling (DGD), er en boreteknologi som er ideell for boring på ultra-dypt vann. Bruk av DGD kan vise seg å bli en viktig del av utvinningen av ressurser fra felt som er umulig å bore per i dag. Dette kan være med på å øke verdens totale produksjon av hydrokarboner.

Per i dag er ikke DGD fullt ut akseptert i boreindustrien, og sees fortsatt på som ukonvensjonell teknologi. I denne rapporten gjøres simuleringer som undersøker trykkontroll i et DGD system. Både begrensninger og muligheter presenteres. Det gjøres også en studie av hvordan utfordringene på Macondo-feltet kunne blitt løst på en bedre måte ved bruk av DGD, i stedet for ved bruk av konvensjonelle boremetoder.

Et program som simulerer styring av det hydrauliske pumpesystemet er laget i MATLAB. Programmet leser inndata fra et excel-ark. Mange simuleringer utført, der inndataene er endret etter tur, noe som viser påvirkningskraften hver parameter har på styringen av systemet. Ved å sette kriterier for hva som regnes som en vellykket simulering, og deretter kjøre mange simuleringer der inndataen endres manuelt fra gang til gang, er grenseverdien for hver parameter som gir et vellykket resultat funnet.

I denne rapporten bevises det at pumpekapasitene som er tilgjengelige per i dag ikke er høy nok til å kunne kontrollere trykket så smidig og raskt som annen ukonvensjonell boreteknologi kan gjøre. Det behøves en undervannspumpe med en rate på 13000 LPM, mer enn det dobbelte av det som er tilgjengelig per i dag, for å kunne kontrollere trykket tilstrekkelig raskt. Ved bruk av et smalere stigerør kan hastigheten på trykkendringer økes med 171%, fra 0.045bar/s til 0.121 bar/s. Til sammenligning, så vil en dobling av pumperate gi en dobling i trykkendringshastighet.

En del av konklusjonen i denne rapporten er at det bør utvikles et DGD-system som bruker et smalere stigerør i tillegg til en undervannspumpe med en høyere pumperate. Det finnes annen ukonvensjonell boreteknologi, som for eksempel Managed Pressure Drilling (MPD), som med god margin overgår DGD sin hurtighet og nøyaktighet når det gjelder trykkendringer i borehullet.

Table of Contents

List of Figures

1. Introduction

From the first oil well drilled, in Pennsylvania, USA in 1859 by Edwin L. Drake, and further through the centuries that lead up till today, drilling technology has been in a continuous developing process. As early as in the 1890s, oil wells were drilled in water, from land connected platforms in lakes and along the coastline, and in the late 1940s wells were drilled from platforms in the open sea. Today, wells drilled in water depths of more than 3'000m are not unusual, and offshore wells with a measured depth of more than 10'000m have been drilled. This line of developing new ways of reaching the hydrocarbons in the ground has not come to an end, and further technological improvements are still needed to reach the hydrocarbons the world will need in the years to come.

To drill oil wells safe and problem free in ultra-deep (a greater depth than 1500m) waters, accurate pressure control is required. The main topic in this thesis, Dual Gradient Drilling (DGD), is a drilling technology that separates from conventional drilling by simultaneously utilizing two different fluids with different densities in the wellbore. This enables both a quicker way of adjusting the bottom hole pressure (BHP), and the ability to make the wellbore pressure curves fit better with the formation pressure curves. DGD is ideal for use in ultra-deep waters, and primarily by reducing drilling cost, but also by increasing the production rate when the well is completed, the use of DGD can add great value to a prospect. Both details and challenges for the DGD technology, and possible benefits will be discussed in more detail in this report. Conventional drilling and other unconventional drilling techniques are also presented and compared with DGD.

The well-known catastrophe that happened in the Gulf of Mexico (GoM) on the Macondo prospect in April 2010 is presented and the field data acquired from Macondo is used as input data for the simulations. It is also discussed how the use of DGD could mitigate problems faced on Macondo.

This thesis describes how to optimize the control of the hydraulic pumping system used in DGD to ensure maximum safety during different cases of; (1) tripping; and (2) sudden loss of rig pump functionality and hence the circulation friction pressure. Both these cases describe a sudden and severe change in the wellbore pressure, and the DGD system is tested in simulations for capability of keeping the BHP as stable as possible and within the drilling pressure window through these changes. Theory regarding how pressure fluctuations when tripping are created and details regarding the mathematical modelling of this is presented.

The simulations are programmed in MATLAB, and the results are discussed and compared to both conventional and other unconventional drilling technology. At the end of the report,

conclusions regarding pressure control with DGD are made, including recommendations for required future technological developments, and limitations for situations that are controllable with DGD. The MATLAB program takes field specific input from an excel sheet, and can therefore be used for analysis of several, and not only the Macondo formation.

2. Unconventional drilling

In this thesis, "conventional drilling" is understood as drilling with an open-to-air annulus, where one type of uniform mud is used in the system. When circulating the mud, it is pumped down the drillstring and up in the riser annulus, where it pours over the riser brim on the rig and flows into the mud pits for the cleaning process.

The BHP of the well is hence described with Eq. 2.1. The first term on the right hand side is the hydrostatic pressure and the second term is frictional pressure loss in the annulus during circulation; the latter term consequently being zero when there is no circulation.

$$BHP = \rho_{mud} * g * TVD + P_{friction} \qquad \textbf{Eq. 2.1}$$

Where:

ρ_{mud} = Density of the drilling fluid

g = Gravity constant $= 9.81 \frac{m}{s^2}$

TVD = Total Vertical Depth; vertical distance from the drillfloor to the bottom

$P_{friction}$ = Friction pressure loss in the annulus when circulating

The only fluid pumping system that is used is the main rig pump system.

Managed Pressure Drilling (MPD) is considered drilling where the pressure control deviates from the above described situation. MPD will here be divided in two parts; Dual-Gradient Drilling (DGD), described in section 2.1, and pressurized (or back-pressurized) MPD, described in section 2.2. Back-pressurized MPD will be denoted as "MPD".

Because DGD is the main topic of this thesis, it will be described in more detail than MPD.

2.1 Dual Gradient Drilling

2.1.1 Basic principles of DGD

DGD is a technology that differs from conventional drilling by the use of two fluids, with different densities, simultaneously while drilling. The light fluid floats on top of the heavy weight fluid in the riser. The heavy fluid is used for the same purposes as the fluid in conventional drilling, but the lighter fluid is only pressure-inducing, and otherwise inactive.

A sketch of the depths in DGD is shown in Figure 1 and the principle difference between conventional drilling and DGD is shown in Figure 2.

When drilling with a drilling riser that goes from the rig to the seabed, the lighter fluid, which can be both a liquid and a gas, fills the annulus from the RKB level (RKB, an abbreviation for Rotary Kelly Bushing, denotes the level of zero depth) down to the depth of the fluid interface (denoted as D_{fi} in Figure 1).

Figure 3 shows a principle sketch of the equipment close to the riser, and as shown, the heavy mud is circulated from the pumps on the rig, down through the drillstring, up the wellbore annulus, through the subsea pump intake in the riser and is then pumped through a conduit line up to the rig by a subsea pump. The circulation differs from that in conventional drilling by not circulating through the upper part of the drilling riser, but rather through the subsea pump.

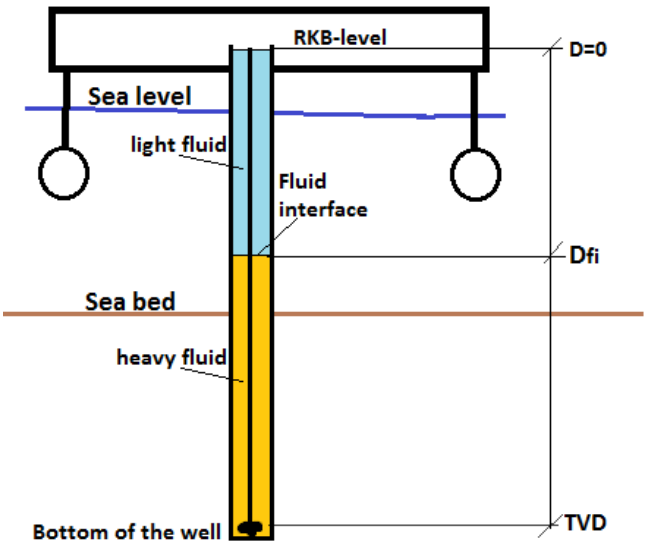

Figure 1: DGD schematic overview

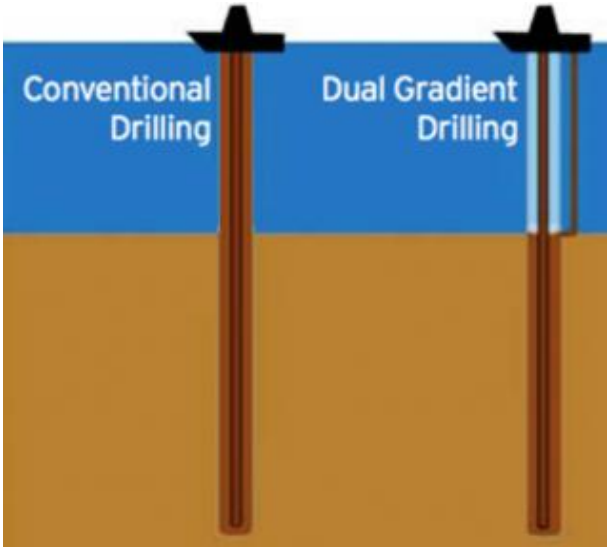

Figure 2: Principle difference: Conventional and DGD

With reference to Figure 1, the BHP when using an open DGD system is described by Eq. 2.2.

$$BHP = \rho_1 * g * D_{fi} + \left(TVD - D_{fi}\right) * g * \rho_2 + P_{friction} \qquad \textbf{Eq. 2.2}$$

Where:

ρ_1 = Density of the light drilling fluid

ρ_2 = Density of the heavy drilling fluid

D_{fi} = Depth of the fluid interface

Compared to Eq. 2.1, Eq. 2.2 offers the possibility of changing D_{fi} to change the BHP. A higher value of D_{fi}, meaning a deeper position of the fluid interface in the riser, gives a lower BHP

because the column of heavy mud is reduced. When saying "*reduce level in the riser*" in this thesis, it describes an *increasing* depth of the fluid interface, giving a *reduced* BHP.

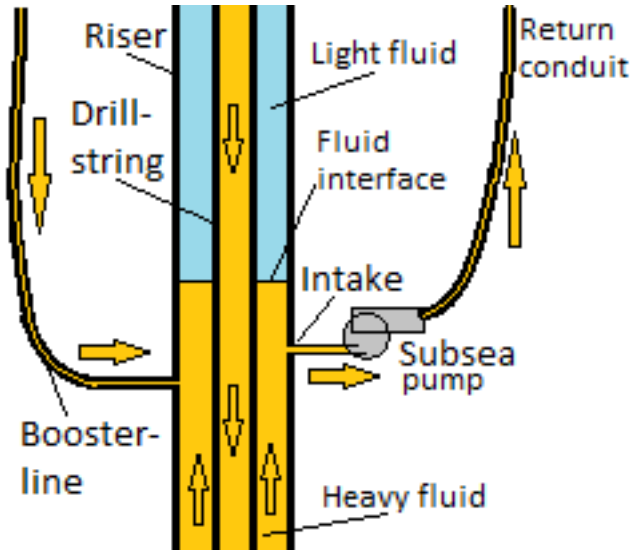

Figure 3: DGD fluid circulation

The booster line transports fluid from the booster pump, a pumping system on the rig that can pump heavy fluid directly into the riser to increase the BHP, independently of the rig pump and the subsea pump. A booster pump is not strictly required to utilize DGD, but in the simulations in this thesis, a booster pump has been included. It would be possible to locate a booster pump system subsea, at the same level and in the same way as the subsea pump, but because this is not strictly required, the placement of the booster pump is most convenient at the rig topside. This makes adjustments and repairing of the pump more accessible. The downside is that a large friction pressure in the booster line has to be overcome, which requires a highly burst-resistible line at the pump output. Another disadvantage by placing equipment topside is that rig space is expensive. The more equipment that can be placed subsea, the better. It would also be possible to have a booster pump system that injects heavy weight fluid down the inside of the marine riser. This would mitigate problems regarding extra umbilicals and lines on the outside of the riser, but it could be a challenge to increase the fluid interface level fast enough, because of the latency from circulating past the light fluid.

The subsea pump sucks fluid from the intake in the riser and pumps it up to the rig. To avoid any of the light fluid being sucked into the subsea pump, the depth difference between the fluid interface and intake has to be more than a specific value, set to 20m in the simulations in this thesis.

The relation between the pump rates, and change of the depth of the fluid interface is described with Eq. 2.3.

$$\Delta D_{fi} = \frac{\left(Q_{sp} + Q_{loss} - Q_{rp} - Q_{bp} - Q_{influx}\right)}{A_{riserannulus}} * \Delta t \qquad \textbf{Eq. 2.3}$$

Where:

ΔD_{fi}	=	Change in fluid interface depth
Q_{sp}	=	Pump rate of the subsea pump
Q_{loss}	=	Rate of fluid loss to the formation
Q_{rp}	=	Pump rate of the rig pump
Q_{bp}	=	Pump rate of the booster pump
Q_{influx}	=	Rate of formation fluid influx to the formation
Δt	=	Time increment
$A_{riserannuli}$	=	Cross sectional area of the marine riser annulus

In Eq. 2.3, a flow that fills the wellbore with fluid is defined as negative. This makes Eq. 2.3 consistent with Eq. 2.2. The subsea pump, which removes fluid from the annulus, makes the *depth* of the fluid interface *increase*, and therefore the BHP in Eq. 2.2 to *decrease*. The new fluid interface depth is found by addition: $D_{fi,2} = \Delta D_{fi} + D_{fi,1}$

The annulus in the wellbore is found by Eq. 2.4.

$$A_{cs,annulus} = \frac{\pi}{4}\left(ID_{hole/casing/riser}{}^2 - OD_{pipe/BHA}{}^2\right) \qquad \textbf{Eq. 2.4}$$

Where:

$ID_{hole/casing/riser}$	=	Inner diameter of the open hole, casing or marine riser
$OD_{pipe/BHA}$	=	Outer diameter of the drillpipe or bottom hole assembly (BHA)

2.1.2 Different companies' variants of the technology

Even though the main principles are the same, different companies have developed different variants of how to use the technology.

2.1.2.1 AGR Group's EC-Drill

The Norwegian based petroleum technology company AGR Group delivers a full set of DGD equipment, consisting of (AGR, 2012):

- Topside equipment
  - Control container
  - Office tool container
  - Umbilical winch
  - Hose handling platform
- Subsea equipment
  - Modified riser joint with in outlet that feeds fluid into the subsea pump module
  - EC-Drill subsea pump module consisting of several subsea pumps
  - Mud return hose

This is the only equipment needed for initiating a DGD operation with EC-Drill. The system integrates into the conventional drilling units already placed on the rig.

The fluid interface is monitored by integrated pressure sensors in the riser joint, sending signals to instruments located topside.

The normal number of pumps to have in a series connection in the subsea pump module is three, each with a flowrate of approximately 4500LPM. This flowrate, in addition to the maximum allowed mud weight could vary from rig-up to rig-up, depending on pump depth, and other customer preferences. The subsea pumps can handle cuttings up to the size of 4in.

The light fluid used is air, which makes a large reduction in the BHP possible, but also makes the riser more vulnerable for collapse due to the pressure differential from the inside to the outside of the riser.

Different from some other unconventional drilling solutions, EC-Drill utilizes no rotating blow-out preventer (RBOP), and is therefore more fit for use in harsh weather conditions. This is a clear advantage to minimize non-productive rig time.

The EC-Drill system does not currently involve a booster pump module (Aasebø, 2012), which means that in case of a rig pump malfunction during drilling, only the mud u-tube effect from the full drillstring into the reduced level annulus, can be used to fill the riser with drilling mud. If possible to open the subsea pump for hydraulic communication with the annulus, a riser filling u-tube effect could also be created from the return conduit to the annulus.

Another feature using EC-Drill, is that the use of a normal drilling riser makes a switch back to conventional drilling easy, simply by isolating the subsea pump module, and pumping return up the drilling riser, as when drilling conventionally.

2.1.2.2 Ocean Riser System's Low Riser Return System

Ocean Riser Systems (ORS), a Norwegian offshore drilling technology company, have developed the Low Riser Return System (LRRS). LRRS utilizes the following equipment (Tonning, 2011):

- Riser interface outlet joint with a Suction Hose going to the subsea pump
- Subsea Mud-Lift Pump
- Return Line going from the subsea pump to the rig
- Modified choke line
- Subsea choke
- Nitrogen purging system

A schematic of the equipment rig-up for LRRS can be seen in Figure 4 (Fossil, et al., 2004). Figure 4 includes some features not yet developed. The 12 ¼" ID marine riser is currently under development, and has not been tested in the field. The Rotary Control Device (RCD) (RCH in Figure 4) is not included in the currently available system either.

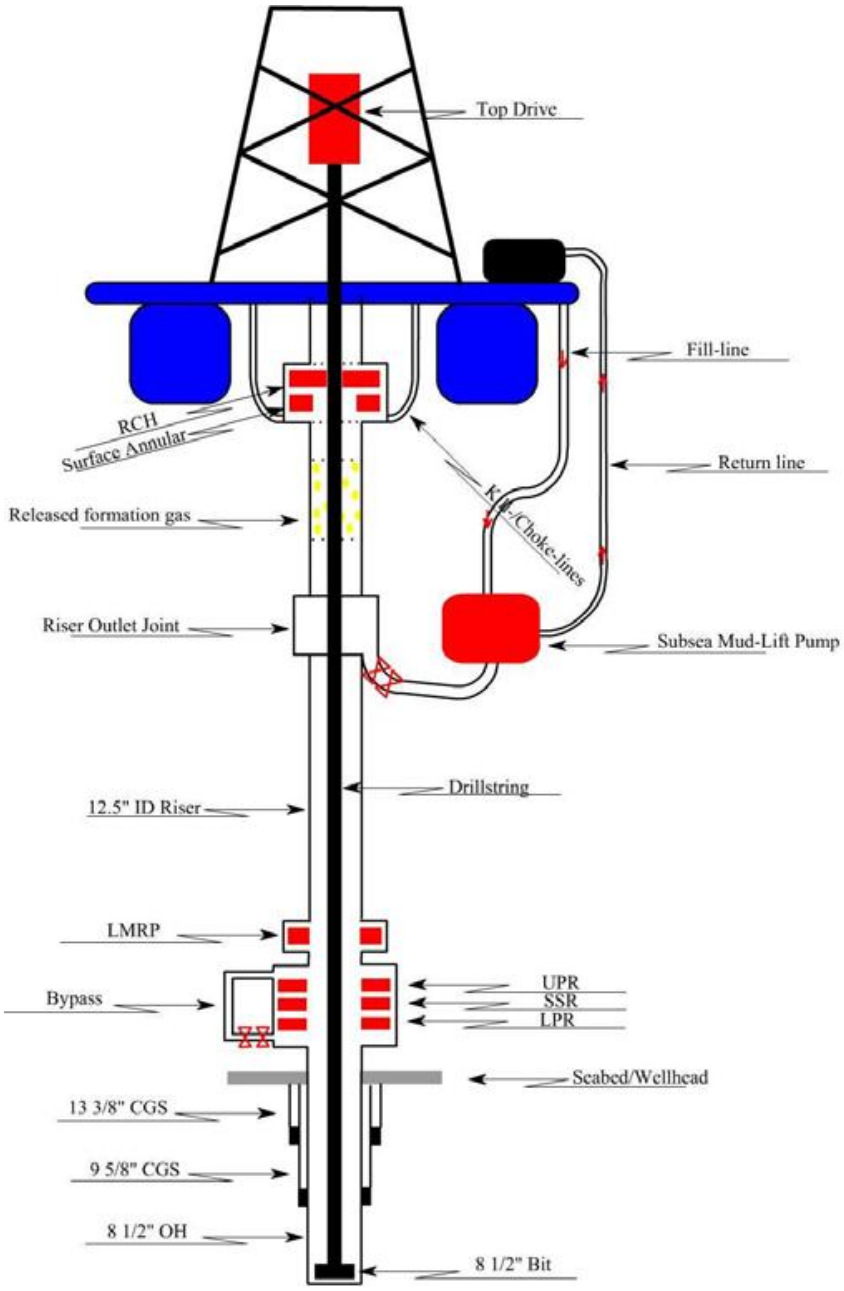

Figure 4: LRRS schematic equipment rig-up

The main feature with the system, the subsea pump module, is a centrifugal pump operating at a rate of 6000 LPM, able to pump mud with a maximum density of approximately $\rho_{mud} = 2100\frac{kg}{m^3}$.

LRRS includes a fill line that goes from the mud pits on the rig to the riser outlet joint, enabling re-filling of the riser with mud, independently of the circulation through the drill string (ORS website, 2012). This gives the same ability as the booster pump previously described. This is a clear advantage compared to AGR's EC-Drill.

The RCD would make it possible to operate as a hydraulically closed MPD system (discussed in section 2.2.2). The development of an RCD in the LRRS system is not fully complete, but has been described in (Fossil, et al., 2004). This way, LRRS could combine the great feature of MPD with the features of DGD; the best of two technologies. The inert gas nitrogen is used in the riser for safety reasons to reduce risk of methane explosions when circulating out formation gas.

The system described in (Fossil, et al., 2004) also utilizes a marine riser with a diameter of 12½", smaller than the normally used 21" (19.5" ID) riser. This makes the procedure of altering the fluid level in the riser quicker even, because the cross sectional area in the annulus is reduced. In addition, less mud is needed to fill the riser, which reduces fluid cost related to both purchase, transportation and conditioning at the rig.

Parts of the LRRS system is under development, and the exact time for when the full system depicted in Figure 4 will be commercially available is uncertain.

2.1.2.3 AGR Group's Riserless Mud Recovery

When drilling conventionally, the top-hole section, drilled from the seabed to the setting depth of the surface casing, is drilled with sea water as drilling fluid, combined with regularly pumped high viscosity fluid "pills". The "pills" clean out the well bore, and increases hole stability. A hole with a small diameter, called a pilot hole, is often drilled prior to a widening of the same hole segment. The pilot hole is made to check for shallow gas or shallow high pressure formation, which is difficult to handle with no way of circulating it out of the well. The process of making the pilot hole can add 1-1.5 extra days. When drilling, cuttings and return drilling fluids are dumped at the seabed.

The Riserless Mud Recovery (RMR) system, another system developed by AGR, makes it possible to bring the return mud from the top-hole section to the rig, without using a riser. This enables the use of weighted drilling fluid in the top-hole; eliminating discharges to the sea, fitting the wellbore pressure profile better to the formation pressure curves and improving well cleaning. This is a use of two fluids when drilling, which makes it a dual gradient system.

The equipment needed for RMR is listed below (AGR, 2012):

- Topside equipment
    - Control container with control system. Linked to the drillfloor and operator container.
    - Umbilical winch. Handles and installs the subsea pump module.
- Subsea equipment
    - Subsea suction module (SMO), placed on top of the well.

- Suction hose, carrying returns from the suction module to the subsea pump module.
- Subsea pump module (SPM), pumping return mud to the rig.
- Electrical cable, enabling communication between the suction module and the pump module.

Visual surveillance of the operation is ensured by cameras placed on the top of the SMO. These live images make accurate adjustment of the mud level possible, which is needed to control the BHP.

Figure 5 (AGR, 2012) shows the suction module, the subsea pump module and the connections to the topside equipment. RMR permits drilling of a longer surface casing section, which extends

Problems regarding shallow gas will be mitigated to a very large extend, both by the use of heavier drilling mud, and by the improved monitoring of the process. This makes the drilling of a pilot hole unnecessary, and therefore, rig time can be saved.

Figure 5: RMR equipment

Figure 6: Drillstring being lowered into the SMO

Figure 6 (AGR, 2012) shows how the drillstring is being lowered into the SMO. The red fluid seen in the open SMO is the weighted drilling fluid. The two cameras monitoring the operation are also visible on both side of the SMO.

Currently, the SMO is only designed for water depths down to 450 m. This depth is too shallow for reaching the whole of the potential drilling market, including many wells in the GoM.

Equipment functional in water depths close to ultra-deep waters (more than 1500m depth) are most likely needed for the technology to be embraced by the whole of the drilling industry. Still, RMR has reached wide acceptance in the drilling industry, after several successful projects around the world that have shown its potential for safety improvement and cost reduction.

2.1.2.4 Chevron, Pacific Drilling and GE's collaboration

In May 2012, the US energy corporation Chevron is doing a cooperative project with drilling contractor Pacific Drilling, where they are putting the world's first deepwater drillship especially designed for DGD into work. AGR Group is also involved in this project, managing deployment and operation, while the major oil service company Weatherford International delivers a RCD that could enable drilling with a hydraulically sealed annulus.

The ship, Pacific Santa Ana, is equipped with the subsea pump "MaxLift 1800", developed by the US technology company group General Electric. MaxLift 1800 has technical data has described below (Refinery News, 2012):

- Maximum pump rate: $6814\ LPM$
- Maximum mud weight capacity: $\rho_{mud} = 2217 \frac{kg}{m^3}$
- Maximum discharge pressure: $455\ bar$
- Maximum water depth: $3048m$
- Maximum object size: $1.5in$

With the only minor shortcoming of the maximum object size, which is less than that of comparable subsea pumps, these highly impressive pump capacity data makes Santa Ana suitable for most of the GoM, a huge drilling market for the years to come.

With this project, Chevron has to be considered a pioneer within the DGD technology. The embracement of DGD by one of the world's oil company giants could very well be the main kick-off for the DGD technology to become the "new conventional drilling".

2.1.3 Benefits from using DGD

2.1.3.1 Fewer casing strings needed to reach total well depth

By the reducing the fluid pressure gradient above sea floor, heavier fluid can be utilized below sea floor. This will make the pressure curves in the well bore fit better with the formation pressure than when using a single fluid gradient. This is visualized by comparing Figure 7 and Figure 8 (Durkee, et al.). Fewer casing strings means both reduced material cost and reduced rig time cost related to the casing setting operation. This is a major benefit. In the figure below, the formation pressure curves are drawn as red (pore pressure) and brown (fracture pressure).

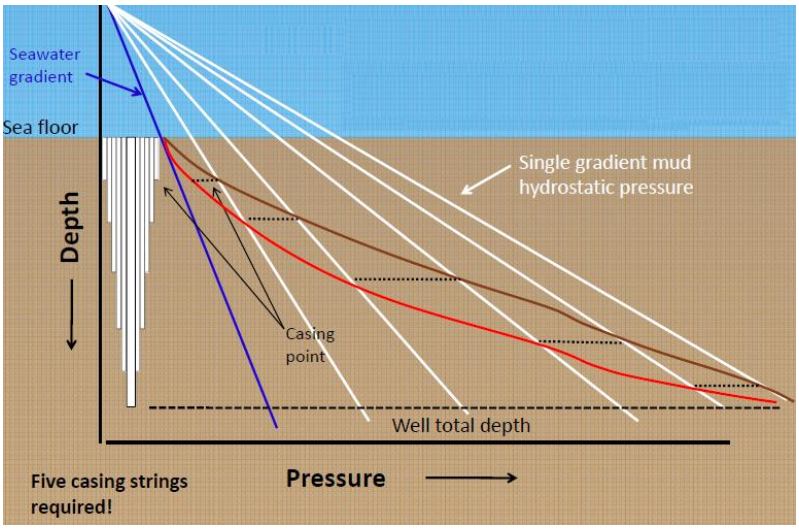

Figure 7: Pressure curves, conventional drilling

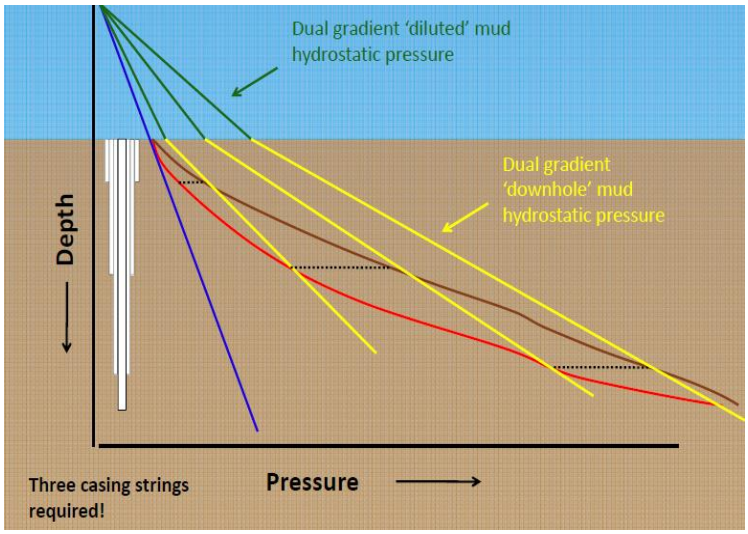

Figure 8: Pressure curves, DGD

When setting a casing, the hole diameter is reduced, and the open hole to be drilled in the next section, has to be smaller than the previous hole. By reducing the number of casings required, the diameter of the end hole can be larger than when drilling conventionally. This means that the production rate can be increased, which again will increase the early income, and hence profit, from the project. From an economical point of view, this is one of the main benefits from using DGD.

Drilling of an exploration well most often means that if a commercially exploitable reservoir is found, the wellbore is stilled plugged and abandoned. Later, when knowing that producible hydrocarbons are in the reservoir, new production wells are drilled. Because of the high cost of an exploration well, energy companies desire to use the exploration wellbores for production; bringing in early income and avoiding to just losing the material and value put into the exploration wellbore.

With the increased wellbore diameter made available by DGD, it is more economically feasible to convert an exploration well into a production well, because of the higher possible production rate. By doing this, high value can be added to a project by not abandoning the exploration wellbores. Convertion of exploration wells into production wells is a hot topic for oil companies todya, especially in deep and ultra-deep waters, where the cost of a well is extremely high.

2.1.3.2 Quicker and more versatile pressure control

In conventional drilling, the hydrostatic BHP can only be changed safely by altering ρ_{mud}, as seen from Eq. 2.1. To do this requires a minimum of one circulation of the whole annulus volume, which typically takes a minimum of 3 hours when drilling in a well at 5000mMD. In addition comes the time needed for mixing the new mud and often additional circulation. The mud weight is increased many times during drilling of a conventional well to adjust for formation pressure changes.

With DGD, the BHP can be changed simply by altering D_{fi} in Eq. 2.2. As an example, consider a system of a 21" ocean drilling riser with an ID of 19.5" and 5" OD drillpipes, giving a riser annulus cross-sectional area of, $A_{cs,ann} = 0.1801m^2$. Further, assume fluids utilized to be seawater ($\rho_{sw} = 1030\frac{kg}{m^3}$) and a drilling mud $\left(\rho_{mud} = 1850\frac{kg}{m^3}\right)$, a subsea pump rate of 5000LPM, and the desired pressure change to be 10 bar. That gives the below shown result

$$\Delta T = \frac{\Delta V}{Q_{sp}} = \frac{A_{cs,ann} * \Delta H}{Q_{sp}} = \frac{A_{cs,ann} * \Delta H}{Q_{sp}} = \frac{A_{cs,ann} * \frac{\Delta P}{(\rho_2 - \rho_1)g}}{Q_{sp}}$$

$$\Delta T = 4.48min$$

Because this way of changing the BHP is much quicker than the conventional way, it allows for more accurate pressure control, as the fluid level in the riser can be continuously adjusted. This makes it possible to eliminate the friction pressure loss from Eq. 2.2, by adjusting D_{fi} accordingly, keeping the BHP completely constant during ramping up and down of the pumps. This has previously been described in more detail in (Gaup, 2011). A constant BHP will make it easier to drill in a narrow mud window, in for example a depleted reservoir or in deep water. This is often impossible with conventional drilling because the friction pressure cannot be eliminated, hence representing the theoretical absolute minimum width of the mud window. With DGD, this problem is manageable.

2.1.3.3 Drilling with riser margin

To have a riser margin when drilling means that the hydrostatic pressure inside the riser at the seabed is lower than the water pressure on the outside, so that in case of an emergency riser

disconnect from the wellhead, the well will still be in pressure overbalance to the pore pressure. When drilling conventionally in deeper waters, this is often completely impossible, because the long column of heavy mud needed would fracture the formation.

By reducing the level in the riser, the pressure exerted from the mud column is reduced, and hence, drilling with riser margin is possible.

2.1.3.4 Early kick and loss detection

The fluid level in the riser is monitored by integrated pressure sensors in the riser or by visual surveillance. Sudden changes in the fluid interface depth, and the following changes in the subsea pump rates, gives indications of either loss of fluid to the formation, or formation fluid influx. This can be discovered earlier than by conventional drilling. In addition to the quicker detection, the measures can be taken during the first minutes after discovery. This mitigates the consequences in case of a well control accident.

2.1.3.5 Possible to obtain optimal circulation rate

The optimal circulation rate, with regards to hole cleaning and rate of penetration often gives a too high ECD for the fracture pressure limit. Because DGD can compensate for the friction pressure by reducing the heavy fluid level in the riser and therefore keep the BHP constant when changing circulation rate, this is no longer a problem. An increased rate of penetration will reduce drilling time and therefore rig cost.

2.1.4 Disadvantages and Challenges with DGD

2.1.4.1 Subsea equipment

Subsea technology is a fairly new technology that is being continuously improved. Not having easy access to the equipment is a challenge, because malfunctions take longer time than topside equipment to repair, either if the repair happens under water, or if the equipment has to be moved to the surface first. As long as the technological development cannot provided 100% faultless equipment, the fact that pumps and other engines operate subsea is a challenge.

The many lines, umbilicals and wires used to control the subsea equipment could easily get entangled because of the sea currents and other motions. This could create problems when wanting to disassemble parts of the equipment, because it could be stuck in the other parts, or because the lines could be deformed, and therefore dysfunctional.

2.1.4.2 Risk of riser collapse

If a gas, for example air or nitrogen, is used in the drilling riser, the risk of inward collapse in the riser has to be assessed. The hydrostatic pressure in the seawater will create a great pressure on the outside of the riser, while the pressure on the inside of the riser will be close to atmospheric

in an open system. As an example, a 20" #133.00 K-55 casing with a collapse resistance of 1490psi (Bourgoyne, et al., 1986) is considered. With atmospheric pressure inside the riser, a pressure differential of the magnitude of the collapse resistance is reached at a water depth of 1017m. The depth is here found by using the below shown equation.

$$D = \frac{\Delta P}{g * \rho_{sw}}$$

If required to use a gas-fluid DGD system at a deeper water depth than 1017m, a stronger casing or a counter-acting pressure on the inside of the riser has to be considered.

2.1.4.3 Conservative and cyclical industry

The drilling industry is often viewed upon as a conservative branch, where new ideas and technology is not easily implemented. Safety and efficiency is highly important, and the risk associated with using brand new technology could be regarded too high for the possible gain.

General investment costs related to DGD is currently higher than for conventional drilling, but as more and more companies start using the equipment, higher volumes of pump modules, winches, riserjoints, pressure sensors, etc will be ordered, and the production cost for each unit will decline, along with the price of the equipment. This likely price decline at the higher produced volume will be a motivator for other companies to adapt the DGD technology.

DGD was a hot prospect already in the early 2000s, but a moderate oil price of just above USD 20/bbl (Inflation Data, 2012) didn't boost risk appetite for the oil companies. Rig contracts lasted shorter time periods than at present, roughly around 12-18 months (Redden, 2010). The expensive investment in DGD equipment might have seemed too risky for such a short time period was not considered right. Now, rig contracts are typically lasting 4-5 years, which gives better incentive to invest in equipment for the rigs. However, the oil prices are volatile, and the very fragile and uncertain economic situation seen in Europa and the USA today could make those companies currently considering investing in DGD systems reconsidering.

2.1.5 How DGD is understood in this thesis

In the simulations made in this thesis, a DGD system with a booster pump, but without a RCH (as described as possible in LRRS) is assumed. The main focus here is to show how the subsea and booster pump can control the hydrostatic BHP by altering the D_{fi} in given situations. Therefore, the feature of adding a backpressure by the use of a RCH in a DGD system has not been investigated.

2.2 Managed Pressure Drilling

2.2.1 Basic principles of MPD

MPD is drilling where the whole of the hydraulic system is pressurized. This is possible because the annulus is not open to the atmospheric pressure in the top, but closed in by a hydraulic seal around the drillstring; the return mud is flowing through an adjustable choke at the rig that regulates a "backpressure" exerted on the mud column in the wellbore. The magnitude of the backpressure is controlled by the circulation rate through it and the opening size of the choke. The hydraulic sealing device, often called an RBOP, enables rotating and vertical movement of the drillstring with a high pressure differential over the device. A schematic of a hydraulic seal, with 4 independently seals, is shown in Figure 9 (SIEM WIS, 2012).

Only one density drilling fluid is used at a time. The BHP is therefore described by Eq. 2.5.

$$BHP = \rho_{mud} * g * TVD + P_{friction} + P_{choke/back} \qquad \textbf{Eq. 2.5}$$

Where:

$P_{choke/back}$ = A pressure exerted on the top of the mud column by a back pressure pump or by a choke

Figure 10 (Evaluating New Automatic Well Control Procedure.., 2010) shows the fluid circulation from the mud pump, down the drillstring, through the bit, up through the annulus, through the choke and further to the mud cleaning process (not shown).

The choke can be both automatically and manually operated. Previous studies have shown that an automatically operated choke is more accurate, even when the choke is operated by a specially trained crew (Godhavn/Statoil, et al., 2010). The automatic choke is controlled by a control system, that could use a hydraulic model to estimates the BHP or the downhole measure while drilling (MWD) data of the BHP, to find the optimal choke size opening.

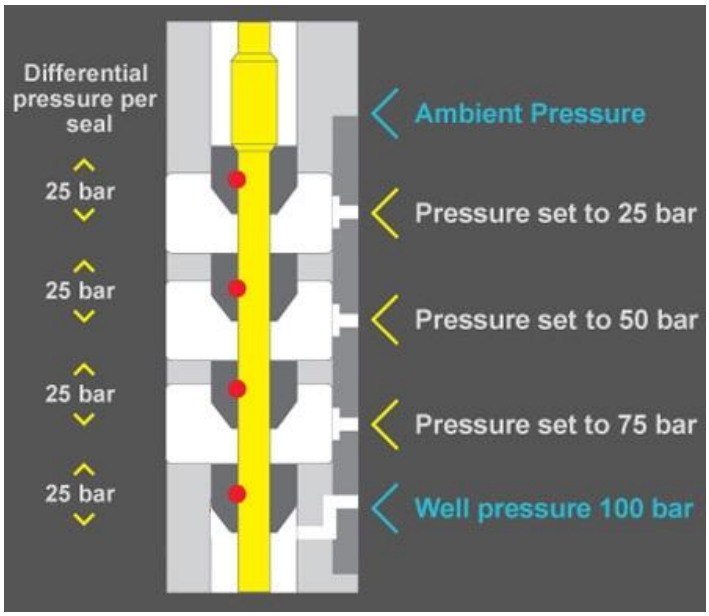

Figure 9: MPD: Hydraulic seal arund the drillstring

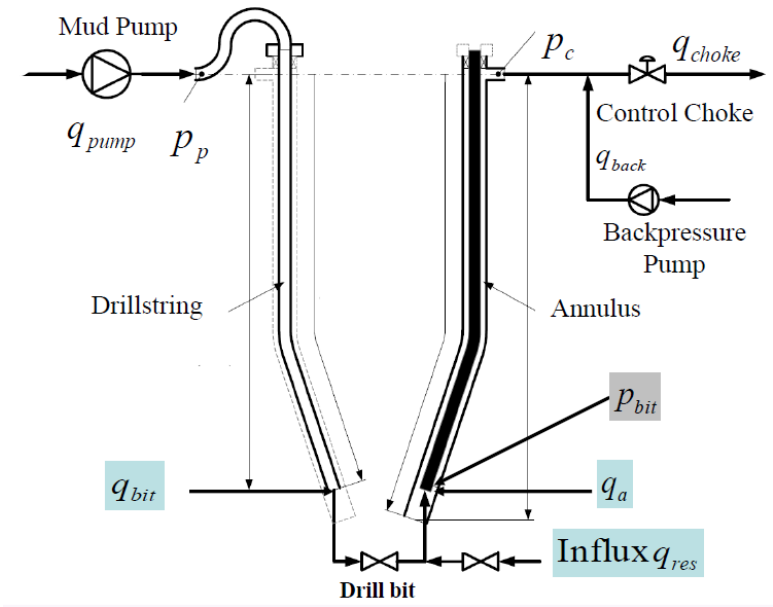

Figure 10: MPD schematic

Required equipment for MPD includes:

- Hydraulic seal around the drillstring that allows for rotation and axial movements of the drillstring, while still keeping the pressure in the top of the annulus higher than atmospheric. This is made by several service companies, including Siem WIS, with their unit called PCD, and Weatherford's RCD.
- Annulus control choke guiding the return mud out of the riser. A small choke opening gives a higher backpressure to the annulus.
- A hydraulic model and a real time control system to coordinate the opening of the choke, mud pumps and the backpressure pump. Schlumberger, through the acquired company @balance and Weatherford, through the acquired company Secure Drilling, are two of the companies delivering a control system. The control system has a very important task of coordinating the equipment, because even minor imprecision could result in large pressure deviations.

Other equipment that improves the performance, without being absolutely essential in MPD mode includes:

- Continuous circulating system (CCS), allowing for circulation of the drillmud in the annulus even when the rig pump is disconnected from the drillstring during connections. This avoids mud sagging in the annulus, and keeps the ECD constant, giving a constant backpressure.
- Backpressure pump, increasing the backpressure without circulation.

(MPD Simulations, 2010: 03.11 & 05.11) has been a base source for understanding of the MPD concept.

2.2.2 Pressure control using DGD

By adjusting the term P_{choke} in Eq. 2.5, it is possible to keep the BHP constant as the friction pressure varies. This is done automatically by the control system. The pressure profile in the annulus becomes like shown in Figure 11 (Gaup, 2012). As visible from the reduced slope of the MPD-line, MPD makes it possible to use a fluid with a lower density than in conventional drilling, to reach the same BHP.

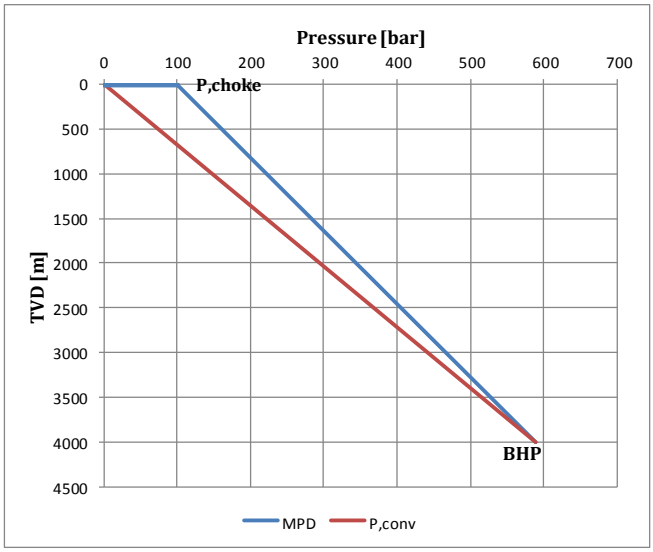

Figure 11: Pressure profile

The adjustment of the choke takes only seconds.

Fluid influx to the wellbore is discovered rapidly, because the system is hydraulically sealed and controlled by sensitive sensors.

2.2.3 Benefits from using MPD

Benefits from using MPD include

- Change BHP instantly
- Accurate pressure control reducing wellbore problems like ballooning and differential sticking, in addition to reducing the number of casing sections needed to reach total depth. The accuracy depends on the hydraulic model's ability to simulate the pressure and the automatic control module's ability to react correctly.
- Possibility to drill with reduced mud weight, reducing hydraulic friction pressure.

- Eliminate the net effect of the annulus friction pressure in Eq. 2.5 by compensating for changes in $P_{friction}$ with $P_{choke/back}$.
- Early kick detection, making it possible to control the influx to prevent an uncontrolled situation
- BHP can be kept constant, even when the pressure varies because of fast movements of equipment in the wellbore, like surge and swab.

2.2.4 Disadvantages and Challenges with MPD

- MPD requires more complex equipment and rig-up than when drilling conventionally. This comes with an increased material cost, additional training for the rig crew and the place requirements for the rig.
- As for DGD, it is difficult to gain full entry into the drilling industry, because of conservative and risk averse attitudes.
- Use of MPD on Mobile Offshore Drilling Units (MODU) is being tested, but not fully possible. Siem WIS's PCD is meant for use on a MODU, but testing is still ongoing and a targeted use in late 2012 is considered realistic

2.3 Comparing unconventional drilling technology

The two technologies DGD and MPD are both developed to control the wellbore pressure faster and more accurate, in order to enable drilling of reservoirs that are undrillable when using conventional drilling methods.

Changing the fluid interface depth in a DGD system gives a new dimension of altering the wellbore pressure. The time needed to alter the DGD pressure is amongst other parameters dependent on the density difference between the fluids utilized, available pumping rates and cross-sectional area in the riser. The pressure in an MPD system can be changed in an instant, simply by changing the position of the Control choke. So, even if DGD is much faster than conventional methods, MPD is even faster than DGD. As will be investigated through the simulations in chapter 5, this difference in quickness means that MPD has better premises to compensate for quick pressure fluctuations in the wellbore.

MPD is not intended for drilling the whole well, but only drilling through specific intervals in the formation with an extremely narrow pressure window. Using MPD when drilling long wellbore section in for example normally pressurized shale creates an unnecessary wear and tear on the RBOP. In normal pressure conditions, which make up most of the well, the accurate control offered by MPD is simply not required. MPD is well suited for the niche of drilling in extremely narrow pressure window. MPD can reduce the number of casing strings needed by offering a more accurate pressure control, which reduces the need for high safety margins.

DGD, on the other hand, is intended for use throughout the whole formation. The pressure profile created with DGD is more parallel to the formation curves, than those created both by MPD and by conventional drilling. This makes it possible to extend the casing sections longer with DGD.

Using an RBOP on a MODU is a challenge. Harsh weather conditions, and heave motions make it difficult to create a redundant seal. MPD is therefore currently marginalized to drilling operating from fixed platforms, which basically means water shallower than around 500m. Even though this covers a large part of the drilling market today, drilling in deeper waters is a huge market, and the full potential of MPD is not reached before solutions including the use of an RBOP from a MODU is commercially available.

Using DGD from MODUs is not a problem, because no hydraulic seal is needed other than the BOP, placed on the sea floor.

3. The well on the Macondo Prospect and its challenges

A well-known and now well-documented accident happened in the Mississippi Canyon Block 252 (MC252) in the Gulf of Mexico (GoM) in April 2010, on the BP-operated Macondo Prospect during the drilling of an offshore well. The accident caused a world-wide debate regarding safety in offshore drilling. MC252 lies 77 kilometers south-east of the nearest shore and 183 kilometers from the shipping supply point in Louisiana, US. The Macondo well was an exploration well, drilled vertically by the rig Deep Water Horizon. The well was planned to be converted into a production well at a later stage if producible hydrocarbons were found. In this thesis, this well will be referred to as "the Macondo well" or "MC252".

The Macondo well has been used in this thesis for a case study. One reason for the selection of this well as a case study is the well data that is publically available in numerous accident investigation reports. Another reason for using the well as a reference is the fact that this was a challenging operation, were mistakes were made, and the potential for improvement is obvious.

It is here shown how the introduction of DGD could have improved well safety and mitigated the risk of the uncontrolled well incident.

3.1 Drilling in the Gulf of Mexico

If not otherwise denoted, the source of information in section 3.1 is (BP, 2010).

3.1.1 The Macondo accident

Prior to the main accident, the Macondo well suffered from several potentially dangerous situations. These incidents were not directly linked with the main accident, but are included here, to describe the many challenges faced. In November 2009 the hurricane Ida damaged the drilling rig, which therefore had to be replaced. In March 2010, an unexpected high pressure sand zone formation was penetrated, an incident which led to the drillstring becoming permanently stuck. The lower part of the wellbore had to be plugged and abandoned and sidetracked with a revised casing design.

Lost circulation was experienced close to the final depth, when penetrating a thief zone in early April 2010. The mud density was reduced, and drilling could continue to the final depth of 5598mTVD.

After logging operations and well integrity testing, the 9 7/8" x 7" casing was run and cemented at 18304ft. When the crew was preparing for the temporary abandonment procedure, on the evening of April 20, 2010, formation gas reached the surface, ignited and created an explosion on the rig which killed 11 and injured 17 of the rig crew. 115 people were evacuated from the rig, including the injured crew member. Deep Water Horizon sank on April 22, 2010.

3.1.2 Key Findings from the accident investigation report

After the accident investigation, it was officially concluded that 8 Key Findings were the most probable reasons for the accident (BP, 2010). Here, only specific drilling related Key Findings are presented, and the Key Findings related to malfunctions of packers, valves, other stationary equipment and the findings related to misinterpretation of well data are not discussed. The below selected Key Findings are discussed because the challenges met could have been eliminated by introducing DGD. If not stated otherwise, source for information in section 3.1.2 is (Close, et al., 2008).

3.1.2.1 Key Finding 1 – The annulus cement did not seal sufficiently

The 7" x $9^{7}/_{8}$" casing was run and cemented at 18304 ft. When cementing the casing, a hydraulic friction pressure from the cement being pumped is exerted to the formation. Because of the narrow drilling window, the focus of the cement slurry design was to ensure an acceptable equivalent circulation density, to prevent fracturing the formation. This took some of the attention away from the design issues to ensure cement stability, contamination issues and cement fluid loss potential. When pumped, the cement slurry design and procedures did not meet the requirements of the Engineering Technical Practice (ETP) recommendations (BP, 2010).

To get a good hydraulic seal when cementing, it is important to displace the drilling fluid with the cement without the cement rifting and creating hydraulic channels. This is best done at a high pumping rate, especially when displacing in a narrow annulus. A high pumping rate creates a higher frictional pressure drop, which again could fracture the formation. As visible from Figure 12, and discussed in section 3.1.3.1, the casing scheme used on Macondo created very narrow annuli.

As will be discussed in section 3.1.3.1, DGD could both have widened the casing annuli, and lowered the wellbore pressure to allow for a higher pump rate; both measures mitigating the problem identified in Key Finding 1.

3.1.2.2 Key Finding 4 – Hydrocarbon influx was not recognized quick enough

A fluid gain of 39bbls in the mud pits was taken at 20:58 hours while displacing the well fluid to seawater. This indicated formation fluids entering the well; hydrocarbons that eventually exploded on the rig. However, the fluid and pressure readings were not recognized as hydrocarbons before 21:38 hours, when the hydrocarbons entered the riser. Well control actions were taken at 21:41 hours; 43 minutes after the first hydrocarbon influx.

When drilling with DGD, more sensitive pressure control with a faster response is used. The fluid interface level in the riser is continuously monitored, along with the pump rate of the subsea pumps. When the first hydrocarbons entered the well, the level of the fluid interface in the riser

would have changed, which would have been a critical change in drilling parameters; undoubtedly causing actions to be taken by the crew members at an earlier stage than when drilling conventionally.

3.1.3 Other challenges faced during drilling on Macondo

The challenges discussed in this section were faced during the drilling of the Macondo well. This gives an impression of the difficult environment the drilling was happening in. As will be discussed below, the problems experienced on the Macondo well could have been solved more efficiently using DGD.

3.1.3.1 Ultra-deep water

The water depth at the Macondo well was 1545 m. This is classified as ultra-deep waters, the highest rating for water depth. In general, deep waters make the drilling pressure window narrower, and hence it becomes more difficult to keep the pressure within the boundaries for a stable well. Shortly explained, this is because the sea water gives a high overburden pressure to the formation; only representing an increased load, but not increased formation strength, as the same interval of rock would have done. This can cause problems when drilling conventionally, because the hydrostatic heavy weight mud column has to go all the way from the rig to the sea bed, exerting a high pressure on the shallow and weak formation, potentially causing damage to the formation.

On the Macondo, this was solved by setting several casing strings to protect the top formation. A normal casing program for deep waters include five casing strings, with diameters ranging from 30” to 7” (Close, et al., 2008). On the Macondo well, nine casing sizes were used, diameters ranging from 36” to 7”. The two casing programs are illustrated in Figure 12 (Close, et al., 2008), showing the casing program used on Macondo on the left-hand side. The narrow space between the casing strings that are created in the Macondo casing program makes it difficult to get a sealing cement barrier in between the casings. In addition, the many casing strings represent high material cost and also give a high load hanging on the well head, which could cause fatigue.

By applying DGD, the hydrostatic pressure exerted from the mud column could have been reduced, to make a better well pressure profile fit with the pressure in the weaker top formation. Thus, a conventional deepwater casing program could have been used, which would have improved the cement hydraulic sealing ability, reducing stress on the wellhead and reducing material cost.

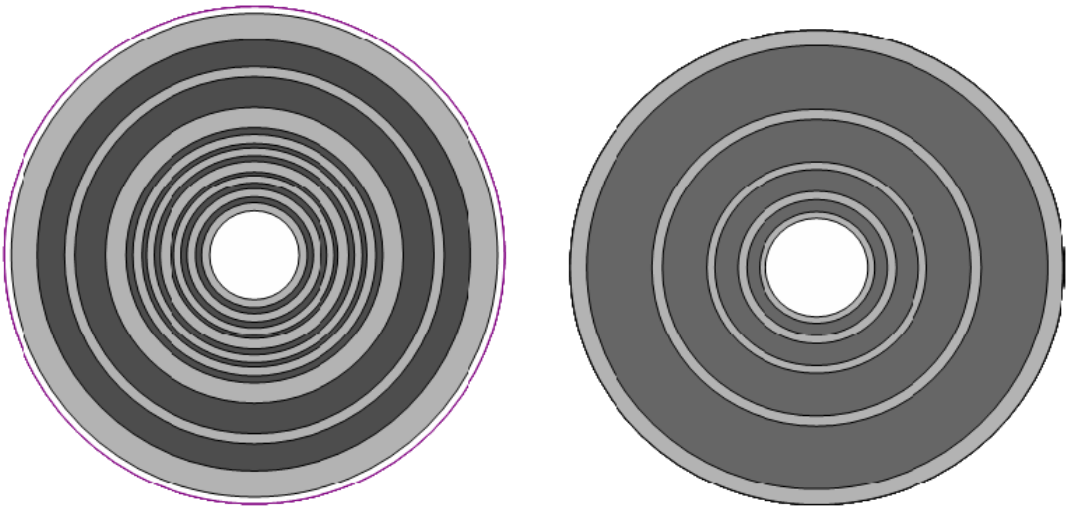

Figure 12: GoM casing program and conventional deepwater casing program

3.1.3.2 High pressure gas zones

On March 8, 2010, the wellbore became underbalanced, resulting in a kick situation. Formation fluid influx were taken into the well, as the well was in an underbalanced condition for an estimated 33 minutes before required measures were taken. The situation occurred as an unexpected high pressure sandformation was penetrated. This incident eventually lead to the drill pipe becoming stuck, and the wellbore had to be abandoned and side tracked.

As discussed in section 3.1.2.2, the situation could have been avoided using DGD, in the same way as the main accident gas influx could have been discovered sooner. By taking measures earlier after the influx, the consequences could have been mitigated.

3.1.3.3 Fluid losses to "thief zones" causing lost circulation

When drilling the 8 ½" x 9 $^{7}/_{8}$" section at 18260 ft, lost circulation was experienced. This is a situation where drilling fluid is lost to the formation when circulating, so that return fluid cannot be returned to the rig. Lost circulation is regarded as a potentially very dangerous situation, because mud, which acts as the stabilizer for the open hole stability and the primary barrier against the formation pressure, is lost. If the mud is lost, not only can the open hole collapse, or the drillstring get stuck, but the well can get in underbalance to the pore pressure, which can result in an un-controlled blow out. The mud weight on Macondo had to be reduced from 14.3ppg to 14.17 ppg, and lost circulation pills were pumped before the well became stable, and

drilling could continue to the final depth. As described in section 0, the change in BHP could have been done much quicker using DGD.

The possible great reduction in time spent for lowering the wellbore pressure by using DGD would both mitigate the consequences of lost circulation, and save cost related to rig operation time.

3.1.4 Other general challenges when drilling in the Gulf of Mexico

The formation pore pressure of Macondo was estimated to be around 13000psi, with a bottom hole static temperature (BHST) of 242°F. These conditions are challenging for the downhole equipment, which increase the probability of receiving the wrong information regarding formation from the bottom hole instruments.

In the formation, there are high pressure gas zones in shallow parts of the formation, as well as hydraulically sealed “thief zones” with lower pressures then the surrounding in both shallow and deeper parts of the formation. This can create a very narrow drilling window, which makes the pressure control during drilling very challenging.

There are also zones with trapped sediments differing from the surrounding formation types, which complicates the formation behavior when in contact with the drilling fluid, and salt zones with sudden pressure variations that are hard, and sometimes impossible, to predict.

The reservoirs are often of high pressure and high temperature (HPHT), which raises demands for equipment, casing and cement robustness.

The above discussed challenges all require accurate pressure control in the wellbore. The accuracy and rapidity provided using DGD, is ideal for the handling of these challenges.

4. Surge and swab

4.1 Theoretical explanation of Surge and swab

'*Surge*' and '*swab*' are terms used for the pressure changes that are created in the drilling fluid when the drillstring, or other bodies, are moving in the wellbore.

When running the drillstring *down into* the fluid filled borehole, the volume of the body of the drillstring displaces the drilling fluid up along the wellbore annulus. This fluid flow creates a frictional pressure in the wellbore that comes in addition to the hydrostatic pressure. Hence, this is *surging* (increasing) the borehole pressure. The same thing happens, when pulling the drillstring *out of* the hole; fluid has to flow down in the borehole annulus to fill the vacuum from the removed drillstring. This creates a pressure suction effect which *swabs (*decreases) the mud pressure, as the mud flows in the annulus between the drillstring and the hole to fill the empty space. This is illustrated in Figure 13.

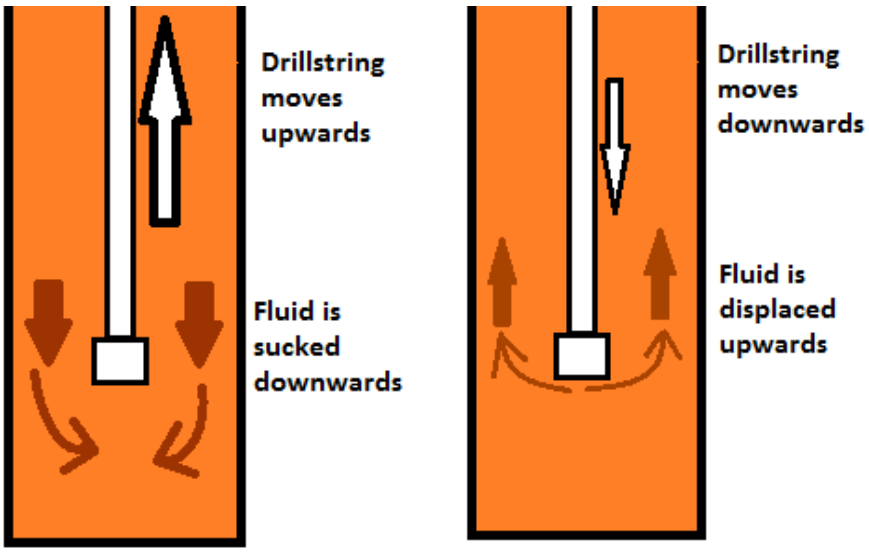

Figure 13: Surge and Swab

The swabbing and surging effects are often talked about together, and denoted "surge and swab". Surge and swab can also be experienced when rotating the drillstring and handling casing, and other equipment, in the borehole. In explaining the pressure changes, the effect will here be divided into two parts; Stationary and Transient movements.

In general, the pressure at a specific depth z in the wellbore when tripping *without* circulation can be described by Eq. 4.1.

$$P_{well}(z) = \rho_1 g Z_{fi} + \rho_2 g(z - Z_{fi}) + \Delta P_{surge/swab} \qquad \textbf{Eq. 4.1}$$

In Eq. 4.1 the first two terms are the hydrostatic pressure, while the term $\Delta P_{surge/swab}$ describes the pressure created by the motion of the drillstring. The calculation of this term is discussed in more detail in section 4.2. Eq. 4.1 assumes no circulation through the rig pumps, and therefore no friction pressure is included.

4.1.1 Transient movement

Transient movements are here considered as the acceleration phase, before the movement of the pipe and the annulus flow of the fluid becomes stationary.

4.1.1.1 Breaking of the gel structure

Drilling mud is a non-Newtonian fluid, and therefore its shear stress is larger at lower shear rates. After a time period of still stand, drilling muds even gel; going from fluid into gel consistence. When stirring a gelled drilling mud, it takes a bit of extra force to break the gel and make the mud into fluid. This breaking of the gel exerts an extra pressure in the wellbore, compared to the pressure experienced if the fluid was water (or other Newtonian fluid). This extra pressure only lasts for a moment, until the gel structure has been broken, and the mud flows as a fluid.

4.1.1.2 Fluid Inertia

Newton's 2nd law says that a force is required to accelerate a body with a mass. This is also valid for drilling fluid, and the force needed to put the fluid in motion is experienced as a change in pressure.

4.1.2 Stationary movement – the viscous drag

When the pipe is being moved at a stationary velocity, a steady fluid flow profile in the axial direction is created in the annulus. Because both the friction force between the moving fluid and the annulus surface, as well as the fluid shear stress, are forces working against the flow, a pressure change is experienced in the wellbore. In the theoretical example of fluid having infinitely low density and no shear stress, there would not be a pressure deviation, since no forces would be counteracting the movement.

Because there are frictional forces between a fluid and a solid, the fluid *clings* to the solid. Due to this *clinging effect* of the drilling fluid on the drillstring surface, drilling mud is moving along with the pipe during movements. This fluid clinging is increasing the effective diameter of the drillpipe, causing the effect of the surge and swab to be more severe. Pipe movement and the corresponding fluid cling effect is illustrated in Figure 14 (Crespo, et al., 2010); which shows movement of the drillstring out of the hole. Here, the mud flows in the opposite direction of the pipe movement, to cover up the removed volume from the pipe and the clinging mud. The clinging fluid behaviour and shear stress of the fluid is described in more detail in (White, 2006).

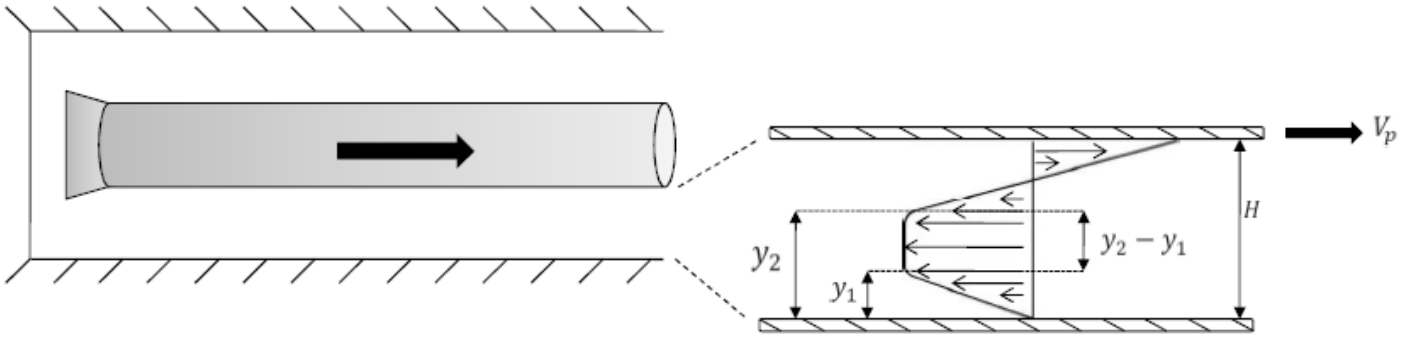

Figure 14: Slot model representation of a concentric annulus. Causing swab effect

A vertical well will in an ideal case create a concentric annulus between the drillpipe and the borehole wall, while a deviated or horizontal well will cause the drillstring to lie down on the low side of the borehole to create an eccentric borehole annulus. Studies have shown that an eccentric borehole reduces the effects of surge and swab compared to that of a concentric borehole (Hussain, et al., 1997). The cross section of an eccentric borehole annulus has a more complicated shape, and is more difficult to make models of. Because the Macondo well is vertical, and the fact that the most severe cases of surge and swab problems happens for a concentric annulus, the envisioned borehole annulus in this thesis is assumed to be perfectly concentric.

4.1.3 Parameters affecting surge and swab

The effect of most of the parameters described below will be studied and illustrated in the simulations made in this thesis.

4.1.3.1 Pipe velocity

When moving the pipe faster, the volume of fluid that must flow in the annulus to compensate for the pipe volume is larger. This gives a higher flow rate, which again gives a higher frictional pressure loss.

4.1.3.2 Slot width

In general, when other parameters are kept stable, fluid flow through a narrow opening creates a higher frictional pressure drop than fluid flow through a wide opening. The same is valid for the flow in the annulus during pipe movement. A small annulus width, “H” as seen in Figure 14, will give a higher surge and swab.

The diameter ratio $\frac{d_{pipe}}{d_{hole}}$ is regarded as maybe the most important parameter, and has been shown to have a great influence on the surge pressure. An increase from $\frac{d_{pipe}}{d_{hole}} = 0.2$ to $\frac{d_{pipe}}{d_{hole}} = 0.7$ could see the exerted surge pressure go from 70 psi to 500 psi, a 700% increase, keeping other parameters fixed (Crespo, et al., 2010).

4.1.3.3 Length of drill pipe in the hole

Because the stationary pressure change is caused by the fluid flow in the annulus, a longer drillpipe will increase the volume of fluid that has to flow along the pipe body, and therefore also the pressure change. For example, when running the drillpipe in the hole from a depth of 1500mTVD to a depth of 4000mTVD, the same tripping motion will cause a larger pressure surge per tripped meter at 3500mTVD than at 2000mTVD, simply because of the longer pipe segment exposed to the fluid.

4.1.3.4 Open or closed pipe

If the end of the pipe is open, fluid can flow inside the drill pipe to compensate for the changed volume in the annulus. This will make the cross section area of the fluid flow path larger, which again will reduce the needed flow rate, and hence reduce the frictional pressure loss when moving the pipe. An open drillpipe can either be made by a circulation hole in the pipe body, by having so large bit nozzles that they can effectively be used for flow both in and out, tripping without a bit (for well intervention operations) or by pumping fluid out of the bit when tripping out (to reduced swab).

In this thesis, a reversed safety valve will be considered included in the drillpipe, making u-tubing and circulation up through the drillpipe impossible. This is done to simplify the simulations, and to isolate the effects from other parameters when simulating.

4.1.3.5 Fluid rheology, density and compressibility

The fluid shear stress, τ, both during motion and at still-stand is important, but has a greater influence at a lower shear rate, due to the non-Newtonian behaviour of the drilling mud called shear thinning. Previous literature show that an increase from $\tau_o = 5\frac{lbf}{100ft^2}$ to $\tau_o = 30\frac{lbf}{100ft^2}$ gives a surge pressure increase from 60psi to 220psi, when keeping other parameters fixed (Crespo, et al., 2010).

Higher fluid density will increase the viscous drag in the annulus, and also influence the change in hydrostatic pressure that is discussed in section 4.1.3.7. Through testing with conventional drilling, the density has been regarded as having a *"relatively small effect on the surge pressures"* (Lal, 1983).

For simplicity, altering of fluid properties due to change in pressure or temperature is neglected in this thesis. This also means that fluid compressibility is neglected. Neglecting the compressibility is regarded as a conservative assumption, because it eliminates the slowing "buffer effect" of a high fluid column. For deep wells, like the Macondo well, pipe movement in the shallow parts of the wellbore will not generate as high a pressure at the bottom of the well as when moving the BHA at the wellbore depth. In addition "*the lack of fluid compressibility is considered a conservative assumption because it predicts a higher flow rate, which generates a higher frictional pressure drop*" (Mitchell, 1988).

4.1.3.6 Borehole and drillpipe properties

Both the borehole and the drill pipe are elastic to some extent. As the pressure varies, the borehole will either expand or contract, and therefore change the volume of the bore hole. The same thing happens with the drill pipe. These changes in volume will alter the cross sectional area of the annulus, and hence change the frictional pressure loss. These effects have been considered negligible in this thesis.

Other annulus features that will affect the flow, for example the drill string joints and other irregularities on the drillpipe, the tortuosity in the wellbore and similar properties, are also neglected. In most cases including these properties will give a higher frictional pressure loss, because the normal assumption of a plain pipe will estimate a smooth flow in whole of the annulus. Still, mathematical modelling of these properties has been regarded as unnecessary complicated, with an effect not great enough.

4.1.3.7 Change in the fluid interface depth in the riser

When tripping with conventional drilling equipment, the added drill string body will cause the mud in the annulus to run over its top and pour into the put pit (assuming that the annulus was brim-full as the pipe was completely out of the hole). This will not change the hydrostatic pressure from the mud column, because the same height of hydrostatic communication from the RKB to the bottom of the hole will be present.

When tripping with DGD and the BHA is below the fluid interface level, the added pipe body will cause the fluid interface in the riser to become shallower. This increases the hydrostatic part of the mud pressure in the well, because the heavy mud makes up a larger part of the wellbore annulus depth. However, the effect can be mitigated by adjusting the fluid interface depth with the subsea- and booster pump, keeping it at a constant level.

In section 4.2.4.2 it will be demonstrated how the pumps could be controlled to eliminate this effect, and keep the hydrostatic part of the wellbore pressure stable.

4.1.4 Potential problems caused by Surge and Swab

If the BHP is not kept within the mud pressure window, it is likely that the well becomes unstable. In environments like the GoM, the mud pressure window is often very narrow, and therefore the surge and swab pressure changes caused by pipe movements could easily bring the pressure outside the mud window.

Problems and consequences resulting from surge and swab will be simulated and discussed in more detail later in the thesis.

4.2 Analytical modelling of Surge and Swab

4.2.1 Choice of hydraulic model for Surge and Swab analysis

Models for both a concentric and an eccentric annulus have been developed. Studies have shown that the surge and swab effects in an eccentric annulus is reduced by around 40% compared to that of an concentric annulus (Srivastav, et al., 2012). However, because the Macondo well was a vertical well, only a concentric annulus will be considered in this thesis. A concentric annulus will also be a better guidance for the most critical surge and swab, the most conservative situation.

4.2.2 Literature review

Studies made in the 1930s stated that "*most blow-outs in rotary drilling occur when the drillpipe is being withdrawn from the hole*" and further that "..*pressure reductions of over 400 psi were observed*" (Cannon, 1934). Mud properties were stated as the most important parameter of influence to the pressure changes; with gel strength being the most influential. (Goins, et al., 1951) supported much of the previous findings, and it was stated that 14 of 22 instances of lost circulation in an example well could be associated with pipe movements in the wellbore.

The first analytical model describing the effects of surge and swab pressure was proposed by (Burkhardt, 1961), who divided the pressure resulting from pipe movements into three parts; inertial effects, breaking of mud gel and viscous drag. Thus, the model takes the unsteady phase into consideration, but not the elasticity of the pipe, nor the compressibility of the borehole wall or the drilling fluids. However, the greatest weakness with this model is that it is based on the assumption that the drilling fluids behave like Bingham fluids. This makes the model inaccurate, because the Power-Law (PL) model and the Yield-Power-Law (YPL) model often provide a more accurate description of the drilling fluid behaviour. Therefore, this model is not used here.

In 1974 it was concluded that "…*control of instantaneous drill string speed while tripping and making connections is necessary to minimize pressure changes downhole*" (Clark, et al., 1974),

suggesting that the most important periods during tripping was in the acceleration (and deceleration) phases, rather than the periods with average or stationary velocity. This conclusion has been taken into consideration when modelling the pressure changes in this thesis, and an extra correction factor has therefore been included, as will be discussed in section 4.2.4.3.

One of the first models that recognized the compressibility of the fluid and borehole expansion as important parameters was presented in (Lal, 1983). The model, which was based on the findings of A. Lubinski in 1977, also considers the effect of several other parameters, including hole geometry and different bit sizes and types. (Lal, 1983) also recognized the tripping depth, relative to the total well depth, as an parameter. A useful equation for this model has not been obtained, and therefore the model has not been utilized in the thesis.

(Mitchell, 1988) integrated the effects of pipe-, formation- and cement elasticity and temperature effects on the drilling fluids into a model. It was here concluded that for deep wells, steady-state models often tended to overestimate the magnitude of the surge pressure, and it was shown clear discrepancies between measured data and the results of the model presented by (Burkhardt, 1961).

Other models were developed during the 1990s and early 2000s (Rommetveit, et al., 2005) and (Wagner, et al., 1993). These models included temperature effects to the rheology and the effect of well deviation causing eccentric wellbore annuli. These models have been considered too complicated and accurate for the scope of this thesis, and are hence not utilized.

A steady-state model for YPL fluids was developed and presented in (Crespo, et al., 2010). This is a *"narrow slot model"* which assumes that the flow in the wellbore annulus behaves like flow between two parallel plates, where the one plate is moving; illustration of this can be seen in Figure 14. The steady-state model has been thoroughly tested and found to be more accurate than the previously developed models for Power-Law and Bingham fluids. Through testing, the model has shown its ability to clearly include the effects of the different important parameters. The effect of each isolated parameter is shown; including tripping speed, annulus width and fluid yield stress.

The model presented in (Crespo, et al., 2010) has been chosen as the model to base the simulations in this thesis on. Equations are openly available, and the assumptions made are in line with the assumptions made in this thesis. The model is also simple, but effective, and because the main point in this thesis is to analyse the DGD system, and not to calibrate a hydraulic model, a model without the more advanced features shown in other models have been preferred.

4.2.3 Equations used for modelling

The selected model uses 6 equations for calculating 5 dimensionless coefficients. The equations used for are listed below (Crespo, et al., 2010):

$$\phi_1 = A{\phi_2}^B{\phi_3}^C(\phi_4 + D)^E{\phi_5}^F \quad \textbf{Eq. 4.2}$$

$$\phi_1 = \frac{H}{k}\left(\frac{H}{V_p}\right)^n \frac{\Delta P}{\Delta L} \quad \textbf{Eq. 4.3}$$

$$\phi_2 = \frac{\rho H^n {V_p}^{2-n}}{k} \quad \textbf{Eq. 4.4}$$

$$\phi_3 = \frac{W}{H} \quad \textbf{Eq. 4.5}$$

$$\phi_4 = \left(\frac{H}{V_p}\right)^n \frac{\tau_o}{k} \quad \textbf{Eq. 4.6}$$

$$\phi_5 = n \quad \textbf{Eq. 4.7}$$

Where

ΔP = Pressure change created by the motion (bar / Pa)

ΔL = Length of the pipe in motion (m)

H = Height of the annulus flow slot (thickness of annulus); as seen in Figure 14 (m)

W = Circumference of the wellbore annulus (m)

ρ = The density of the fluid ($\frac{kg}{m^3}$)

n = Fluid behaviour index ($-$)

τ_o = Fluid shear stress (Pa)

k = Fluid consistency index ($Pa \cdot s^n$)

V_p = Velocity of the pipe in motion ($\frac{m}{s}$)

The factors H and W used in Eq. 4.5 are calculated as:

$$H = \frac{ID_{hole} - OD_{pipe}}{2} \qquad \textbf{Eq. 4.8}$$

$$W = \frac{\pi}{2}\left(ID_{hole} + OD_{pipe}\right) \qquad \textbf{Eq. 4.9}$$

When doing simulations, values for H and W are found for each wellbore section with varying hole or pipe diameter.

The empirically found correlation constants of Eq. 4.2 are defined in Table 1. These values were obtained after performing regression analysis of the model (Crespo, et al., 2010).

Table 1: Correlation Constants for Different Rheological Models

Fluid Rheological Model	A	B	C	D	E	F
Power-Law	0.267	-0.068	1.497	0.001	-0.032	0.702
Bingham Plastic	0.041	0.001	1.842	3.900	0.919	-4.076
Yield-Power-Law	0.351	0.096	2.403	0.833	1.806	-4.106

To find the pressure change during tripping, Eq. 4.2 and Eq. 4.3 are merged and solved for ΔP. The result is shown in Eq. 4.10.

$$\Delta P = \frac{\phi_1}{\frac{H}{k}\left(\frac{H}{V_p}\right)^n}\Delta L$$

$$\Delta P = \frac{A * {\phi_2}^B * {\phi_3}^C * (\phi_4 + D)^E * {\phi_5}^F}{\frac{H}{k}\left(\frac{H}{V_p}\right)^n}\Delta L \qquad \textbf{Eq. 4.10}$$

As visible from Eq. 4.10, the pressure change has a linear relation to the length of drillpipe exposed to the fluid, when keeping the other parameters constant.

4.2.4 Calibrations of the of the model

4.2.4.1 Dependence on pipe velocity

When checking the effect of the velocity, V_p, it turned out that the model returned a rising value for ΔP the lower V_p got, when V_p<$0.4 m/s$. This was alarming, since the logical sense implicates $\Delta P = 0$ when $V_p = 0$. Therefore, the mathematical dependence of V_p in $\Delta P\left(V_p\right)$ was tested.

By writing out the equations dependent of V_p as a parameter into Eq. 4.10, Eq. 4.11 is derived. Equations for parameters not depending on V_p are not written in full length, but are kept as previously shown.

$$\Delta P = \frac{A * \left(\frac{\rho H^n {V_p}^{2-n}}{g_c k}\right)^B * {\phi_3}^C * \left(\left(\frac{H}{V_p}\right)^n \frac{\tau_o}{k} + D\right)^E * {\phi_5}^F}{\frac{H}{k}\left(\frac{H}{V_p}\right)^n} \Delta L \qquad \textbf{Eq. 4.11}$$

By singling out all the factors containing V_p, Eq. 4.12 is achieved.

$$\Delta P = \frac{A * \left(\frac{\rho H^n}{g_c k}\right)^B \left({V_p}^{2-n}\right)^B * {\phi_3}^C * \left(\left(\frac{H}{V_p}\right)^n \frac{\tau_o}{k} + D\right)^E * {\phi_5}^F}{\frac{H^{n+1}}{k}\left(\frac{1}{V_p}\right)^n} \Delta L \qquad \textbf{Eq. 4.12}$$

By further separating V_p in Eq. 4.12, the below shown equations are gotten.

$$\Delta P = \frac{A * \left(\frac{\rho H^n}{g_c k}\right)^B \left({V_p}^{2-n}\right)^B * V_p^n * {\phi_3}^C * \left(\left(\frac{1}{V_p}\right)^n H^n \frac{\tau_o}{k} + D\right)^E * {\phi_5}^F}{\frac{H^{n+1}}{k}} \Delta L$$

$$\Delta P = K_*\left({V_p}^{2-n}\right)^B * {V_p}^n * \left(\frac{1}{{V_p}^n} K_{**} + D\right)^E$$

And by further deriving, Eq. 4.13 is found.

$$\Delta P = K_* * {V_p}^{2B-nB+n} * \left(\frac{1}{{V_p}^n} K_{**} + D\right)^E \qquad \textbf{Eq. 4.13}$$

Here

$$K_* = \frac{A * \left(\frac{\rho H^n}{g_c k}\right)^B * {\phi_3}^C * {\phi_5}^F}{\frac{H^{n+1}}{k}} \Delta L \qquad \textbf{Eq. 4.14}$$

$$K_{**} = H^n \frac{\tau_o}{k} \qquad \textbf{Eq. 4.15}$$

Both Eq. 4.14 and Eq. 4.15 are made up of positive numbers, resulting in $K_*>0$ and $K_{**}>0$.

For $\lim_{V_p \to 0}\left[f(V_p) = V_p^n\right] = \infty$, when $n < 0$. In the same way, ΔP will be rising towards infinity for low values of V_p if the net exponent of V_p is negative in Eq. 4.13.

For ΔP in Eq. 4.13 not to increase when $V_p \to 0$, "$2B - nB + n$" must be positive, and at the same time, the contribution to the exponent of V_p from the term $\left(\frac{1}{{V_p}^n} K_{**} + D\right)^E$ must not give a net exponent lower than zero for V_p in $\Delta P(V_p)$. Because $0<n<1$ (from the definition of the YPL fluid model (Skalle, 2010)); "$2B - nB + n$">0 when B>0, which it is from the definition of B seen in Table 1. Therefore, E is identified as the parameter that could give a negative exponent to V_p. By trial and error, the value of $E = 0.400$ has been found to give values of ΔP that are in line with examples shown in (Crespo, et al., 2010). This reduction in parameters is hence made to calibrate the model used to the well and the fluid used on the Macondo well.

With the use of $E = 0.400$, the example values of surge and swab shown in Figure 15 is achieved.

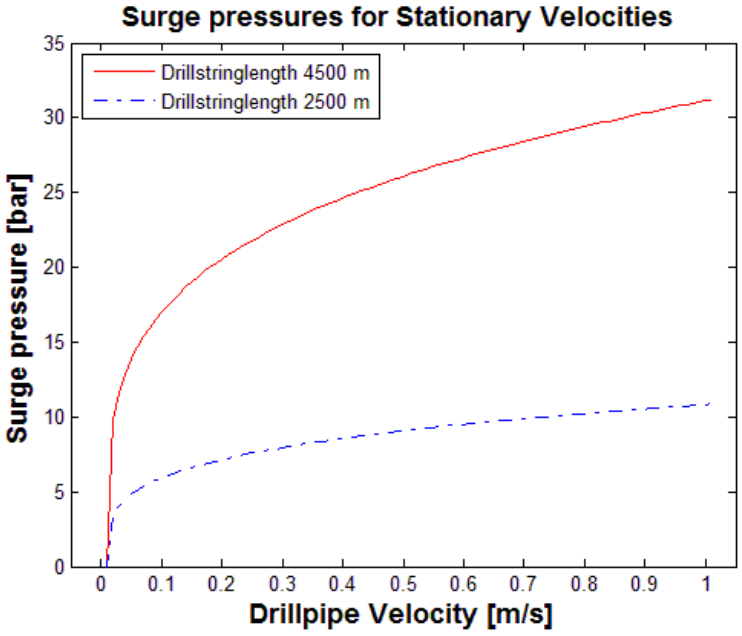

Figure 15: Surge pressure for different pipe velocities

Because no calibration or field testing of the model is possible on the Macondo, it is impossible to know for certain exactly how accurate the model is. However, based on comparison with various field data studies described in section 4.2.2, the results presented in Figure 15 seems likely, and probably are they not far from real values.

4.2.4.2 Adjusting for the use of dual gradient drilling

All of the models presented in section 4.2.2 are made for conventional drilling. Therefore, the models are assuming a wellbore annulus that is filled with a uniform density drilling mud from the bottom of the wellbore to the top of the riser. When running in hole, the annulus can never be "fuller than full", which implicates that as the drillstring body is taking up space in the wellbore, the displaced mud is overtopping the annulus and pouring into the mud pits. When pulling the drillstring out of the hole (tripping out) the conventional annulus is assumed to be constantly refilled by the drilling fluid to cover up for the lost volume of the drillipipe. The hydrostatic part of the BHP is therefore assumed constant, without change in height or density.

When drilling with dual gradient drilling, this will be different. If the subsea pump and the booster pump are shut-off, the fluid interface depth in the drilling riser will change as the drill string body is lowered into the wellbore below the fluid interface level, as illustrated in Figure 16. This change of the fluid interface depth will also change the BHP, and this effect is therefore added manually in this thesis to the selected model.

An example shows that when tripping 27 m of a 5.0" drill pipe into a casing with a 19.5" ID, drillpipe volume of V_{add} is added as shown below:

$V_{add} = A_{cross-section} * L = \frac{\pi}{4} * 5.0^2 \frac{1}{(12*3.28)^2} * 27m^3 = 0.3422m^3$. This gives a change in depth ΔH of the fluid interface in the riser of $\Delta H = \frac{V_{add}}{A_{cs,riser}} = \frac{0.3422m^3}{(0.1801m^2)} = 1.90m$

Hence (when using a drilling mud with $\rho_{mud} = 1850 \frac{kg}{m^3}$ and seawater with $\rho_w = 1030 \frac{kg}{m^3}$ in the DGD system) a pressure change ΔP as shown below is experienced:

$\Delta P = (\rho_2 - \rho_1) * g * \Delta H = (1850 - 1030) * 9{,}81 * 1.90 * \frac{1}{10^5} bar = 0.153bar.$

When tripping multiple stands of 27 meters, this pressure change will add up significantly, and this pressure change has been adjusted for when implementing the model in the simulator.

To compensate for this increase, the added volume, $V_{add} = 0.3422m^2$, must be removed by the subsea pump (or added by the booster pump when pulling out) equally fast. With a velocity of 0.2m/s, tripping one stand takes approximately $\Delta t = \frac{27m}{0.2\frac{m}{s^2}} = 135s$. With a velocity of 1m/s, it takes approximately 30 seconds, including the acceleration phase.

The required average pump rates to compensate for the increased hydrostatic pressure will therefore be:

$$Q_{sp,req} = \frac{0.3422m^3}{135s} = 0.0025\frac{m^3}{s} = 152LPM$$

and

$$Q_{sp,req} = \frac{0.3422m^3}{30s} = 0.0114\frac{m^3}{s} = 684LPM$$

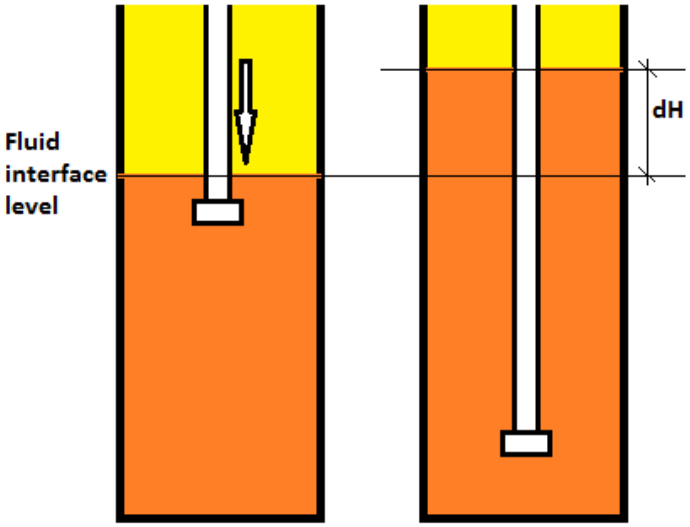

Figure 16: Change in fluid interface depth

4.2.4.3 Adjusting for transient pipe movements

The most important part of pipe movements is in the unsteady parts (Clark, et al., 1974). Because the selected model is a steady-state model, which does not include the effect of unsteady pipe movements, this has been added as a correction factor.

In the right hand side of Figure 17 (Mitchell, 1988), an example of difference in estimated pressure changes from a dynamic and a steady-state model is shown. The left hand side of Figure 17 shows the velocity profile of the pipe. The negative acceleration at the start is when the pipe is lifted up and out of the slips, before being run down into the well. In the early acceleration phase, the steady-state model clearly under predicts the real pressure changes. The 'steady pressure' in the right hand side of Figure 17 shows a minimum value of approximately $-48psi$, while the measured data shows approximately $-212psi$. Hence, the stationary model under predicted the real value by a factor of $\frac{-212}{-48} = 4.42$ in the acceleration phase.

Figure 17 also show that, while running the pipe into the hole at a positive speed, a negative surge pressure can still be experienced, due to a negative acceleration. In the simulation, this will be included in the model by adding a correction factor to the calculated pressure at negative acceleration. This negative surge comes as a result of the inertia of the mass of the already moving fluid, as discussed in section 4.1.1.2.

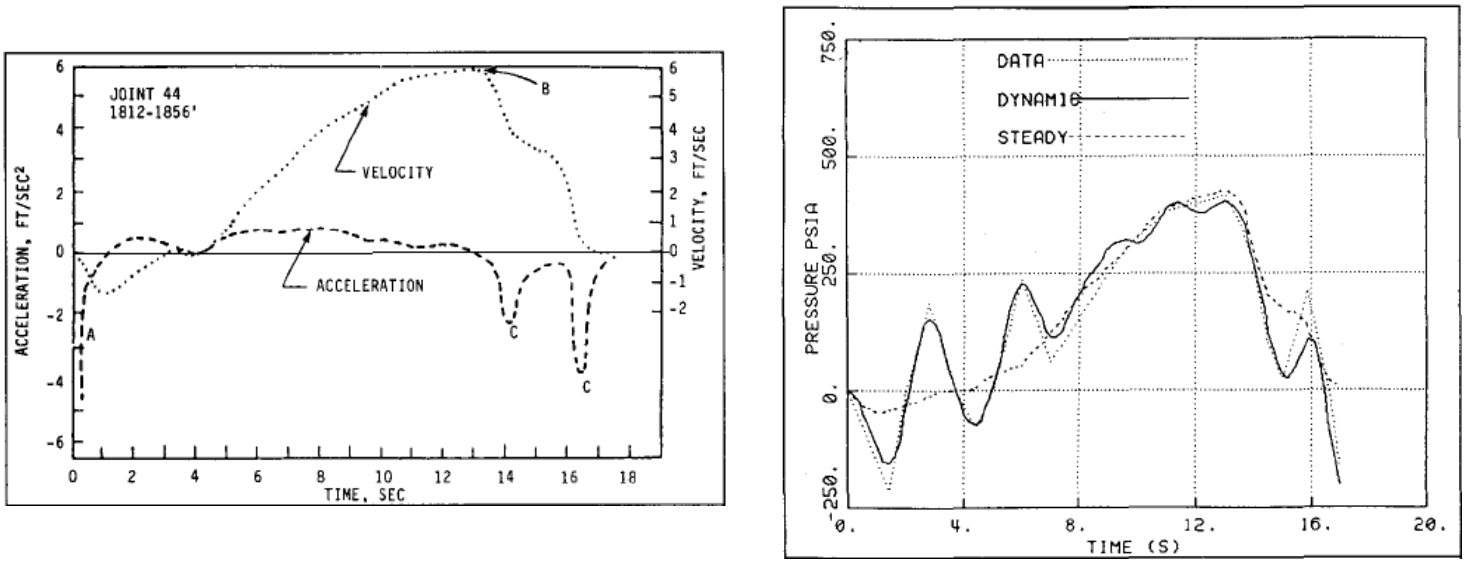

Figure 17: Velocity profile and corresponding surge/swab pressure

These findings were later supported, as an example in Figure 18 (Samuel, et al., 2003) shows. Here, the steady state pressure during the last few seconds is approximately $35psi$ $(1793 - 1758)psi$, while the measured data shows a pressure swab of $86psi$ $(1793 - 1707)psi$. This means an under prediction by the stationary model by a factor of $\frac{86psi}{35psi} = 2.46$ in the acceleration phase.

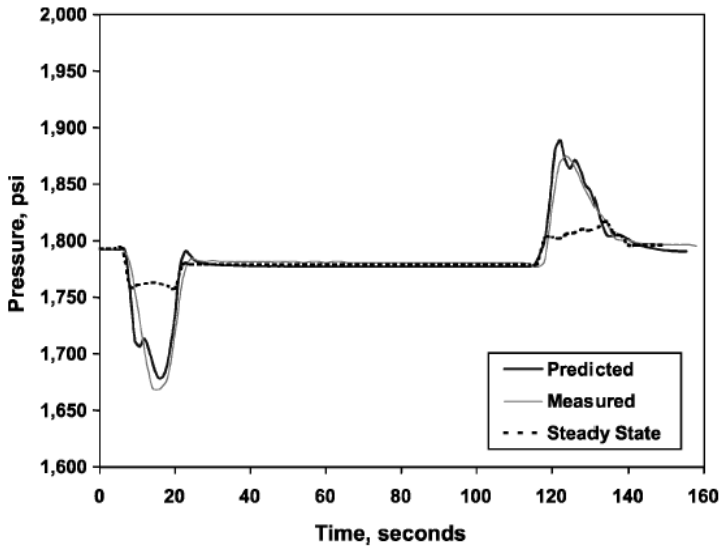

Figure 18: Surge/Swab pressure.

Based on these two examples, a correction factor $F_{corr,acc} = \frac{4.46+2.46}{2} = 3.46$ for the acceleration phase of the tripping movement seems likely, and is what will be used in this thesis.

When $a > 0$ the adjusted pressure will be calculated as shown in Eq. 4.16.

$$\Delta P_{adjusted} = \Delta P_{model} * (1 + a * F_{corr,acc})) \quad \textbf{Eq. 4.16}$$

where a is the acceleration of the pipe. Early testing of Eq. 4.16 for tripping when $a < 0$, showed that to get a realistic effect of the negative pressure that can be created in the well, Eq. 4.17 had to be used when $a < 0$.

$$\Delta P_{adjusted} = \Delta P_{model} * a * F_{corr,acc} \quad \textbf{Eq. 4.17}$$

Hence, if $a < 0$, the resulting $\Delta P_{adjusted}$ will be negative, but reduced, magnitude depending on the acceleration.

These adjustments have been included in the program code for the acceleration phase of the movement. To include this factor is important because the acceleration phase represents the pressure spikes, which in turn represent the most critical moments when it comes to controlling the wellbore pressure. Eq. 4.16 and Eq. 4.17 have proven to give fairly sensible results in the test examples.

4.2.4.4 Oversensitivity regarding hole ratio

By inspection of Eq. 4.5 and Eq. 4.10, it is observed that the exponent C has a great influence on the effect of the hole diameter ratios. When testing the simulator, the value of $C = 2.403$ proved to be somewhat too high for the Macondo well, as the surge pressure simulated in the well skyrocketed when the BHA entered the casing, ending up at around 150bar at TVD. This is shown Figure 19; the pressure surge experienced in the wellbore at a constant tripping speed, as a function of depth of the BHA. The small pressure step-up just before the major incline starts is due to the BHA entering the wellbore, which reduces the slot flow annulus, and increases the friction pressure loss.

On the basis of these findings, the value of C has been reduced to $C = 1.650$. Running the same simulation again, the reduced value of C reduces the pressure surge significantly, to a more realistic level.

The value $C = 1.650$ has been chosen on the background of comparing results with those found in previous literature. Data from tests performed in (Lal, 1983) show that a 4724mMD wellbore, with a $9^{7}/_{8}$" casing shoe set at 4267mMD, experienced a maximum pressure surge of 29.4bar when tripping in at a velocity of $0.6\frac{m}{s}$. By trial and error, the value of $C = 1.650$ was found to give similar results for the same input data. This is shown Figure 20. $C = 1.650$ also lies close to the value used for the P-L model, as viewed from Table 1, which is a similar model to YPL model.

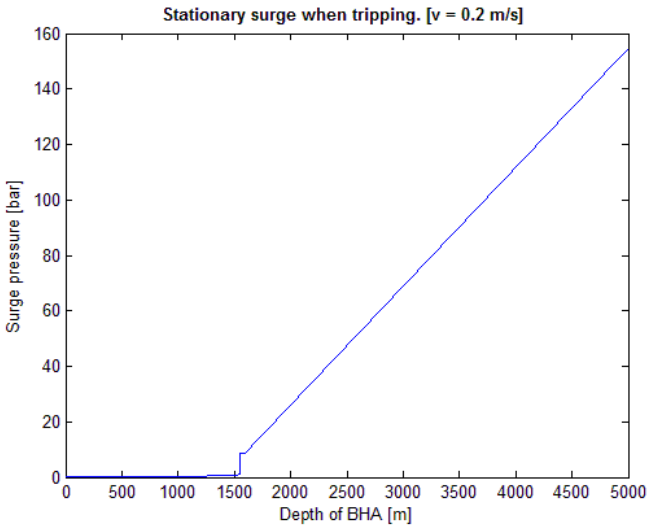

Figure 19: Adjusting C. C=2.403

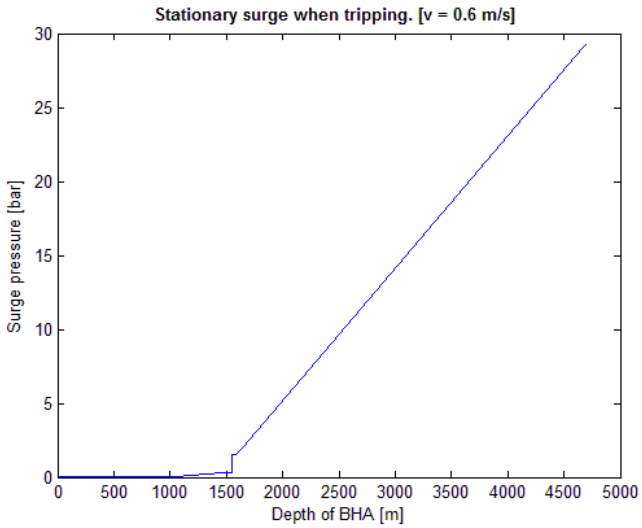

Figure 20: Adjusting C. C=1.650

4.3 Limitations in pressure control with DGD

Ideally one would like to control the wellbore pressure 100% accurately and keep the BHP at a constant level during every situation in a well. When using open DGD, this is not always possible, for example when moving the pipe in the hole; when tripping, and when the drill pipe is kept in the slips in the drill floor, moving up and down in the hole along with the sea heave.

An example of a tripping motion is gotten from the measured field data shown in Figure 21 (Wagner, et al., 1993); pressure is first changing from 6625psi to 6522psi in 15 seconds (blue lines); a pressure changing rate of $\frac{\Delta P}{\Delta t} = -6.87\frac{psi}{s} = -0.47\frac{bar}{s}$. Nearly the same (with an opposite sign) can be viewed later in the same field data, where the pressure increases from 6503psi to 6580psi in 11 seconds; which gives a rate $\frac{\Delta P}{\Delta t} = 7\frac{psi}{s} = 0.48\frac{bar}{s}$. The average tripping speed in this example was $1.8\frac{ft}{s} = 0.55\frac{m}{s}$. Another example shows how the measured pressure increases from 1776psi to 1875psi during 7.4 seconds of pulling the drillpipe out as shown in Figure 22 (Samuel, et al., 2003); a change of $\frac{\Delta P}{\Delta t} = 13.4\frac{psi}{s} = 0.90\frac{bar}{s}$. Below, calculations to find the required subsea- or booster pump rates to compensate for this sudden pressure change is presented.

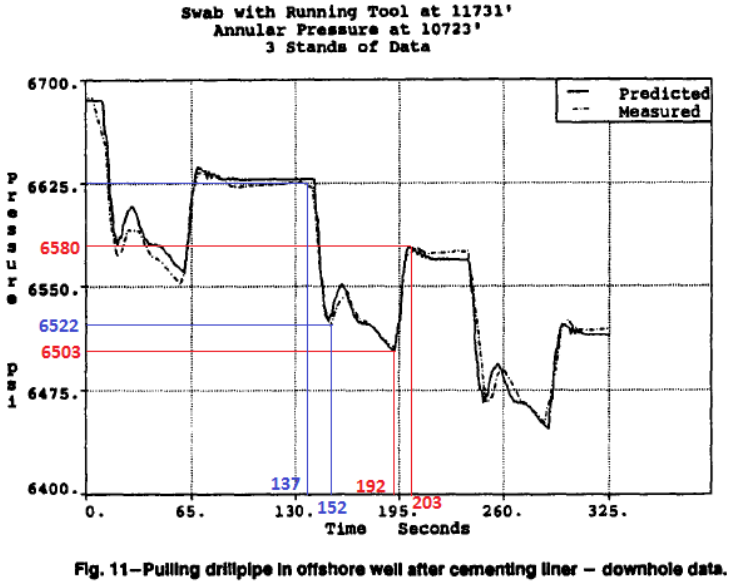

Fig. 11—Pulling drillpipe in offshore well after cementing liner — downhole data.

Figure 21: Pressure changes

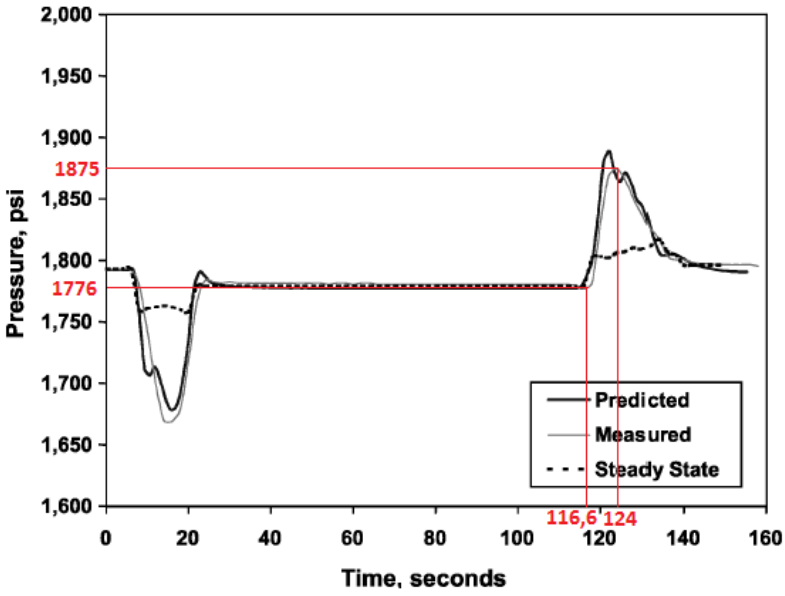

Figure 22: Pressure changes – 2

When changing the pressure by altering the depth of the fluid interface, the pressure change per time is expressed as:

$$\frac{\Delta P}{\Delta t} = (\rho_2 - \rho_1) * g * \frac{\Delta D_{fi}}{\Delta t} \qquad \textbf{Eq. 4.18}$$

When using a standardized ocean drilling riser with an ID of 19.5" and 5" drill pipes, the A_{cs} is calculated with Eq. 2.4:

$$A_{cs,annulus} = \frac{\pi}{4}(19.5^2 - 5^2)in^2 \frac{1}{\left(12\frac{in}{ft}\right)^2 * \left(3.28\frac{ft}{m}\right)^2} = 0.1801m^2$$

From Eq. 4.18 the required average velocity of the fluid interface depth change, $\frac{\Delta D_{fi}}{\Delta t}$, is found, and the required volume change rate in the riser annulus, Q_{pump}, is derived by rearranging Eq. 4.18, and multiplying with the cross sectional area on both sides, which gives Eq. 4.19

$$\frac{\frac{\Delta P}{\Delta t}}{(\rho_2 - \rho_1) * g} * A_{cs} = \frac{d_{fi}}{dt} * A_{cs}$$

$$Q_{pump} = \frac{\frac{\Delta P}{\Delta t}}{(\rho_2 - \rho_1) * g} * A_{cs} \qquad \textbf{Eq. 4.19}$$

When using drilling fluids with densities $\rho_1 = 1030\frac{kg}{m^3}$ and $\rho_2 = 1850\,\frac{kg}{m^3}$, the required subsea pump rate for the examples presented above becomes

$$Q_{pump} = \frac{-0.47\,\frac{bar}{s}}{(1850 - 1030)\,\frac{kg}{m^3} * 9.81\,\frac{m}{s^2}} * 0.1801m^2$$

$$Q_{pump} = -1.06\,\frac{m^3}{s} = -63\ 629LPM$$

And when the pressure change is $0.84\,\frac{bar}{s}$, the required pump rates becomes

$$Q_{pump} = 1.88\,\frac{m^3}{s} = 112\ 995LPM$$

These high pump rates are clearly impossible to create in the subsea pump or the booster pump of a DGD system. Pumps are normally designed to give a maximum rate of ≈5000-7000 LPM, and even though multiple pumps are possible to use theoretically, and hence a very large pump rate is achievable, the total required power to run the pumps would be immense.

On the basis of these calculations, it is concluded that a DGD system without a backpressure possibility, which is what is simulated in this thesis, cannot keep the BHP completely constant during pipe movements.

However, it is possible to optimize the hydrostatic wellbore pressure using DGD, to keep the well as stable as possible and within the drilling window when doing different operations. By predicting how the pressure will behave during an operation, the hydrostatic BHP can be controlled so that the possible consequences of the pressure variations, which are impossible to counteract, are mitigated. This will be the focus of the simulations in chapter 5.

4.4 Formation fluid influx and fluid losses to the formation

When the wellbore pressure varies, it could go outside the mud pressure window. This would cause influx of formation fluid to the wellbore. Influx to the formation used in the simulator has been assumed as linear with relations to pressure deviation from the fracture pressure, as shown in Eq. 4.20, for the situation when $P_{mud} < P_{pore}$.

$$Q_{influx}(P_{mud}) = PI * \left(P_{pore} - P_{mud}\right) \qquad \textbf{Eq. 4.20}$$

Losses to the formation, when $P_{mud} > P_{frac}$, have been defined as shown in Eq. 4.21.

$$Q_{mudloss}(P_{mud}) = PI * (P_{mud} - P_{frac}) \quad \textbf{Eq. 4.21}$$

"*The main reservoir in the Macondo prospect well consist of two oil bearing sands. (…) Based on 300 mD and 86ft net pay, the influx performance curve indicates a productivity index of 49 stb/d/psi. For pressures above the bubble point pressure*" (add wellflow as, 2010). The estimation of the productivity index, PI, has been based on this information. For simplicity, and because it for most cases is the most realistic, the pressure will be assumed to always be above the bubble point pressure. (Even though the situation simulated here does not involve drilling through the reservoir section of the well, it has here been assumed that the formation described here behaves as the real Macondo reservoir.)

By converting into SI-units as shown below, the result in Eq. 4.22 is achieved, and has been used for calculations in the simulation.

$$PI = 49\frac{bbl}{day * psi} * \frac{14.5\frac{psi}{bar}}{6{,}28\frac{bbl}{m^3} * \frac{24 * 3600s}{day} * 10^5\frac{Pa}{bar}}$$

$$PI = 1.308 * 10^{-08}\frac{m^3}{s * Pa} \quad \textbf{Eq. 4.22}$$

As an example, a pressure drop of 20 bar below the pore pressure will cause a formation influx rate of 1570LPM as shown below.

$$1.308 * 10^{-08}\frac{m^3}{s * Pa} * \frac{60 * 10^3 LPM}{\frac{m^3}{s}} * 20bar\frac{10^5 Pa}{bar} = 1570LPM$$

5. Simulations and Results

5.1 The simulated situation

The situation investigated here is described as follows:

- Cased hole from wellhead on seabed to casing shoe @ 5240mTVD, with casing properties: P-110 $9^7/_8$" #47.00 (ID: 8,681" (Bourgoyne, et al., 1986))
- Open hole: 8 ½" hole drilled through $9^7/_8$" shoe cement, to depth of 5260mTVD

The situation is thought of as prior to drilling into the reservoir section of the Macondo well, after the casing is set, and the casing shoe tested. The depth of the $9^7/_8$" casing is found through

graphical investigation of the pore- and fracture pressure curves of the Macondo well (add wellflow as, 2010).

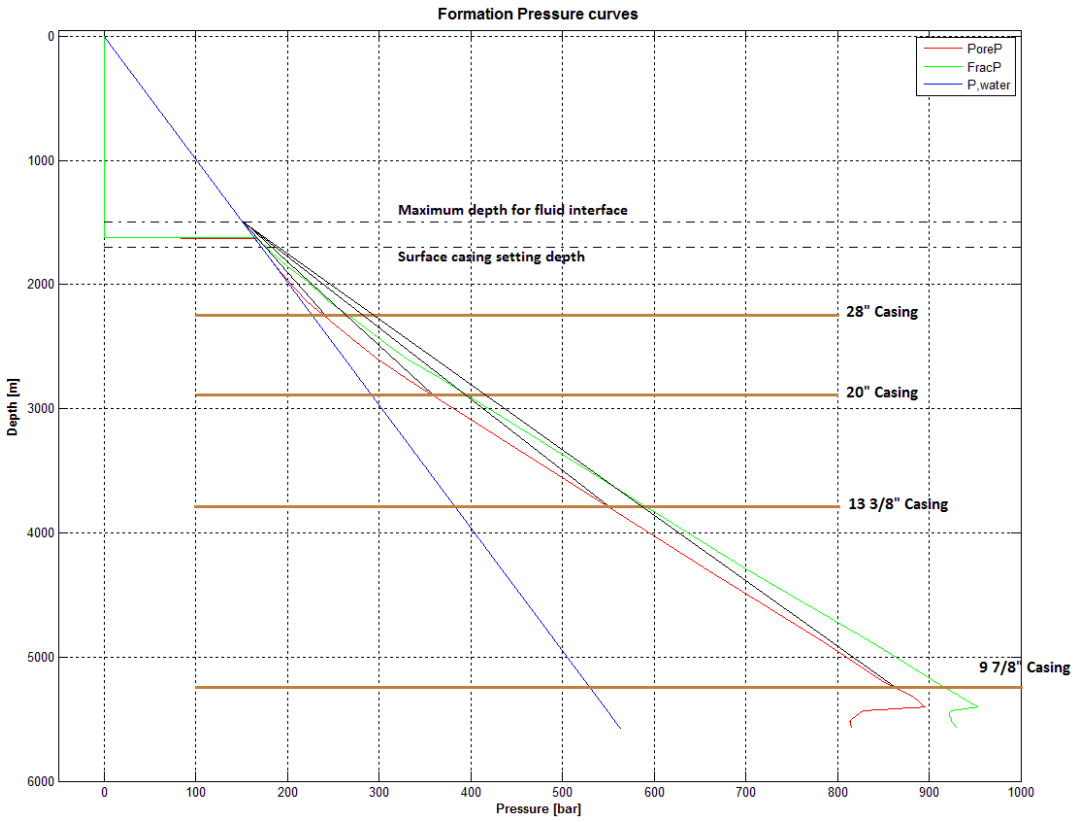

Figure 23: Casing setting depths.

Figure 23 shows the result. It is a coincident that the depth of the $9^{7}/_{8}$" casing is roughly the same as the casing setting depth done on the real Macondo well, which was 5234mTVD (BP, 2010). Even though this example is inaccurate, it is a good example of the improvement that can be made to a casing setting program by using DGD instead of conventional drilling. Here, 5 casing strings are used, while 8 were used in the field on Macondo.

The focus of this report is not to find the exact DGD casing program for the Macondo well, and therefore, a graphical solution has been considered good enough, even though a full mathematical analysis would give more accurate results. The casing sizes have been chosen partly from the casing program used when drilling Macondo, along with a conventional casing program. The setting depth of the surface casing is the same as used when drilling the Macondo well (BP, 2010). Even though liners were used when drilling Macondo, full casing lengths, from the setting depth to the wellhead, has been assumed here.

5.1.1.1 Why the choice of this situation

The Macondo reservoir formation has layers with highly reduced pore- and fracture pressure at around 5400mTVD, as can be seen as a sudden drop in the curves in Figure 23. Under those reduced pressure gradient formations, lay formations in a more normal pressure situation. This creates an extremely narrow pressure window, because the fracture pressure falls down, closer to the formation pressure. Drilling through this reservoir interval of varying pressure is very difficult.

How to best utilize DGD to control the pressure when drilling through that highly challenging interval is not the main focus of this thesis, and therefore the situation investigated here is assumed to be before penetrating the extremely narrow pressure window. Utilization of DGD when drilling through the narrow pressure window at Macondo has been discussed in more detail in previous literature (Tonning, 2011).

5.1.1.2 Pressure margins

Normally when drilling, an extra added safety margin in the mud window is used to keep the pressure well away from the mud window boundaries. Margins often used in the drilling industry are $30\frac{kg}{m^3}$ above the pore pressure, and $10\frac{kg}{m^3}$ below the fracture pressure (Sangesland, 2012). This way of denoting a pressure margin is understood as "the pressure that the specified margin density exerts at the current depth if it was a fluid". This means that the minimum allowed BHP is found by Eq. 5.1 and the maximum allowed BHP is found by Eq. 5.2. These values are shown in the graphs as dotted lines, and denoted as "P-fracture-m" and "P-pore-m".

$$BHP_{min} = P_{pore} + 30\frac{kg}{m^3} * TVD * g \qquad \textbf{Eq. 5.1}$$

$$BHP_{max} = P_{fracture} - 10\frac{kg}{m^3} * TVD * g \qquad \textbf{Eq. 5.2}$$

Because formation strength is regarded to increase with depth, the weakest point in the open hole is assumed to be at the casing shoe; the shallowest part of the open hole section. It is this depth that is investigated for reactions to the pressure fluctuations.

5.1.1.3 Further assumptions and underlying data

- Wellbore data for the examples simulated
  - Casing: P-110 $9^7/_8$" #47.00 (ID: 8,681" (Bourgoyne, et al., 1986)) @ 5240mTVD
  - Open hole: 8 ½" hole drilled through $9^7/_8$" shoe cement, to depth of 5260mTVD
- Pressure Safety Margins
  - 0.01sg below fracture pressure when drilling/circulating
  - 0.03sg above pore pressure when drilling/circulating

    - Hydrostatic pressure not less than 5 bar above pore pressure
- Drilling fluids
    - Light fluid: $\rho_1 = 1030\frac{kg}{m^3}$
    - Heavy fluid: $\rho_2 = 1850\frac{kg}{m^3}$
    - No circulation through the drillstring when tripping
- Pump capacities (based on previously described technology)
    - $Q_{max,subseapump} = Q_{max,booster\ pump} = 6000LPM$
    - $Q_{min,subseapump} = Q_{min,booster\ pump} = 100LPM$
- Drillstring movement
    - Acceleration: $a = 0.1\frac{m}{s^2}$
    - Velocity when at constant speed: $v = 0.2\frac{m}{s}$
- Drillstring tally
    - Reverse safety valve placed in drillstring, making hydraulic U-tubing from annulus and up the drillstring impossible.
    - BHA
        - Length: 50m.
        - OD: 6”
    - Drillstring
        - OD: 5”
        - Pipe joints are neglected
    - One stand equals 3 drill pipe joints, each of 9 metre, a total of 27metres.

5.2 Simulating: Tripping drillpipe into the hole

This case shows the wellbore pressure surges as the drill pipe is being run into the hole, and more importantly, how to compensate for the surges by changing the hydrostatic pressure.

5.2.1.1 Calculating start data

The P_{hyd} at the start of the situation is here set to be 15 bar above the BHP_{min}. This has been chosen because it brings the BHP to the middle of the pressure window, with the largest clearance to both the formation pressure and the fracture pressure. At still-stand, with only the hydrostatic pressure contributing to the BHP, this has been regarded optimal.

By reading from the simulated examples, or from Figure 23, the pore pressure at $TVD = 5240m$ is found to be 861.2bar. Using Eq. 5.1 and adding 15 bar, the start pressure at the shoe is found to be:

$$P_{shoe} = 861.2bar + 30 * 9.81 * 5240Pa\frac{1bar}{10^5Pa} + 15bar = 891.6bar$$

From the calculated P_{shoe}, the D_{fi} is found. Solving Eq. 2.2 for D_{fi} produces Eq. 5.3.

$$D_{fi} = \frac{BHP - P_{friction} - TVD * g * \rho_2}{(\rho_1 - \rho_2) * g} \qquad \textbf{Eq. 5.3}$$

$P_{friction} = 0$ at still-stand, and therefore, D_{fi} can be found as

$$D_{fi} = \frac{891.6bar\frac{10^5 Pa}{bar} - 0 - 5240m * 9.81\frac{m}{s^2} * 1850\frac{kg}{m^3}}{(1030 - 1850)\frac{kg}{m^3} * 9.81\frac{m}{s^2}} = 737.9m$$

The whole tripping motion is assumed to go from the depth of the fluid interface, D_{fi}, to the depth of the casing, D_{casing}.

5.2.1.2 Pipe motion

The acceleration is assumed constant, both during starting and stopping of the pipe motion. Between the velocity changing phases, the velocity is assumed constant. This gives velocity and acceleration profiles, when tripping 27 meters of drillpipe, as shown in Figure 24.

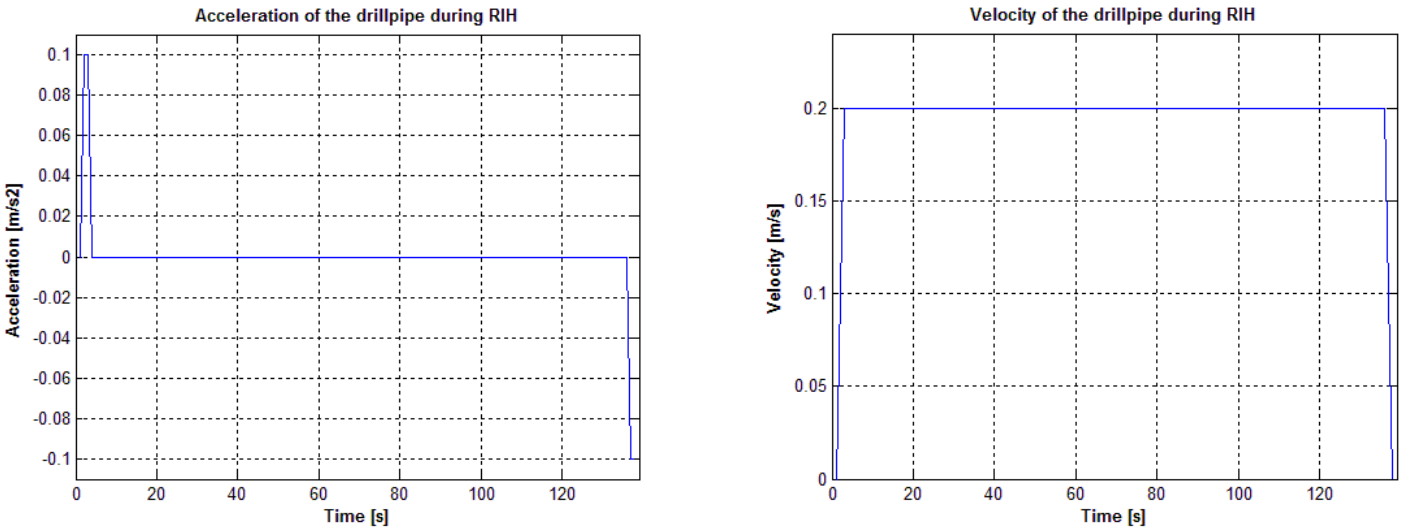

Figure 24: Acceleration and Velocity profiles for tripping one stand when RIH

5.2.2 Case 1 – A theoretical demonstration of the steps in the tripping simulation

Here, a demonstration of the features in the simulation is showed. The example describes tripping from $D_{fi} = 738m$ to $D = 1736$; 200m down into the cased hole section. Some of the numbers used in this example are not necessarily realistic, but have been over exaggerated to magnify the effects of the different features included in the simulator.

5.2.2.1 Surge pressure profile when RIH

Figure 25 shows the surge pressure profile created in the wellbore when running the drillpipe downwards; calculated by Eq. 4.10. The starting depth of the BHA in this example is 4000mTVD, and the velocity profile used is the same as the one shown in Figure 24. At the start, the created pressure is zero (represented by the red line). During the first few seconds, the pressure rises to a peak; representing the acceleration phase of the motion, magnified by the correction factor described in section 4.2.4.3. Then the created pressure stabilizes, as the drill pipe is moved at constant velocity. As more pipe is added into the hole, increasing ΔL in Eq. 4.10, the surge pressure created increases slightly as visible in Figure 25. The last part of the movement creates a negative pressure, as the acceleration goes below zero, even though the velocity is positive. This is also because of the correction factor described in section 4.2.4.3.

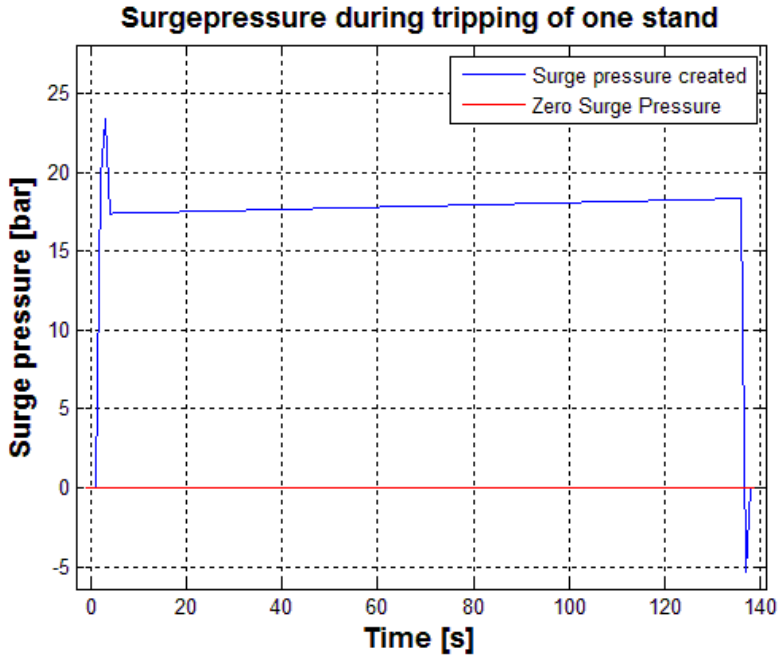

Figure 25: Pressure changes in the wellbore during tripping

5.2.2.2 Example of tripping of multiple stands

This demonstration case is generated to show and explain in detail how the simulator works and how calculations are done, which can be difficult to see from the graphs when a long tripping segment is simulated because the space in the graph is limited. In the demo case, the acceleration correction factor is set to $C_{acc} = 300$, so that an unrealistically excessive effect of the transient phase can be seen. To magnify the effect of the pumping system, the maximum rate of the subsea- and booster pump has been set to 10'000 LPM. It is acknowledged that

pump rates of 10'000LPM is highly unrealistic, but shows the functionality of the pumps and fast change of fluid interface depth better.

Figure 26 shows how the mud pressure at the shoe varies, peaking during the acceleration phase, and having low points during the deceleration phase. The mud pressure is calculated with Eq. 5.4, where P_{surge} is found from Eq. 4.10, and $P_{hydrostatic}$is found from Eq. 2.2.

$$P_{mud} = P_{hydrostatic} + P_{surge} \qquad \textbf{Eq. 5.4}$$

The over excessive acceleration effect gotten by setting $C_{acc} = 300$, causes the high pressure spikes, calculated from Eq. 4.10. During the deceleration movement, the pressure drops below the pore pressure, which causes influx from the formation, shown as positive spikes in Figure 27, calculated by Eq. 4.20.

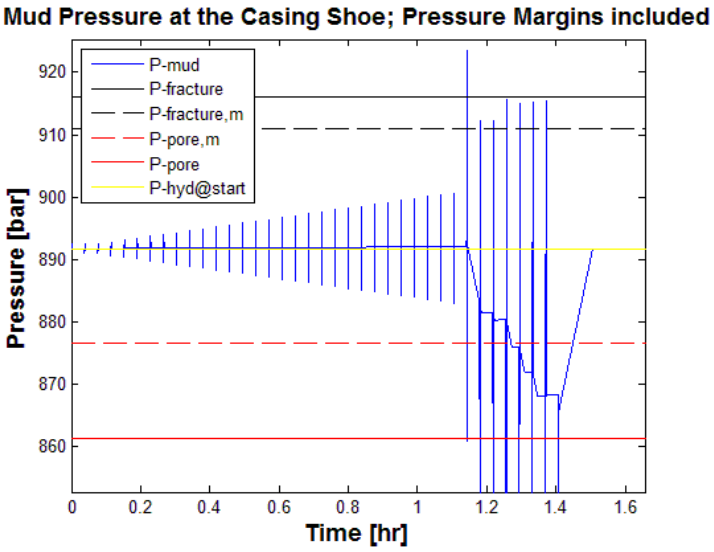

Figure 26: Demo Case – Mud pressure at casing shoe

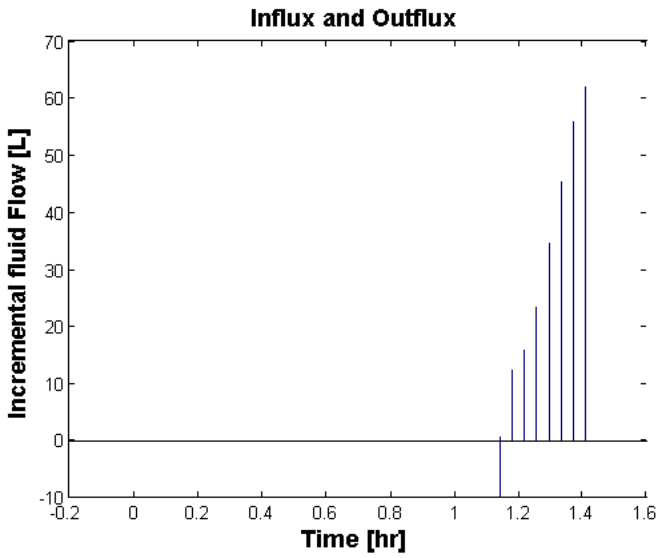

Figure 27: Demo Case – Well flow with the formation

As discussed in section 3.1.3.3, lost circulation is a very dangerous situation that could have severe consequences. Because of this, getting formation fluid influx because the BHP drops below the pore pressure has been regarded as the "lesser of the two evils". Therefore, the subsea pump is ramped up to reduce the fluid level in the riser, to decrease the BHP, and hence keep the pressure below the formation pressure as long as possible.

Before running each stand, the simulator predicts how high the pressure will rise during the tripping motion of the stand, and calculates the ideal target depth for the fluid interface. As the simulator recognizes that the maximum mud pressure during the tripping process of the next stand will go above the safety margin for fracture pressure, as seen at around t = 1.15hr in Figure 26, the target depth is increased incrementally until the predicted well pressure lies

below the fracture pressure. If the maximum interface depth is reached, the target depth is kept at the maximum depth.

The pump rates are controlled by the difference between the current fluid interface depth and the ideal depth found by the prediction. For example, when the fluid interface level in the riser is higher than ideal, the subsea pump rate is found by Eq. 5.5, which increases the rate, and hence lowers the fluid level in the riser. The subsea pump rate is chosen to not be higher than the maximum rate, while the booster pump is set to the minimum required rate.

$$Q_{sp} = minimum\left(\frac{A_{cs,riser} * \left(D_{fi,target} - D_{fi}\right)}{\Delta t} + Q_{bp,min}; Q_{sp,max}\right) \qquad \textbf{Eq. 5.5}$$

The pumprate can be seen in Figure 28 and the corresponding depth for the fluid interface is shown in Figure 29 (note that the y-axis is reversed). The downwards sloping pressure between the spikes at around t=1.15hr in Figure 26 shows the falling wellbore pressure due to the reduced level in the riser.

The pumprates shown in Figure 28 are ramped up and down multiple times, which also is done in the similar figures later in the thesis. This is done deliberately, to show the requirements for pump rates at each stage during the tripping process. A more realistic way of controlling the pumps is to run them continuously for a longer time period at a constant and lower rate. By doing this correctly, the same average rate as when ramping the pumps up and down, could be achieved, by spreading the total pumped volume over a longer time period. This both reduces wear and tear on the pump's engines, and gives a more smooth and dynamic flow in the riser. As discussed in section 6.1, the rates have been chosen to be turned on and off, even though this probably would not be possible in reality.

At around t=1.35hr, the lowest allowed hydrostatic pressure (5 bar above the pore pressure) is reached, and the subsea pump is therefore ramped down to prevent the hydrostatic pressure from falling further.

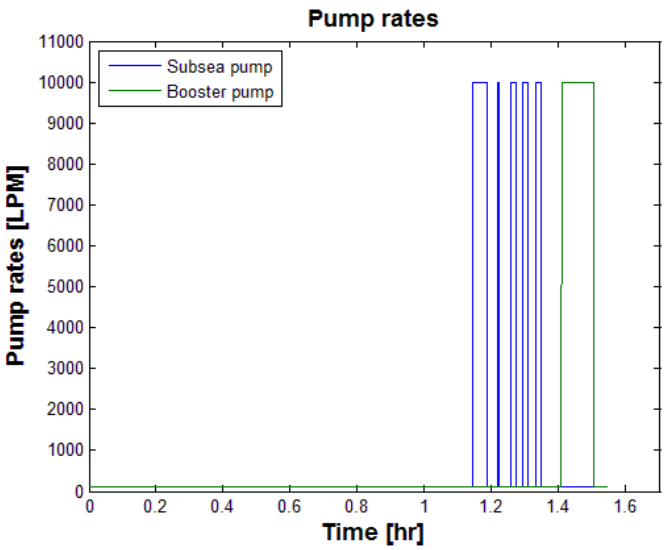

Figure 28: Demo Case – Pump rates

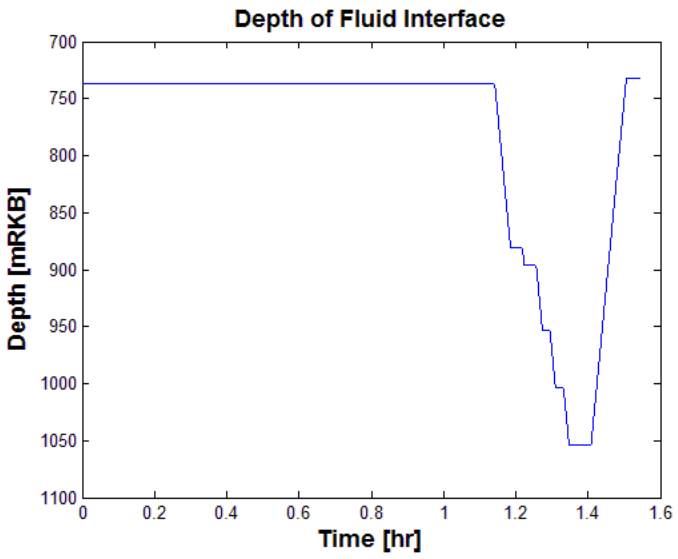

Figure 29: Demo Case –Fluid interface depth

When the target depth for the tripping is reached, the hydrostatic pressure is changed back to the starting level by increasing the rate of the booster pump to change the fluid interface level. This rate change is shown in the green graph in the last part of Figure 28, and the corresponding change in depth of the fluid interface can be viewed in Figure 29. The booster pump rate that is used continuously until the wanted D_{fi} is reached is calculated with Eq. 5.6, where D_{fi} is found with Eq. 5.3.

$$Q_{bp} = minimum\left(\frac{A_{cs,riser} * \left(D_{fi} - D_{fi,start}\right)}{\Delta t} + Q_{sp,min}; Q_{bp,max}\right) \qquad \textbf{Eq. 5.6}$$

The lower pump rates shown for t < 1.10hr in Figure 28, are adjusting the fluid interface level when the drillstring displaces the fluid upwards in the riser, as discussed in section 4.2.4.2.

5.2.3 Case 2 – Base Case

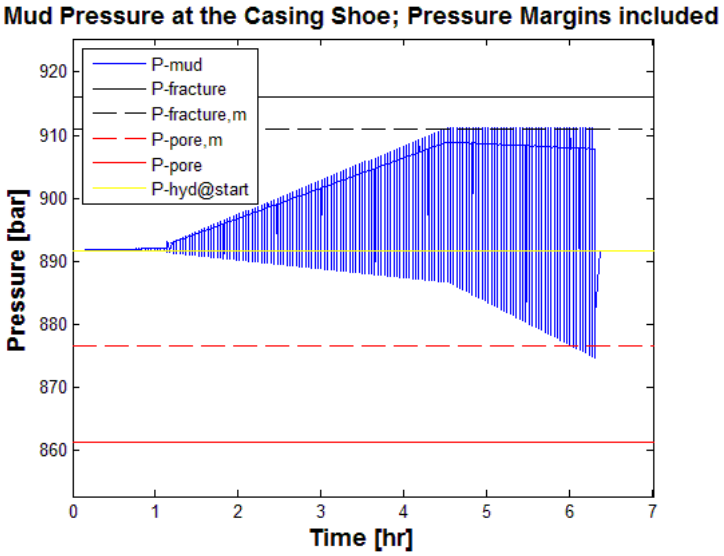

Figure 30: Case 2 – P-mud at casing shoe

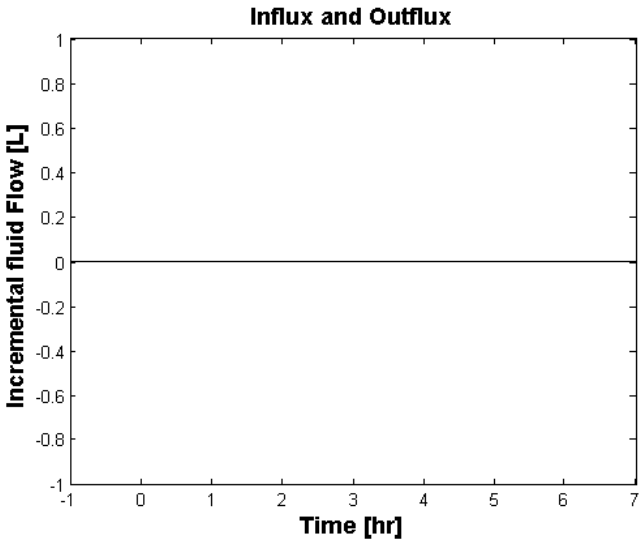

Figure 31: Case 2 – Formation influx

In Figure 30 the pressure development at the casing shoe is shown. As the pressure peaks reach the margin line of the fracture pressure, at around t=4.5hr, the hydrostatic pressure is lowered by the subsea pump to prevent the pressure peaks reaching closer to the fracture pressure. In this example, the pressure does not breach out of the mud window, and no fluid loss or influx is experienced, as can be seen from Figure 31.

In Figure 32, the pump rates are shown. The first part, when t<4.5hr, shows low pump rates that remove the added volume of the drill pipe body to keep the hydrostatic pressure constant. This constant hydrostatic pressure can also be recognized in Figure 33 as the stable depth of the fluid interface. At t>4.5hr, the subsea pump rate is increased to lower the hydrostatic pressure to make sure that the pressure peaks from the tripping movements will not increase above the safety margin of the fracture pressure. This can also be seen in Figure 33 as the increasing depth of the fluid interface, which gives a lower hydrostatic pressure.

When the BHA is at the end depth, the depth of the fluid interface is reduced, to increase the hydrostatic pressure back to the starting level.

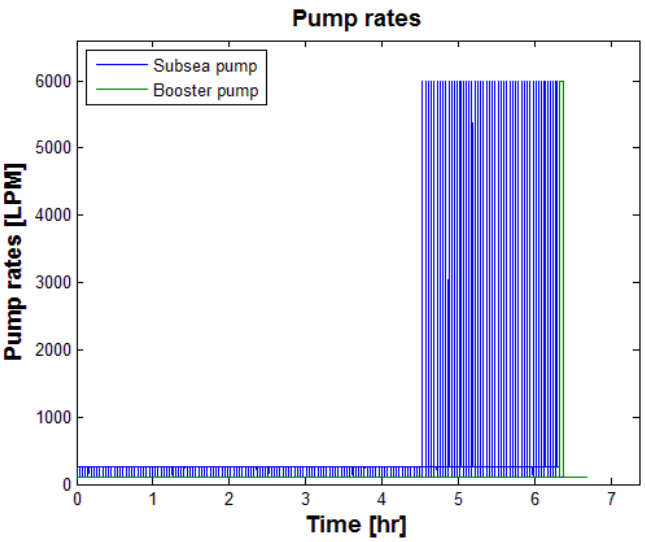

Figure 32: Case 2 – Pump rates

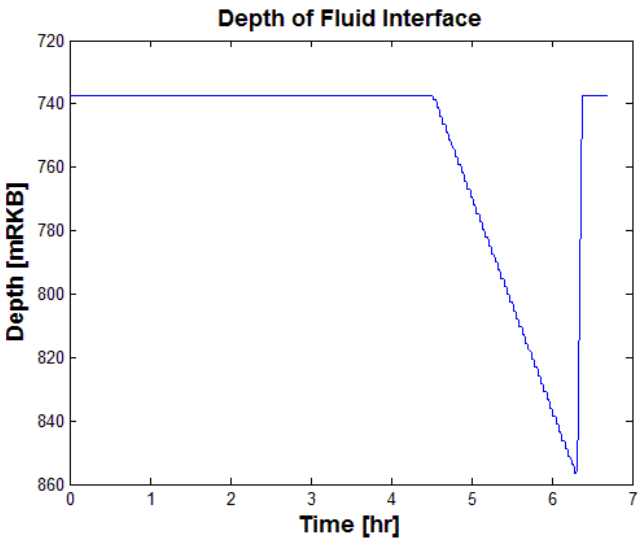

Figure 33: Case 2 – Fluid interface depth

5.2.4 Case 3 – Tripping without pumps

To get an impression of the importance of the pumps, the maximum rates of both the subsea pump and booster pump are set to 1LPM, as visible in Figure 36. Other parameters are the same as in Case 2 – Base Case. The obtained results show how the pressure will develop when the pressure is allowed to evolve freely.

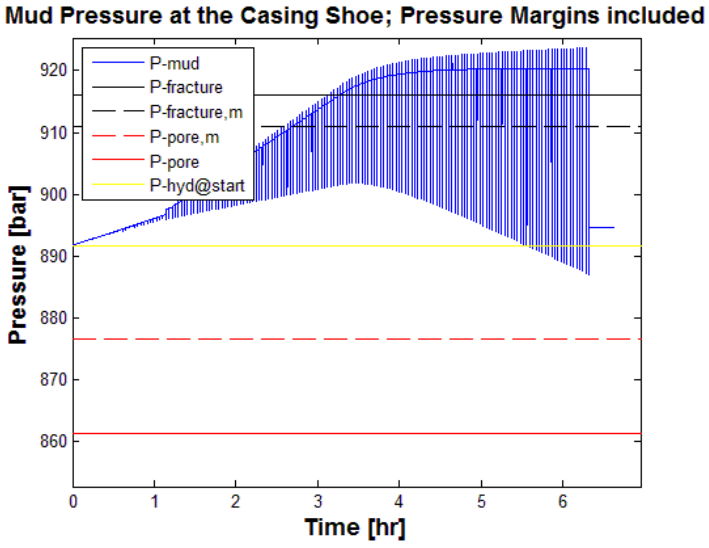

Figure 34: Case 3 - P_{mud} at Casingshoe

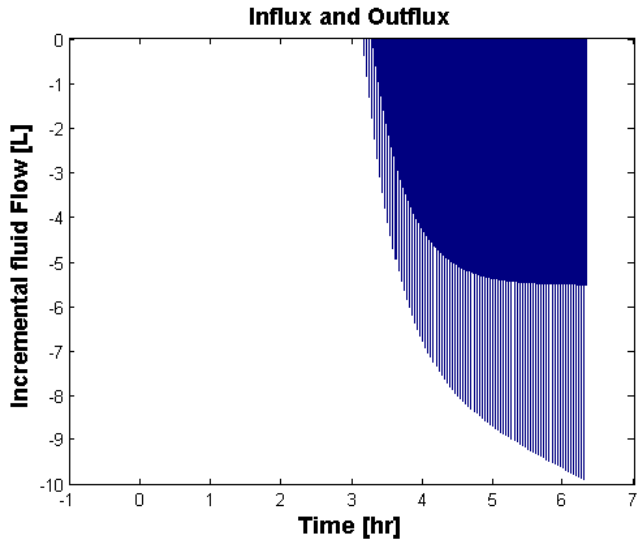

Figure 35: Case 3 - Flow in/out of formation

Figure 34 shows how the mud pressure increases, and eventually goes above the formation fracture pressure. When the pumps are not removing a mud volume amount corresponding to the added drillstring body, the hydrostatic pressure will increase with 0.153bar per stand as

calculated in section 4.2.4.2. There, it was also shown that a 0.2m/s tripping velocity corresponds to an average 152LPM subsea pump rate, which mean that 152LPM plus the minimum required booster pump rate is lacking in this example.

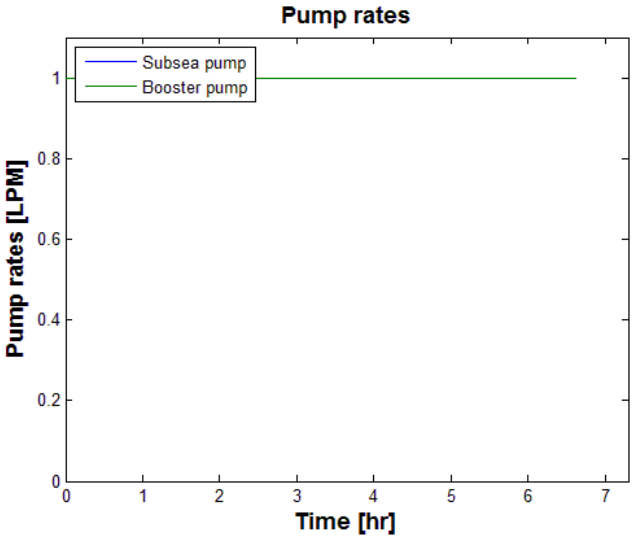

Figure 36: Case 3 - Pump rates

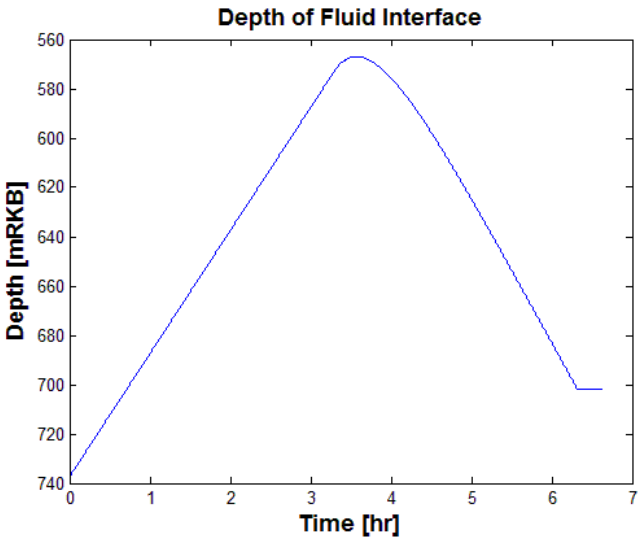

Figure 37: Case 3 – Depth of fluid interface

The fluid interface depth, shown in Figure 37, decreases steadily until the curve breaks off and increases in value at approximately t=3.5hr . The first decrease is what is causing the pressure build up seen in Figure 34.

The interface depth increase when t>3.5hrs is caused by the losses to the formation, which again is caused by the pressure surges during each the motion of each stand. Because the booster pump does not refill the fluid that is lost during the tripping motion, the depth declines for each stand.

5.2.5 Case 4 – Higher tripping velocity and acceleration

This case is included to show how the pressure might influence a wellbore when tripping in an even narrower pressure window than the casing shoe at Macondo. An increased velocity will also increase the pressure surge, as demonstrated in section 4.2.4.1. The pressure fluctuations are magnified, which causes more severe influx and losses.

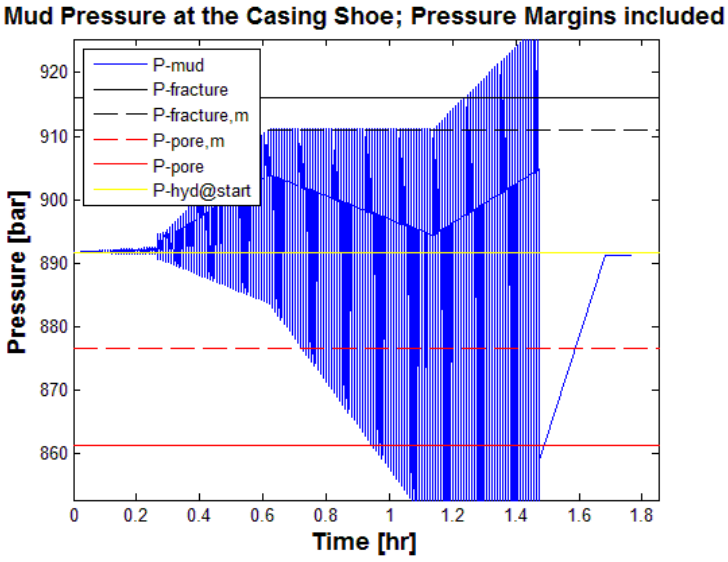

Figure 38: Case 4 – P_{mud} at Casingshoe

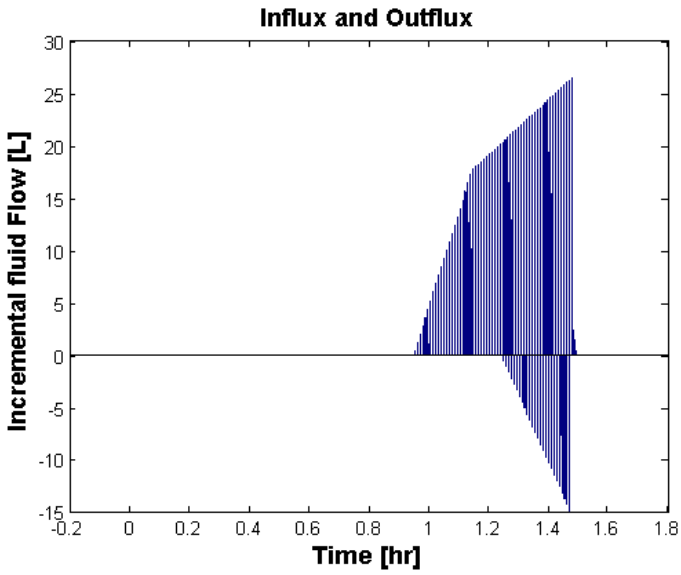

Figure 39: Case 4 - Flow in/out of formation

As seen in Figure 38, the pressure fluctuations increase sharper as the high OD BHA enters the smaller ID casing at around t=0.3hr. The level in the riser is reduced as the pressure fluctuations reach the fracture pressure margin at around t=0.6hr. At just after t=1.2hr, the lowest allowed hydrostatic pressure is reached, which denies the subsea pump a higher rate than necessary to keep the hydrostatic pressure constant, and hence the formation is fractured, causing fluid losses.

The density of the formation fluid has been assumed to be $\rho_{influx} = 800\frac{kg}{m^3}$, which alters the composition of the wellbore mud. A result from this is shown in Figure 41, where the fluid level at the end has to be reset to a higher level in the riser than at the start, to give the same hydrostatic pressure. The new density is calculated with Eq. 5.7.

$$\rho_{new} = \frac{\left[V_{antot} - \left(V_{influx} - V_{loss}\right)\right] * \rho_{mud} + \left(V_{influx} - V_{loss}\right) * \rho_{influx}}{V_{antot}} \qquad \textbf{Eq. 5.7}$$

New density is not calculated at every tripping movement, but only at the end of the whole process. Therefore, results gotten from Eq. 5.7 could be inaccurate, because the fluid lost from the wellbore is assumed to have $\rho_2 = 1850\frac{kg}{m^3}$, but it could already have been mixed by the light weight formation fluid, and hence having a lower density.

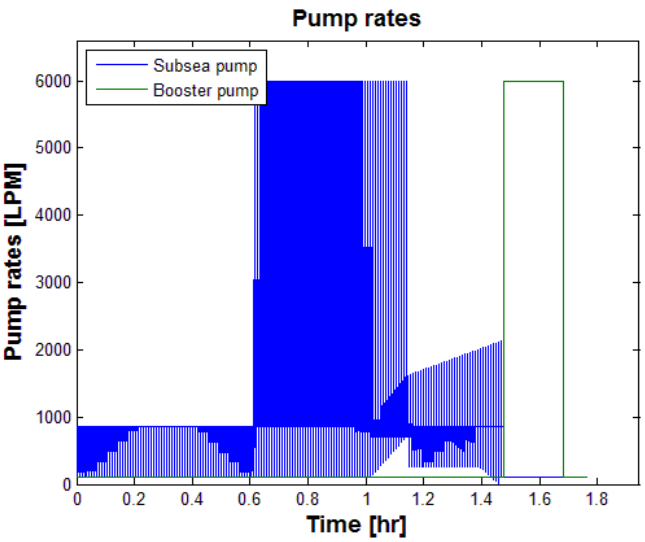

Figure 40: Case 4 – Pump rates

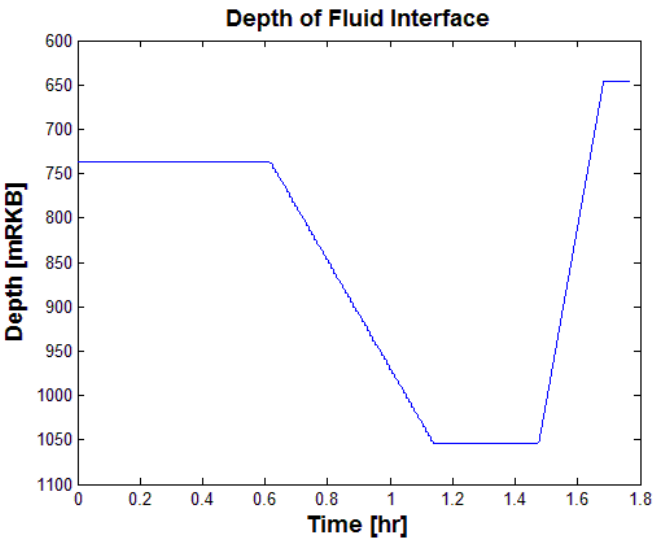

Figure 41: Case 4 – Depth of fluid interface

The reduced subsea pump rate because of the disallowed lowering of the hydrostatic pressure can be seen at t=1.15hr in Figure 40. The booster pump rate which increases the level in the riser to bring the pressure back to the pre-tripping level is seen as the green graph at t=1.45hr. The corresponding increase in interface level in the riser is seen at the end of Figure 41.

5.2.6 Results

Table 2: Results – Running drillpipe into the hole

	Case 1 - DemoCase	Case 2 - Base Case	Case 3 - No pumps	Case 4 - Higher tripping velocity and acceleration
Start depth [m]	737	737	737	737
End depth [m]	1 736	5 219	5 219	5 219
Total well depth [m]	5 260	5 260	5 260	5 260
Maximum pressure variation for tripping of a stand [bar]	101	36	37	86
Total fluid volume lost [L]	-10	0	-50 404	-287
Formation influx volume gained [L]	249	0	0	3 342
Theoretical new density due to formation fluid influx [kg/m^3]	1 849	1 850	1 850	1 832
Theoretical change in hydrostatic pressure due to new mud density [bar]	-0.46	0.00	0.00	-7.21
Change in fluid interface depth due to change in mud density [m]	-6	0	-35	-92
Change in hydrostatic pressure due to change in mud density [bar]	-0.03	0.00	2.85	-0.55
Tripping time [hours]	1.55	6.42	6.63	1.77
Pipe velocity [m/s]	0.20	0.20	0.20	**1.00**
Pipe acceleration [m/s^2]	0.10	0.10	0.10	**0.20**
Acceleration correction factor	**300**	3.46	3.46	3.46
Density, light fluid [kg/m^3]	1 030	1 030	1 030	1 030
Density, heavy fluid [kg/m^3]	1 850	1 850	1 850	1 850
Density of influx [kg/m^3]	800	800	800	800
Max rate, Subsea pump [LPM]	**10 000**	6 000	**1**	6 000
Max rate, Booster pump [LPM]	**10 000**	6 000	**1**	6 000
Min rate, Subsea pump [LPM]	100	100	**1**	100
Min rate, Booster pump [LPM]	100	100	**1**	100

5.2.7 Stripping with MPD pressure compensation

Stripping is when tripping pipe into a pressurized well, through a closed BOP. With a normal BOP, stripping can be done with the annular BOP element closed, but with MPD, the RBOP is the seal. Tests of stripping with MPD in a vertical test well in Dallas, USA showed that an automatic control system could keep the BHP stable within a ±2.5 bar window when stripping in and out, while circulating at 2000LPM (Godhavn/Statoil, et al., 2010). A test of stripping into and out of a well when stabilizing the pressure only with the BPP was also conducted, result being that the

pressure criteria of stability within a ±2.5bar pressure margin was met. Stripping velocities were 3-12m/min (0.05-0.2m/s) for both tests.

Another stripping test at the offshore well Gullfaks C, Norway was done with a circulation rate of 1950LPM. Figure 42 (Godhavn/Statoil, et al., 2010) shows the bit position and pressure- and rate curves for the test when stripping at 9m/min (0.15m/s).

As visible from the top and middle pressure graph when stripping out of the hole at 100s<t<250s, the back pressure increases with 1.5bar from 22.5bar to 24bar, while the measured BHP falls around 3bar, from 290bar to 287bar. Assuming that the friction pressure from the circulation was constant, this indicates that the swab pressure created in the well is around 4.5bar. When investigating the running of the pipe into the hole, it can be seen that backpressure is reduced with 1.5bar from 23bar to 21.5, while the measured BHP increases with 3bar from 287bar to 290bar. This indicates a total surge pressure when tripping into the hole of 4.5bar; the same as experienced when running into the hole. Water was used as fluid for both the tests described here.

The BHP deviated less than ±2.5bar from the desired wellbore pressure, which was within the defined criteria for a success.

The same results were obtained when stripping at a velocity of 12m/min (Godhavn/Statoil, et al., 2010).

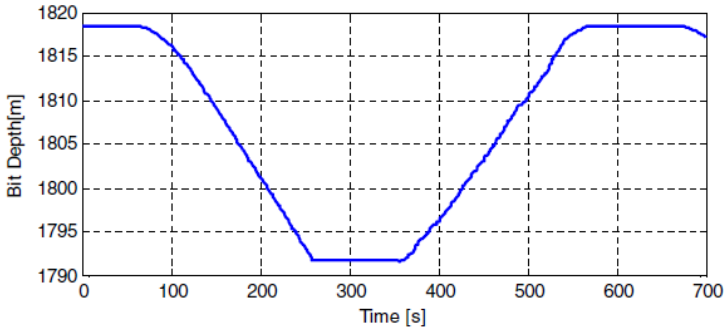

Figure 13. Gullfaks C offshore commissioning swab and surge experiment. Bit depth.

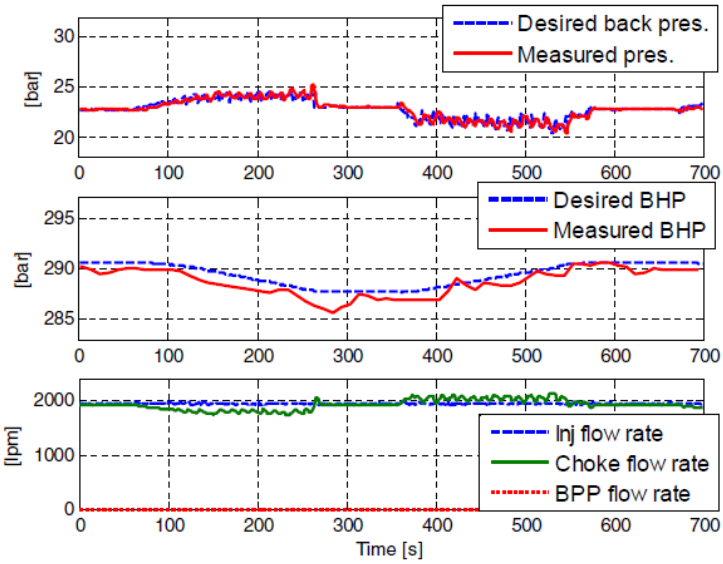

Figure 14. Gullfaks C offshore commissioning swab and surge experiment. Top: back pressure set point and measurement, middle: BHP set point and measurement, bottom: rates.

Figure 42: MPD Tripping test on Gullfaks C

5.2.7.1 Comparing with DGD technology

The 4.5 bar pressure change discussed in section 5.2.7, that is seen over roughly 180 seconds in Figure 42, could be compensated for by using the DGD. The required pump rate is found with Eq. 4.19 as shown below

$$Q_{pump} = \frac{\frac{4.5 * 10^5 Pa}{180s}}{(1850 - 1030)\frac{kg}{m^3} * 9.81\frac{m}{s^2}} * 0.1801m^2 = 0.05597\frac{m^3}{s} = 3358LPM$$

This rate is within the limits of what can be produced with currently available DGD equipment. The GE MaxLift 1800 pump produces a rate of 6814LPM, which makes it possible to compensate for the double surge/swab pressure of that showed in the example from Gullfaks.

5.3 Trapping pressure

5.3.1 The simulated situation

The simulations presented here, describe a situation when circulating with the rig pumps through the drillstring, with a wellbore pressure above the pore pressure, when suddenly the rig pumps stop. This causes an immediate loss of the friction pressure in the well, eliminating ECD, and leaving only the hydrostatic pressure in the mud column. The hydrostatic pressure is lower than the bottom hole pore pressure, which leads to an underbalanced well, and formation fluids flowing into the well. In the situation, the casing shoe has been drilled out, to a total well depth of 5260mTVD, and circulation has commenced, preparing for drilling the reservoir section.

In the simulated example, neither use of a RBOP at the rig topside or use of the BOP at seafloor has been considered. Only pressure control by change of the hydrostatic pressure is simulated. Control of the pressure using other features is presented in section 5.3.11, and later discussed and compared.

5.3.1.1 Friction pressure

Data from the Macondo show that the circulating friction pressure is $608psi = 41.9bar$ in a $18'000ft = 5488m$ wellbore (Transocean, 2011). The details regarding the tally, and especially the length and OD of the BHA, for when these data were measured, are not publically available. Therefore, it has here been assumed a drillstring tally as described in section 5.1. Because the total depth of the wellbore design used in this example is slightly more shallow, with the casing depth being at 5240mTVD and the bottom hole being at 5260, the friction pressure has been slightly adjusted downward to $580psi = 40bar$. The rig pump rate, the very rate creating the friction pressure loss has not been found available either, but this lacking information has been regarded as less important, because the simulation will focus on control of the subsea and booster pump after the rig pump has lost power. The rig pump rate is only included in the graphs to illustrated the difference between before and after power loss on the pumps.

The BHP when circulating is set to be 5 bar above the pore pressure safety margin (Rødland, 2012). To optimize the rate of penetration, the BHP should not exceed the pore pressure by more than necessary to keep the well stable, because the cuttings crushed loose from the formation will be removed easier when the pressure exerted on them from the wellbore is smaller (Skalle, 2010). The pore pressure with the added margin of 0.03sg is 882 bar at bottom hole, which gives a targeted pressure of 887 bar when circulating.

Applying numbers from the specified well design used in the examples in Eq. 5.5, yields the below depth of fluid interface when circulating:

$$D_{fi} = \frac{(887 - 40)bar\frac{10^5 Pa}{bar} - 5260m * 9.81\frac{m}{s^2} * 1850\frac{kg}{m^3}}{(1030 - 1850)\frac{kg}{m^3} * 9.81\frac{m}{s^2}} = 1338m$$

5.3.1.2 Fluid behaviour

It is reasonable to assume that the formation fluid is immiscible with the drilling fluid, and therefore makes up a section of its own in the annulus (Skalle, 2009). The flow of formation fluid into the well is assumed to follow Eq. 4.20. When the formation fluid influx enters the well, it is assumed to displace the wellbore fluid upwards in the well, and take up a length of the wellbore annulus. The hydrostatic BHP is therefore found by Eq. 5.8, with reference to Figure 43 (Gaup, 2012).

$$BHP_{hyd} = \rho_1 * g * D_{fi} + \left(TVD - D_{fi} - H_{influx}\right) * g * \rho_2 + H_{influx} * \rho_{influx} * g \qquad \textbf{Eq. 5.8}$$

In Eq. 5.8, $\rho_{influx} < \rho_1 < \rho_2$, meaning that an increased H_{influx} gives an increased BHP_{hyd}. H_{influx} is the height the formation fluid amounts to in the well, which is found by Eq. 5.9.

$$H_{influx} = \frac{V_{influx}}{A_{cs,BHA-OH}} \qquad \textbf{Eq. 5.9}$$

Because the BHA is longer than the open hole section, Eq. 5.9 is extended to involve the annulus between the BHA and the cased hole if $H_{influx} > L_{OH}$,; and further to include the annulus between the drillpipe and the cased hole if H_{influx} extends L_{BHA}; and the same goes for the rest of the wellbore. More details regarding these calculations can be found in the Appendix.

The fluid interface will be pushed upwards in the riser. Both the influx, which displaces the drilling fluids, and the booster pump rate, will contribute to this. It is here assumed that the light weight fluid displaced upwards, and out of the riser, is taken care of and contained by help of the mud circulation system, as on a conventional rig.

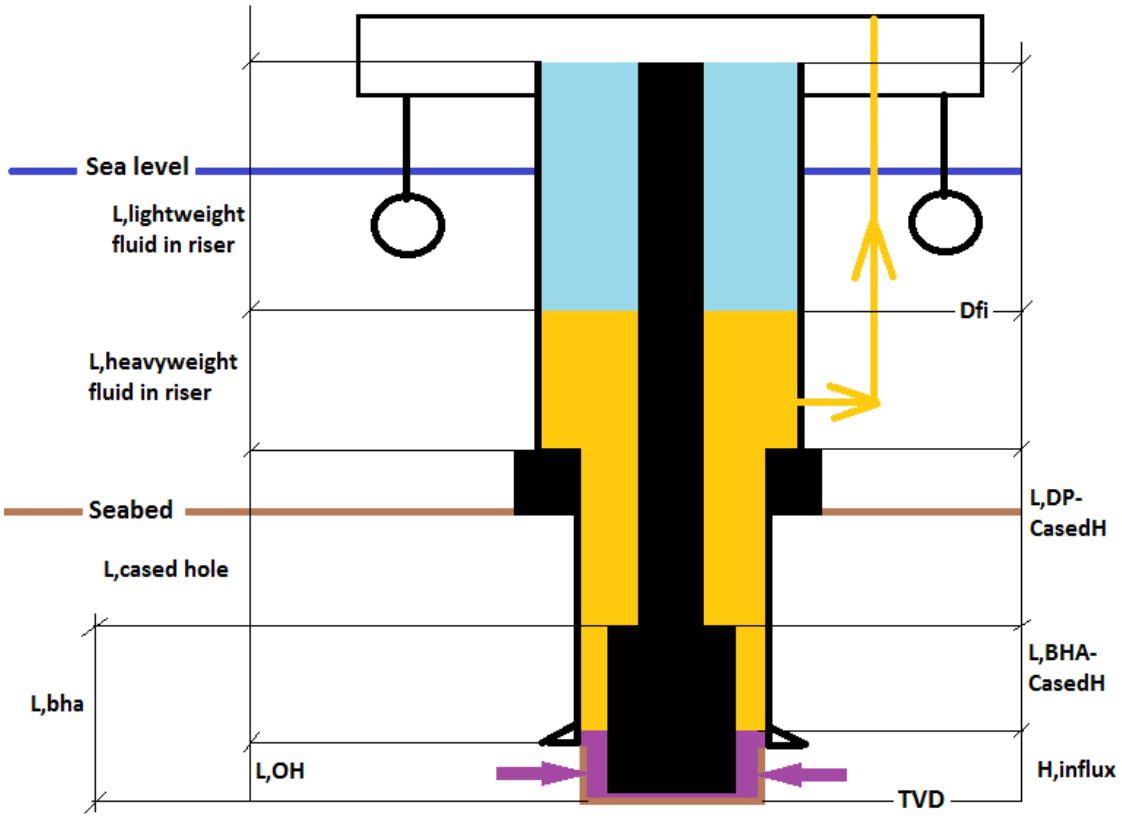

Figure 43: Well sketch for formation fluid influx

General constraints and assumptions:

- Well and drillstring design
  - 9 7/8" casing set @ 5240mTVD.
  - 8.5" open hole drilled to 5260mTVD
  - Drillstring; 5" drillpipes and a 50m 6" BHA, at the bottom of the well
- Fluids
  - Formation fluid immiscible with the drilling fluid
  - Drilling fluids, pump capacities, pressure safety margins and other wellbore data as described in section 5.1
  - Density of the formation fluid: $\rho_{influx} = 800\frac{kg}{m^3}$
- Consider the well a blow-out and well control lost if (one or both):
  - $D_{fi} < 50$
  - H_{influx} reaches above $D_{subsea\ pump\ intake}$
- Other
  - Pump rates change momentarily

- Water hammering, or other effects making the fluid move after the pumps have stopped, are neglected

5.3.2 Case 1 – Base Case

Case 1 is the base case, with a wellbore design and pump specifications as described above. Figure 44 shows how the hydrostatic pressure at the bottom of the well develops when it first drops below the pore pressure. As long as the hydrostatic pressure is below the pore pressure, formation fluid continues to flow into the well. This, in turn, increases the length of the column with light weight formation fluid, and the BHP_{hyd} falls further, leading into a self-energizing process. As visible from the downward concave shape of the hydrostatic mud pressure in Figure 44, the booster pump is not able to increase the level in the riser quick enough to re-establish pressure overbalance in the well. Well control is defined as lost after 12.6 minutes, when the formation fluid reaches the subsea pump inlet.

The first 30 seconds in the simulation are showing the situation when circulating, with 40 bar friction pressure in the well. Figure 45 shows that there is no fluid influx during this time; Figure 46 shows a stable fluid interface depth position at 1388m; Figure 47 shows $Q_{rp} = 3000LPM$, $Q_{bp} = 100LPM$ (minimum value) and $Q_{sp} = 3100LPM$ to remove the volume added by the two other pumps, keeping the fluid interface level stable.

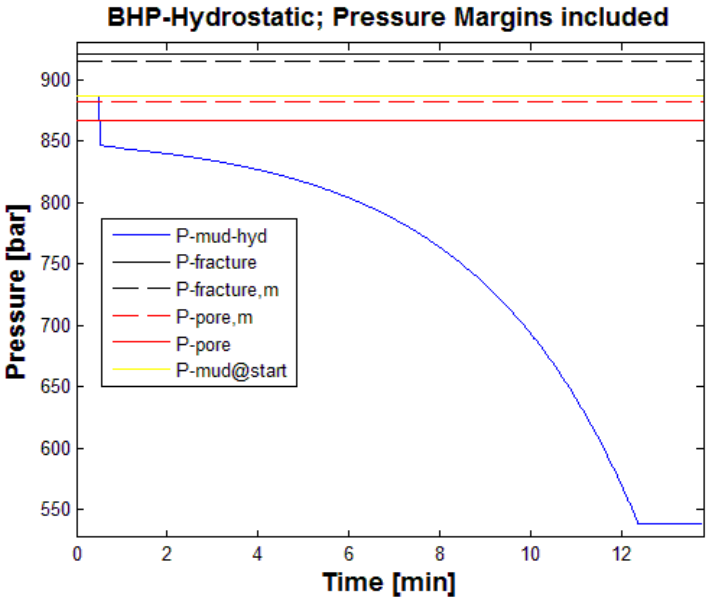

Figure 44: Trapping pressure: Case 1 – BHP

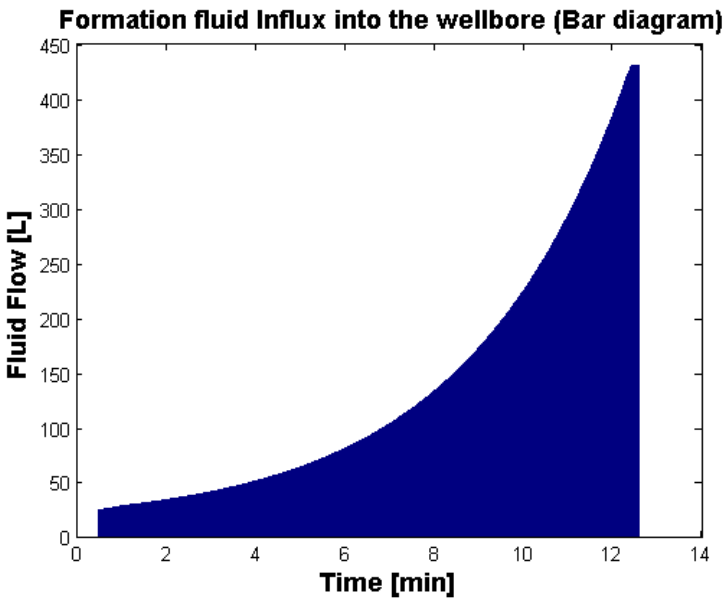

Figure 45: Trapping pressure: Case 1 – Fluid influx

Figure 46 show how the position of the fluid interface is pushed upwards in the well. The drop to zero of the subsea pump circulation rate, the reduction to minimum required rate of the subsea pump and the instantaneous ramp-up of the booster pump is showed in Figure 47.

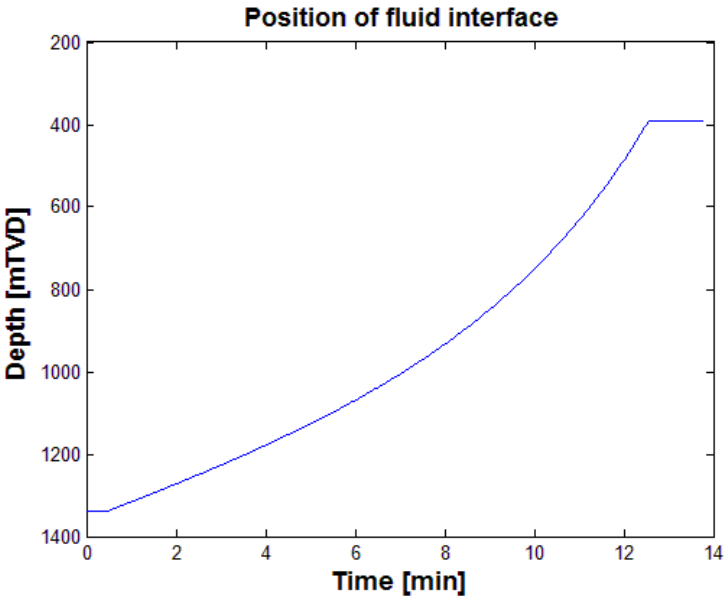

Figure 46: Trapping pressure: Case 1 – Fluid interface

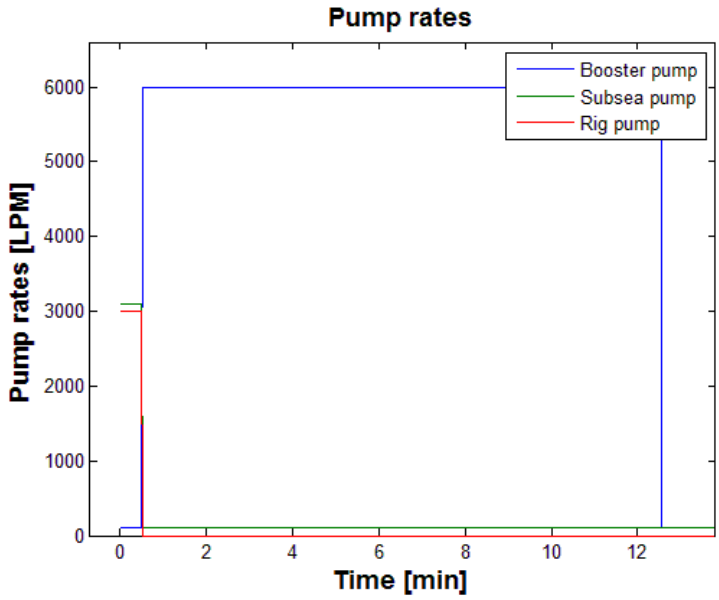

Figure 47: Trapping pressure: Case 1 – Pump rates

5.3.3 Case 2 – Higher booster pump rate

As seen from Eq. 2.3, a higher booster pump rate Q_{bp} will increase the level in the riser faster, and hence increase the pressure faster. By trial and error with the input data, the smallest rate that makes it possible to re-establish the control of the well has been found to be $Q_{bp} = 13550LPM$. The total influx volume is $V_{influx} = 15.2m^3$; 4% of the wellbore annulus volume. The height of the formation fluid column is 608m and the depth of the fluid interface is at 61mTVD; 11m short of the defined failure limit. Full results are included in Table 3.

5.3.4 Case 3 – Smaller ID on the Marine riser

The ORS DGD solution described in section 2.1.2.2 utilizes a marine riser with a 12.5” ID. This will able the subsea pump to change the fluid interface level faster than with a 19.5” ID riser, for the same subsea- and booster pump rate. This can be understood from Eq. 2.3.

When changing the defined ID of the riser to 12.5”, well control is achievable with the standard booster pump rate of $Q_{bp} = 6000LPM$. The behaviour of the BHP can be seen in Figure 48 and the declining formation influx volumes can be seen in Figure 49. The well pressure is in overbalance after just over 5 minutes, and the start pressure is re-established after 8.1 minutes.

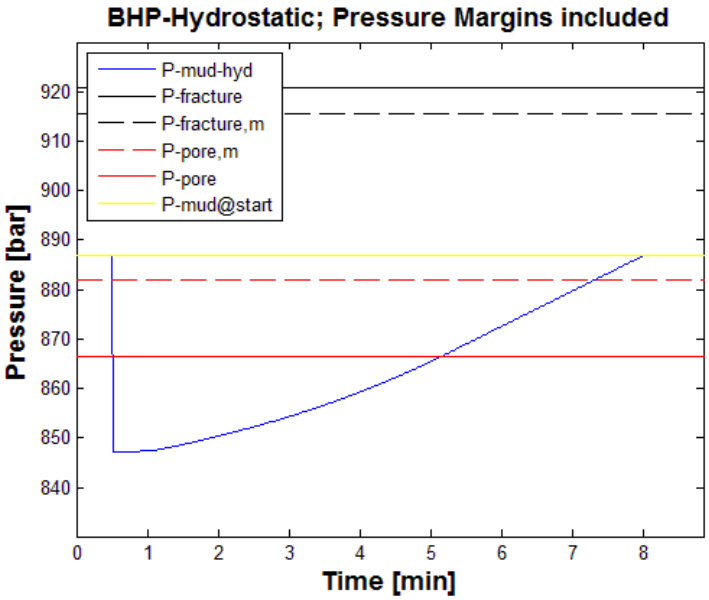

Figure 48: Trapping pressure: Case 3 –BHP

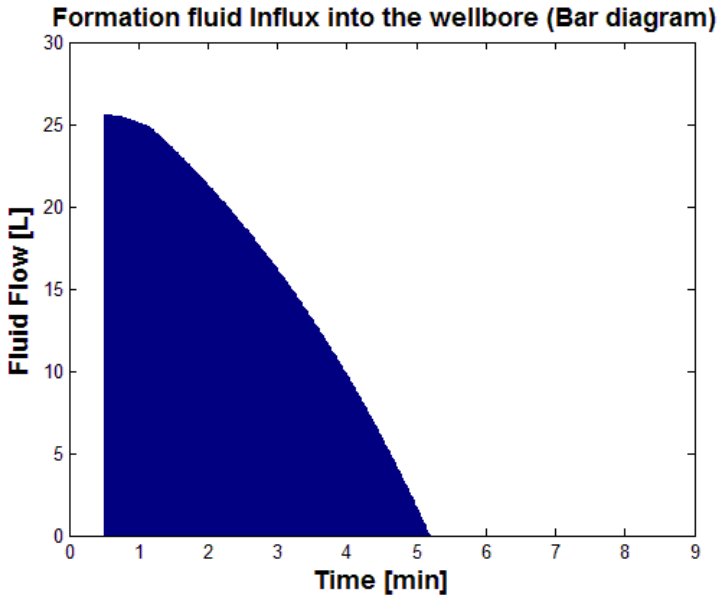

Figure 49: Trapping pressure: Case 3 –Fluid influx

To show the effect of the narrower riser, the following calculations are presented. Rearranging Eq. 4.19 and putting in Eq. 2.4 for A_{cs} yields Eq. 5.10.

$$\frac{\Delta P}{\Delta t} = \frac{Q_{pump}(\rho_2 - \rho_1) * g * 4}{\left(ID_{riser}^2 - OD_{pipe}^2\right) * \pi} \qquad \textbf{Eq. 5.10}$$

Using Eq. 5.10 with input data from the Base Case and $ID_{riser} = 19.5"$ gives a result of $\frac{\Delta P}{\Delta t} = 0.045\frac{bar}{s}$. With $ID_{riser} = 12.5"$ a result of $\frac{\Delta P}{\Delta t} = 0.121\frac{bar}{s}$ is achieved; an increase of 171% in pressure changing speed when keeping other parameters constant.

Because of the linearity between $\frac{\Delta P}{\Delta t}$ and Q_{pump} shown in Eq. 5.10, a doubling of the pump rate, will yield a 100% increase in $\frac{\Delta P}{\Delta t}$.

5.3.5 Case 4 – Smaller riser and maximum time delay

Here, the riser ID has been set to 12 ½", and a *time delay* before the pumps are turned on to increase the pressure, has been set.

Through trial and error with the input data, a maximum allowed delay of 75 seconds before the booster pump is ramped up is allowed. The time period with no booster pump is shown in Figure 51, and the corresponding hydrostatic pressure decline can be seen in Figure 50.

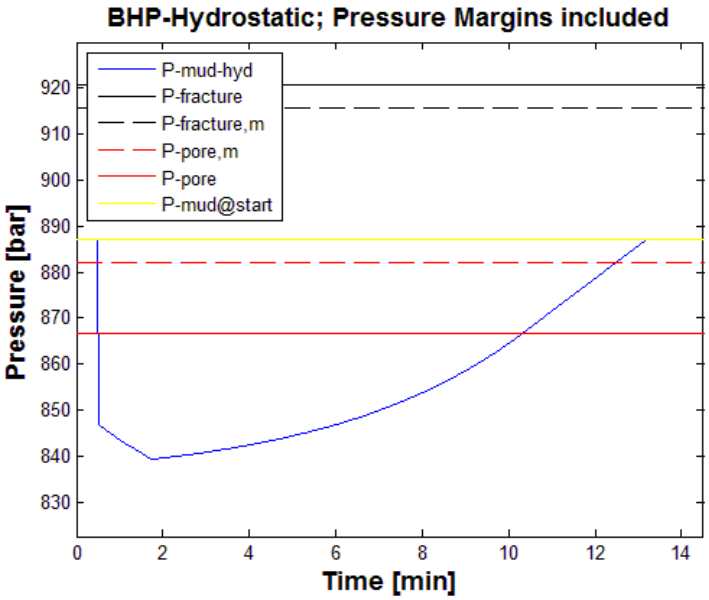

Figure 50: Trapping pressure: Case 4 – BHP

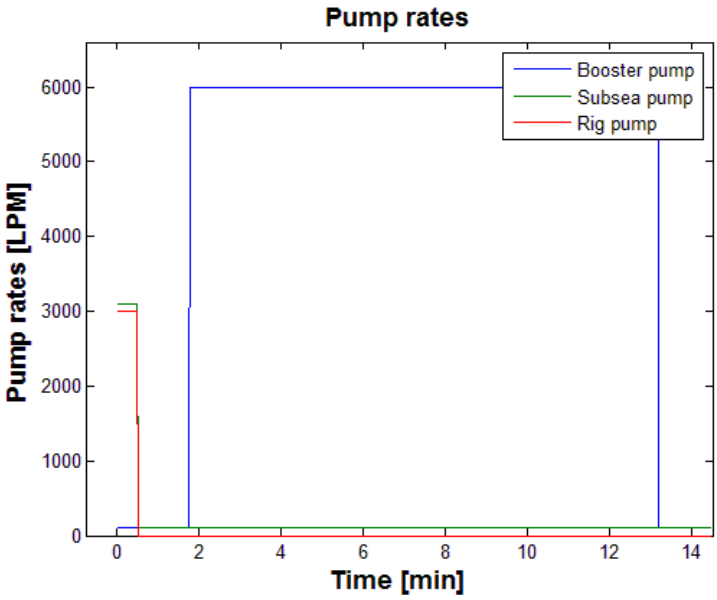

Figure 51: Trapping pressure: Case 4 – Pump rates

5.3.6 Case 5 – Higher pressure margin

In this example, the pressure margin when circulating, prior to the rig pump stopping, has been increased, which means that the mud pressure when the circulation stops does not fall as far below the pore pressure as in Case 1. Through trial and error, the required pressure margin to gain well control has been found to be 17 bar above the pore pressure margin, which means 32 bar above the pore pressure. This pressure, and the margin to the pore pressure can be seen as the yellow line in Figure 52

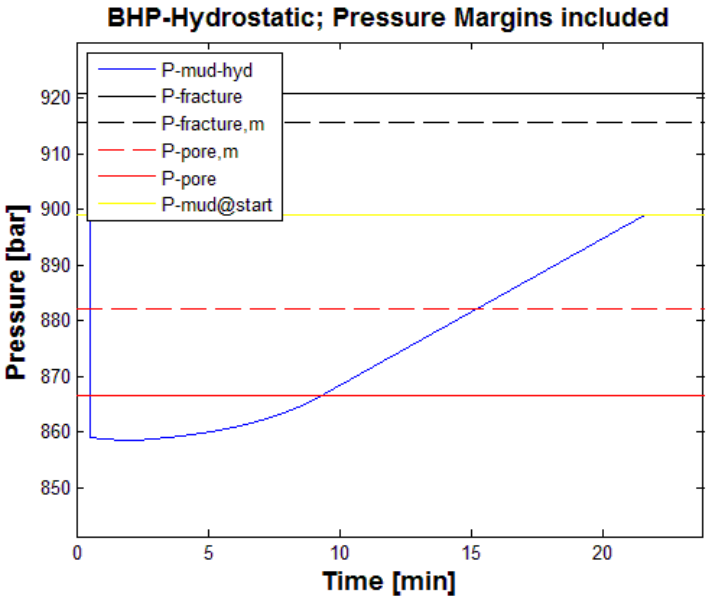

Figure 52: Trapping pressure: Case 5 – BHP

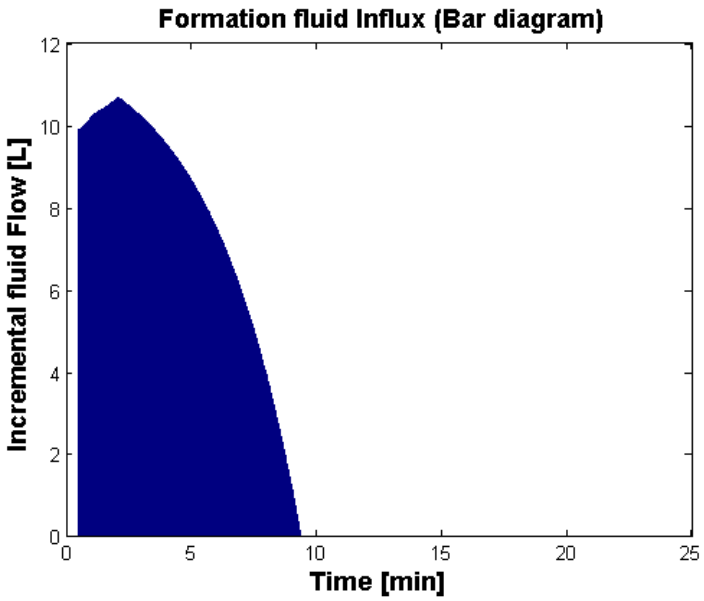

Figure 53: Trapping pressure: Case 5 –Fluid influx

5.3.7 Case 6 – Optimal design. Narrow riser, high pressure margin

By using a 12.5" riser, and increasing the pressure margin to 15 bar above the pore pressure margin, the well can be brought back to the circulation pressure situation in 6.6 minutes, taking a 739L influx volume into the wellbore. This volume corresponds to less than 1% of the wellbore annulus volume, and gives a formation fluid column in the well of 39 m height.

As visible from Figure 54, the wellpressure is quickly re-established, the well being in underbalance for about 2 minutes. The quickly declining influx is shown in Figure 55.

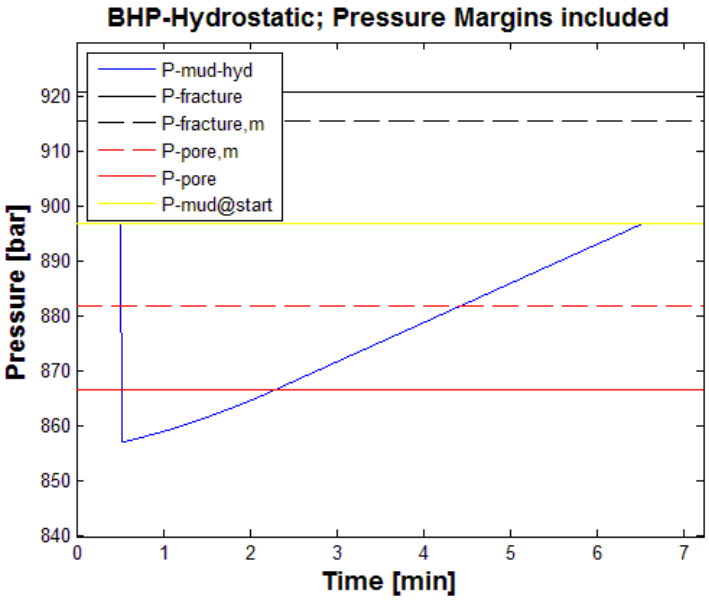

Figure 54: Trapping pressure: Case 6 – BHP

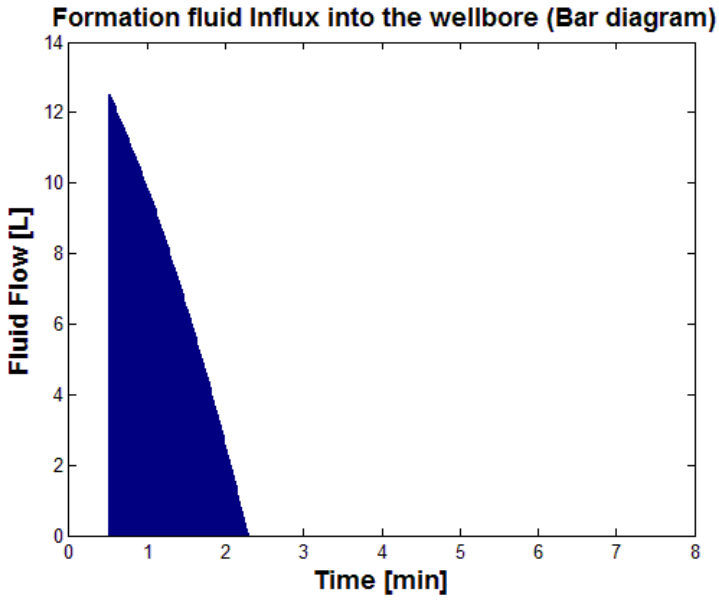

Figure 55: Trapping pressure: Case 6 – Fluid influx

5.3.8 Case 7 – Self-balancing well by very narrow riser annulus

As shown in Case 3 and Case 4, a narrow riser, makes it possible to change the level in the riser quickly. Because the fluid influx helps lift the fluid interface upwards, it contributes to a larger pressure in the well, and hence to counteract the hydrostatic pressure difference that is the reason for the influx. The same effect can be achieved by using a drillpipe with larger OD, which also makes the riser annulus narrower.

Here, an experiment that shows how narrow the annulus has to be, before the influx balances itself out, without the need of changing the level in the riser with the pumps, is conducted. This is done by optimizing the OD of the drill pipe in the riser.

The mathematical criteria for a "self-balancing well" can be set like the inequality shown in Eq. 5.11. On the left-hand side it describes the change in hydrostatic pressure in the marine riser and on the right-hand side it describes the hydrostatic pressure change in the wellbore where the formation fluid influx meets the drilling fluid. The equation says that the pressure increase in the riser must be greater than the pressure increase in the bottom hole.

$$\Delta P_{hyd,fi} > \Delta P_{hyd,influx} \qquad \textbf{Eq. 5.11}$$

Eq. 5.11 is extended to Eq. 5.12 (with reference to section 2.1), and further to Eq. 5.13.

$$(\rho_2 - \rho_1)\Delta h g > (\rho_2 - \rho_{influx})\Delta h g \qquad \textbf{Eq. 5.12}$$

$$(\rho_2 - \rho_1)\frac{Q_{influx}\Delta t}{A_{csan,riser}}g > (\rho_2 - \rho_{influx})\frac{Q_{influx}\Delta t}{A_{csan,wellbore}}g \qquad \textbf{Eq. 5.13}$$

Because the only influx is the formation fluid influx, the factor $Q_{influx} * \Delta t * g$ can be reduced from Eq. 5.13, which gives the relation in Eq. 5.14.

$$\frac{(\rho_2 - \rho_1)}{A_{csan,riser}} > \frac{(\rho_2 - \rho_{influx})}{A_{csan,wellbore}} \qquad \textbf{Eq. 5.14}$$

Further, the cross sectional areas are defined as in Eq. 2.4, to give Eq. 5.15.

$$\frac{(\rho_2 - \rho_1)}{({ID_{riser}}^2 - {OD_{pipe}}^2)} > \frac{(\rho_2 - \rho_{influx})}{({ID_{casing/hole}}^2 - {OD_{pipe/BHA}}^2)} \qquad \textbf{Eq. 5.15}$$

A greater OD_{pipe} makes the left side of Eq. 5.15 greater, and hence contributing to make the inequality correct. In practice, because the riser has a limited length, the difference from the left- and right hand side of Eq. 5.15 has to be so great that $BHP_{hyd} > P_{pore}$ before the fluid interface reaches the rig.

By solving Eq. 5.15 for OD_{pipe}, Eq. 5.16 is achieved.

$$OD_{pipe} > \sqrt{{ID_{riser}}^2 - \frac{(\rho_2 - \rho_1)({ID_{casing/hole}}^2 - {OD_{pipe/BHA}}^2)}{(\rho_2 - \rho_{influx})}} \qquad \textbf{Eq. 5.16}$$

And when entering numbers the below result is found (units in the equation are dropped due to space restraints):

$$OD_{pipe} > \sqrt{19.5^2 - \frac{(1850 - 1030) * (8.681^2 - 5^2)}{(1850 - 800)}}in = 18.46in$$

This result is valid for the situation when the fluid interface between the rising formation fluid column and the drilling fluid is in the cased hole and the drilling fluid interface is in the riser. A drill pipe with an outer diameter of 18.46in, is no-where near convenient. By utilizing the ORS DGD system described in 2.1.2.2, with $ID_{riser} = 12.5in$, the required OD of the drillpipe is calculated to be $OD_{pipe} > 10.81in$ with use of Eq. 5.16. This is a large, but still a slightly more convenient drillpipe diameter.

The length of the increased size drillpipe matters in the meaning that Eq. 5.16 is only valid as long as the light/heavy weight drilling fluid interface is in the narrow riser annulus. To ensure

this, the longer the high OD drillpipe section is; the better. It would not always be necessary to have the high OD the whole way up to the RKB, if the density difference between the drilling fluids used is high enough to balance the influx over a shorter length of fluid.

This increased-OD drillpipe does not need to have this large diameter throughout the entire wellbore; only in the riser, at D_{fi}. (Obviously, it would be impossible to have a 10. 81in drillpipe in a casing with $ID_{casing} = 8.681in.$) For example, it would be possible to only have $OD_{pipe} = 10.81in$ from RKB down to $D \approx 1300m$ to cover the likely depthrange for ΔD_{fi}. Based on the predetermined depth of drilling and knowledge of the formation, this should be planned in more detail in the drillstring tally. This means that drilling with a normal drillpipe program should be done from seafloor to 1300m above the total depth. The last 1300m should therefore be drilled with the increase ID pipe. The pipe cannot be pushed into the wellhead, because of the smaller sized casings, and if drilling deeper than the level reached when having the high OD drillpipe at the wellhead is required, the drillpipe must be pulled out and the diameter changed.

Both the OD of the drillstring (changing from BHA to drillpipe) and the ID of the hole/casing changes near the bottom of the hole, and therefore, simulations in MATLAB has been used to find a solution to the OD_{pipe}, for the specific Macondo well design of the situation described. In these tests, the delay before the booster pump starts is set to be 60 minutes. This is to get enough time to see how the pressure behaves.

The simulator is built to have a uniform OD of the drillpipe from the rig to the BHA. Changing input data for OD_{pipe} in the model means altered geometry through the whole wellbore, not only for the riser. Therefore, for simplicity, the optimized ID_{riser} when using $OD_{pipe} = 5in$ is found through trial and error in MATLAB, and the corresponding OD_{pipe} to give a similar cross section area of the riser annulus when using $ID_{riser} = 12.5in$ is calculated from the MATLAB result.

Through trial and error, this limit for the riser has been found to be $OD_{pipe} = 7.5in$. By comparing cross section areas, the below equation is found:

$(7.5^2 - 5^2)\frac{\pi}{4} = (12.5^2 - OD_{pipe}^2)\frac{\pi}{4}$; which gives the final result: $OD_{pipe} = 11.18in$

The reason for why this differs from the result obtained by Eq. 5.16, is because the MATLAB simulation takes the varying well geometry into account, and the limitation that the pressure must be controlled before the fluid interface depth in the riser reaches any closer to the rig than 50m below RKB-level.

Figure 56 shows how the BHP immediately starts to rise as it drops below the pore pressure. This causes the sharply declining formation fluid influx shown in Figure 57.

Figure 58 shows how the position of the fluid interface is pushed upwards, solely by the pore pressure. It flattens out just below the minimum allowed depth of 50m. The pump rates can be seen in Figure 59. The booster pump rate and subsea pump rate are kept at the minimum level, counteracting each other.

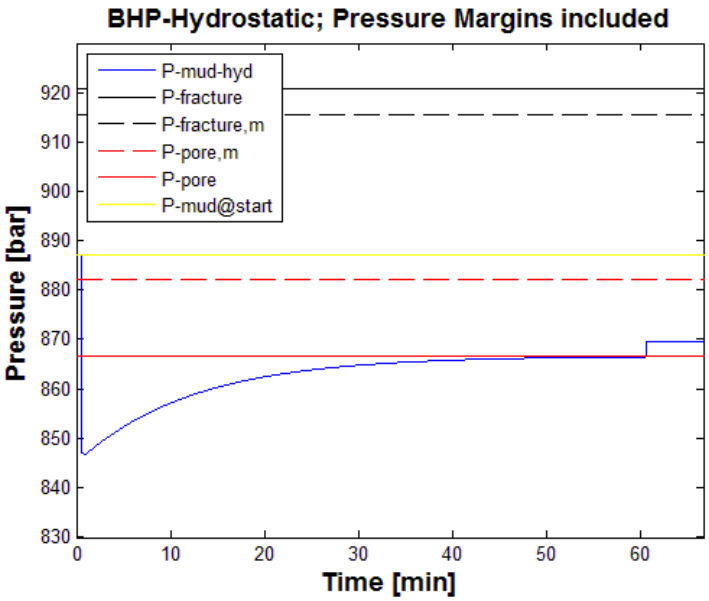

Figure 56: Trapping pressure: Case 7 – BHP

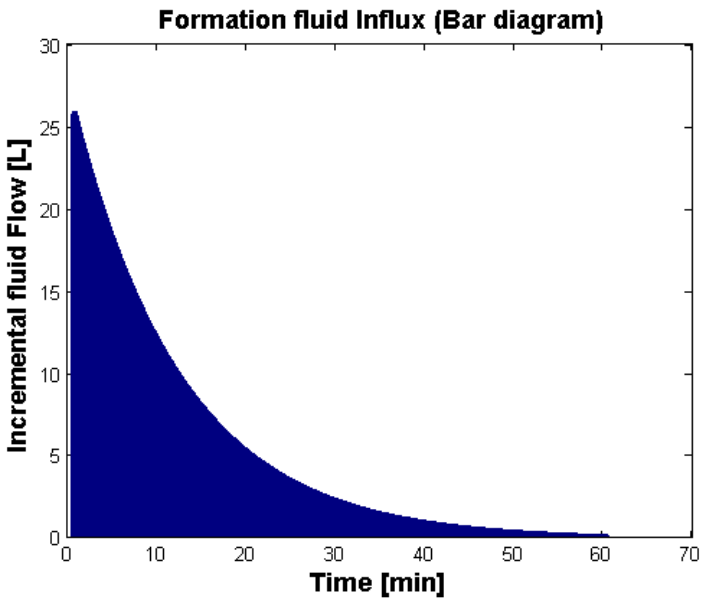

Figure 57: Trapping pressure: Case 7 – Fluid influx

The increased booster pump rate seen around t=60min is when the booster pump is allowed to increase the pressure the last part to insure well pressure overbalance.

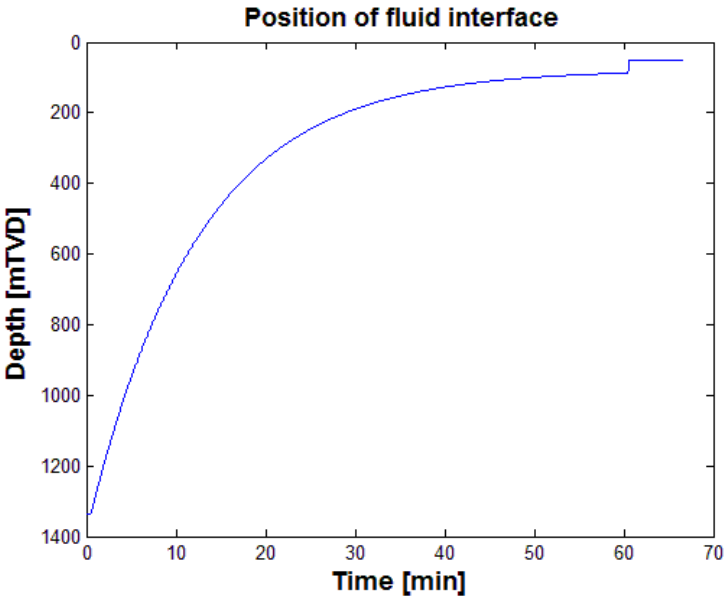

Figure 58: Trapping pressure: Case 7 – Fluid interface

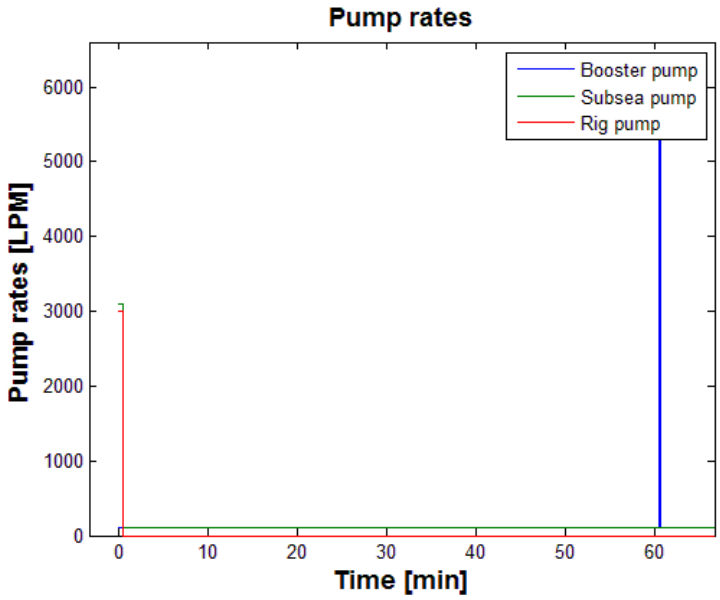

Figure 59: Trapping pressure: Case 7 – Pump rates

5.3.8.1 Drill pipe weight increase

By assuming $ID_{pipe,normal} = 4.125in$ for a normal drill pipe and $ID_{pipe,heavy} = 7in$ for a heavy drill pipe, a substitution of 1000m of normal drill pipe with 1000m heavy weight drill pipe, would increase the maximum mass hung from the topdrive by ΔW, found by Eq. 5.17:

$$\Delta W = \left(A_{pipe,heavy} - A_{pipe,normal}\right) * L_{pipe} * \rho_{steel} * F_{buoyancy} \qquad \textbf{Eq. 5.17}$$

Which gives the result below.

$$\Delta W = \frac{\pi}{4}\left((11.18^2 - 7^2) - (5^2 - 4.125^2)\right) * \frac{1}{12^2 * 3.28^2} m^2 * 1000m * 7900\frac{kg}{m^3} * \left[1 - \frac{1030\frac{kg}{m^3}}{7900\frac{kg}{m^3}}\right] = 237ton$$

$\rho_{steel} = 7900\frac{kg}{m^3}$ is used, and it is assumed that the 1000m pipe length is submerged in seawater ($\rho_{sw} = 1030\frac{kg}{m^3}$) in the riser.

The weight for 5000m of normal drill pipe, 1000m submerged in sea water and 4000m submerged in heavy weight drilling fluid is found from Eq. 5.18:

$$W = A_{pipe,normal} * \rho_{steel} * \left[L_1 F_{buoyancy,1} + L_2 F_{buoyancy,2}\right] \qquad \textbf{Eq. 5.18}$$

By entering numbers, the result shown below is obtained

$$W = \frac{\pi}{4}(5^2 - 4.125^2)\frac{1}{12^2 * 3.28^2}m^2 * 7900\frac{kg}{m^3}\left[1000m\left(1 - \frac{1030}{7900}\right) + 4000m\left(1 - \frac{1850}{7900}\right)\right]$$
$$= 126ton$$

This means that the drillstring weight experienced as a drag in the top drive would increase with $\frac{126+237}{126} = 288\%$, slightly short of the triple weight compared to a normal situation!

Calculations regarding increased torque have not been done.

5.3.9 Results for pressure trapping

Table 3: Trapping pressure. Results

Case number	1	2	3	4	5	6	7
Description	Base Case	Higher booster pump rate	Narrow Riser	Narrow riser and maximum time delay	Higher pressure Margin	Optimal Design	Self-balancing
Total time to control/loose control [min]	12.6	16.5	8.1	13.2	21.7	6.6	60.6
Time delay before Booster pump starts [s]	0	0	0	**75**	0	0	3600
Total Influx Volume [L]	99 019	15 201	4 425	14 264	4 044	739	19 793
Vinflux of total wellbore Volume	27 %	4 %	2 %	7 %	1 %	0 %	17 %
Height of influx when well in overbalance (or when uncontrolled influx reaches Subsea pump inlet) [m]	3 741	608	186	571	171	39	788
Depth of fluid interface at end [mTVD]	392	61	602	108	472	666	50
ID Riser [in]	19.5	19.5	**12.5**	**12.5**	19.5	**12.5**	**7.5**
OD DrillPipe [in]	5	5	5	5	5	5	5
OD BHA & DrillCollar [in]	6	6	6	6	6	6	6
Length BHA&DrillCollar [mTVD]	50	50	50	50	50	50	50
Bottom of the well [mTVD]	5260	5260	5260	5260	5260	5260	5260
Circulation friction pressure [bar]	40	40	40	40	40	40	40
Added pressure margin above Pore pressure margin when circulating [bar]	5	5	5	5	**17**	**15**	5
Density, light fluid [kg/m^3]	1 030	1 030	1 030	1 030	1 030	1 030	1 030
Density, heavy fluid [kg/m^3]	1 850	1 850	1 850	1 850	1 850	1 850	1 850
Density of formation fluid [kg/m^3]	800	800	800	800	800	800	800
Max rate, Booster pump [LPM]	6 000	**13 550**	6 000	6 000	6 000	6 000	6 000
Min rate, Subsea pump [LPM]	100	100	100	100	100	100	100
Min rate, Booster pump [LPM]	100	100	100	100	100	100	100
Regained control of the well	✘	✓	✓	✓	✓	✓	✓

5.3.10 Trapping pressure with MPD

As discussed in section 2.2.2 an MPD system could adjust the BHP either by altering the choke pressure when circulating with the rig pump, or by creating a back pressure when not circulating. Altering of the choke size is done in seconds and hence also the changing of the BHP. The choke creates a pressure by letting the circulated fluid out through a reduced size opening, and hence it will only be functional when there is a flow through it. Therefore, when the rig pump stops, and hence the fluid flow is reduced to zero, the choke will lose its purpose, if not closed quickly enough.

If using an MPD with a backpressure pump, the BHP can be increased without circulation through the choke, as is visualized in Figure 55.

A test conducted in an onshore horizontal test flow loop in Houston,USA explain how wellbore pressure can be kept within a BHP change of ±5bar when the rig pump rates go from 3000LPM to no flow; simulating a critical rig pump malfunction (Godhavn/Statoil, et al., 2010). The backpressure exerted from the choke goes from 14 to 52 bars in 10 seconds. This indicates that the friction pressure at 3000LPM in the flow loop is $52 - 14bar = 38bar$; roughly the same as assumed in the simulated examples described in section 5.3.1.

Three similar tests in a vertical onshore test well in Dallas,USA demonstrated that trapping of wellbore pressure was possible when ramping down rig pump rates from 2000LPM to zero in 5 seconds; (1) with a BPP available; (2) without a BPP available; and (3) by manual control of the choke without a BPP available. The BHP was kept within the criteria limits of ±5 bar.

A result from an offshore test at the platform Gullfaks C in Norway, where the rig pump was instantly ramped down from 2000LPM to no flow, is shown in Figure 60 (Godhavn/Statoil, et al., 2010). The BHP (middle graph) increases to 5 bar above the desired pressure during the transient part of the test, but then declines and is kept close to the desired pressure, which is at a fairly constant level. The backpressure increases from around 23 to 38 bar, simultaneously as the BHP increases with around 2 bars. This indicates that the friction pressure during circulation is about $(38 - 23 - 2\ )bar = 13bar$.

From Figure 60 it can also be seen that the choke flow rate continues to be positive for around 17 seconds, still after the rig pump is zero. This is considered to be driven by the compressibility of the fluid, wellbore and steel in the well. The wellbore used in this test has a depth of 1903mMD.

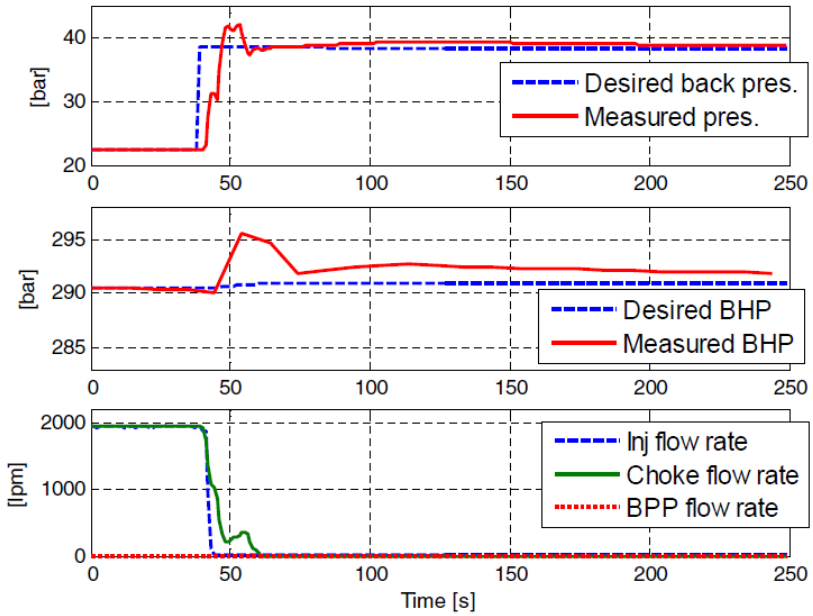

Figure 15. Gullfaks C offshore commissioning powerloss experiment with pressure trapping without BPP available. Top: back pressure set point and measurement, middle: BHP set point and measurement, bottom: rates.

Figure 60: Results from pressure trapping test at Gullfaks

5.3.11 Trapping pressure using the BOP

When experiencing a kick during conventional drilling, the well is most often controlled by closing the BOP, and circulating the kick fluid out through the kill/choke line. This way, the high pressure is sealed off, and kept away from the marine riser and the rig. Here, the possibility of doing the same to keep the pressure in a DGD wellbore when the rig pump power is lost, is investigated.

The 17 seconds of flow through the choke line after the rig pump stop discussed in section 5.3.10 give an indication of the time after rig pump power is lost available for keeping some of the pressure.

It has here been assumed that the delay from experiencing pump stop to the close button on the BOP control panel is pushed, is zero. This means that either an automatic control system has to be programmed to operate the BOP at rig pump failure, or the driller (or another drill crew member) has to be specially trained to close the BOP immediately after experiencing rig pump stop. In practice, the latter would probably not give zero time delay, because of the always existing human errors.

BOP closing times in deep waters is a challenge for the drilling industry. This is because deeper water means a longer BOP umbilical to pressurize if the BOP actuating pumps are placed on the rig, and it means a more challenging pump situation to handle if the actuator is placed at

seabed. Electrical BOP actuators are developed, but the combination of high pressure, seawater and high demands for redundancy makes working with electric equipment challenging. The API requirement for maximum time to close the annular element in the BOP is 60 seconds, and to close a Ram in the BOP the requirement is 45 seconds (API, 2004). The quickest a BOP Ram can be closed is around 25 seconds (Oceaneering International, Inc, 2011). This was done in a mean sea level of about 1300m.

When comparing the 17 seconds of well flow after pump stop to the minimum of 25 seconds it takes to operate the BOP, it is clear that the BOP is not suitable for containing the friction pressure in the ell. The reaction time comes in addition, both for personnel and for possible automatic control systems.

6. Discussion

6.1 Running the pipe in the hole

An important thing to notice here is that the connection breaks during tripping is not included in the simulation. This makes it seem that tripping of the next stand starts immediately after the top of the current stand has reached the drill floor. Of course, this is not so in reality, because moving the rig elevator to the top of the next stand and connecting it, in addition to connecting the pipe one stand to the next with the iron roughneck, takes time. The time given to the pumps to adjust the fluid level is therefore often unrealistically short, and this is therefore seen as a conservative assumption.

The required pump rates found in section 4.2.4.2 of 152LPM and 684LPM to compensate for the hydrostatic pressure build-up, are clearly not a problem for the maximum pump rates. This is therefore not discussed in more detail because there is no real challenge in this.

The simulator is here defined to predict the maximum pressure surge one tripped stand in advance. By predicting pressure surges for 4-5 stands in advance, even more time for the pumps to adjust the interface level is achieved. This would reduce the required pump rate for adjusting the pressure further, and give a more smooth control to the procedure. Still, the pump rates are ramped up and down in the simulated examples, to show the details in when during the process the rate changes are required.

This means that for the tasks simulated here, which don't involve neutralizing the pressure surge itself when the pipe is in motion, the subsea pump pressure rate is not a real challenge.

6.1.1 Case 2 – Base Case

By lowering the hydrostatic pressure in the riser when RIH, a pressure that normally would go outside the pressure window can be kept within the boundaries. This avoids fracturing of the formation, and formation fluid influx.

In the simulation, the subsea pump is run at the maximum rate, which is not really necessary in a real test, because of the added connection time between the stands. Still, it shows that even with this reduced simulation time, the pump maximum capacity is enough to keep the pressure within the mud window.

The highest pressure fluctuation experienced of 36bar, is when the BHA is run in the open hole, with the drillstring length at its longest. Based on comparing with previous literature, this seems a likely magnitude for the surge pressure in the described situation.

6.1.2 Case 3 – Tripping without pumps

This case shows the importance of using the pumps to adjust the fluid interface to control the wellbore pressure and reduce the hydrostatic pressure build-up. Figure 34 shows how the pressure increases to above the fracture pressure, and therefore causes losses, and probable lost circulation. Lost circulation is discussed in section 3.1.3.3. Comparing with Figure 31, in which the pressure is never allowed higher than the fracture pressure margin, the importance of adjusting the fluid level in the riser with the pumping system is visualized. This means that when not utilizing the pumps, the non-existing fluid ex-change with the formation in Case 2 is switched with the severe fluid loss of 13 504L; representing 7.4% of the heavy weight drilling fluid in the wellbore. This is seen by comparing Figure 31 and Figure 35 along with the results in Table 2. The density of the mud is not altered, because the pressure is never lower than the pore pressure, and hence no light weight fluid comes into the wellbore.

Somewhat ironically, the losses to the formation reduce the primary problem, which is the increased hydrostatic pressure. Therefore, the maximum of the pressure curve seems to stabilize in Figure 34. However, if now needing to pull the drill pipe out of the well, still without pump capacity, the hydrostatic pressure will decline, and the risk of an underbalanced situation becomes severe.

It has been shown that the subsea pump must be functioning when tripping with DGD, otherwise, severe losses could be experienced. The ability to control the pressure on beforehand of the tripping motion is a great advantage compared to tripping conventionally.

6.1.3 Case 4 – High tripping velocity

If experiencing such high pressure surges as in this example when tripping into a wellbore in the field, the tripping velocity would be reduced immediately to keep the pressure within the mud window. Here, it deliberately is not, to show how the pumps can mitigate the wellbore damage.

As explained in section 5.2.2.2, influx is preferred to losses, and this thought is the base for the pump control here. Influx is also a potentially very dangerous situation, because it will alter the mud properties. Not only the density, which creates the hydrostatic pressure, but also the rheology, which could change cutting transportation ability and the surge and circulation friction pressure, along with several other important features provided by the mud. It could be an even greater problem if the formation fluid is gas. This will reduce the hydrostatic pressure even more than a liquid would do, and it would also expand as the pressure is reduced upwards in the well; magnifying the problem.

6.1.4 Stripping with MPD

To compare the simulated examples with the results from the field test on Gullfaks described in section 5.2.7 is not unproblematic. First of all, the fluid used is water, which separates in many

ways from the drilling mud assumed in the simulations; the density is lower and the shear stress is likely to be lower as well; depending on the shear rate during pipe motion. As can be seen from inspection of Eq. 4.11, this would decrease the friction pressure loss, when keeping the other parameters constant. Secondly, the well geometry differs; in the Gullfaks well, a 7" casing is set at 2595mMD, while a 9 $^{7}/_{8}$" casing set at 5240mTVD is used in the Macondo simulations. The smaller ID of the hole on Gullfaks gives a higher pressure surge, as can be seen from the relation of Eq. 4.8 and Eq. 4.9 to Eq. 4.10. And thirdly, the Gullfaks test was done under continuous circulation at 2000LPM, which eliminates the transient pressure peaks because the mud is in motion the whole test period. As discussed in section 4.2.4.3, the transient motions have been regarded as the most severe part in the simulations.

As shown in section 5.2.7.1, DGD technology can compensate for the magnitude of surge/swab experienced at Gullfaks with a pump rate of 3358LPM. However, this is dependent on the elimination of the most challenging surges; the transient ones. Without a circulation system that circulates the mud independently of the top drive, a CCS, it is not likely that an elimination of the transient surges is possible when tripping with DGD, simply because a CCS is not normally used together with DGD equipment. Therefore, doing the same tripping motion as done on Gullfaks solely with DGD equipment would involve a transient pressure surge, which would be impossible to fully eliminate by changing the hydrostatic pressure in the DGD riser.

Other literature, as presented in section 4.3, show that more severe pressure surges than those on Gullfaks is likely to be experienced. This is a problem to handle with DGD, because of the high pump rates required. The Gullfaks test is therefore not regarded as fully representable for the situations to occur when drilling in deeper waters. In addition, the Gullfaks platform is a Gravity Based Structure (GBS), a platform type not used in deeper waters.

6.1.5 General discussion

The results achieved from the sure model are highly uncertain. For a more accurate model to be developed, field tests from the Macondo well should have been used to calibrate the model before simulating. This has not been possible. Even if the magnitude of the calculated surges is not correct, the behaviour of the surges, and the increase as the pipe goes deeper into the hole is reasonable.

6.2 Trapping pressure

The procedures described here, of how to re-establish pressure overbalance in the well, does not include procedures of what to do at a later stage, when the influx should be circulated out of the wellbore. However, the situation that the wellbore is left at when overbalance is re-established, makes it possible to circulate the formation fluid out of the well by well-known

procedures. For more details regarding these circulation procedures it is referred to (Skalle, 2009).

6.2.1 General assumptions

6.2.1.1 Assumptions

It has here been assumed that the formation fluid and the drilling fluid are immiscible, and that the formation fluid fills the bottom of the well. This is regarded as a conservative assumption, because, especially when using an oil based mud (OBM), the formation fluid is likely to be more dispersed in the wellbore. This would reduce the length of the light weight formation fluid column, and therefore increase BHP_{hyd}. Only a liquid has been considered as the formation fluid. A formation gas would probably be even more likely to disperse in the wellbore, because of the reduced viscosity and shear stress in the gas, but the main difference would be the increasing gas volume, as it expands due to the lower pressure in the upper wellbore. This would give a more challenging situation, because the length of the low weight column would increase and therefore reduced the BHP_{hyd} further.

Friction pressure in the annulus has been neglected. The fluid being pumped by the booster pump through the riser will create a friction pressure loss that will be exerted down the mud column, increasing the counter pressure towards the pore pressure. This is not included here, and is a conservative assumption.

The pumps and the flow rates have been assumed to stop momentarily. In reality, partly because of the compressibility of the fluids, the wellbore and the metal, the fluid flow probably would have continued for some seconds longer than assumed here and hence given a few seconds longer for the well control procedures to commence. An example of this is shown in Figure 60, where the transient flow through the MPD choke continues for about 17 seconds after the rig pump is shut down. This is for a 1903mMD wellbore, and the 5260mMD Macondo wellbore would probably give even more transient flow because of the increased wellbore volume. However, the choke in that example was already at a partly closed position when the rig pumps stopped, which kept the pressure and the flow in the well more than in an open system, as discussed here. Even though no accurate analysis is done on the subject, Figure 60 is considered a good guideline for the after-flow. The assumption of no after-flow is therefore regarded as conservative, because the pressure is assumed to drop quicker than it would realistically.

The rig pumps are assumed to instantly increase the rates to a high level. In previous literature, the increase of a pump rate from 335 LPM to 1233 LPM in 7 seconds is described as “challenging” (Sigbjørn Sangesland, 2007), and on the background of this (and normal sense and

logic) instantaneous rate changes is clearly optimistic. More realistically, this would take time, which would slow down the ability to change the BHP.

Water hammering effects and pressure waves that would appear in the wellbore due to a sudden circulation stop are not included. In reality, water hammering would make the pressure fluctuate after the pump stopped. This would give a more unstable pressure condition in the well, and could possibly lead to fluid losses to the formation. Fluctuating pressure is also likely to disperse the formation fluid more, and prevent it from forming a long column in the wellbore.

The influx from the formation is assumed to start immediately after the pressure drops below the pore pressure. This is regarded as a conservative assumption, because the mud cake and the drilling fluid filtrate having been pushed into the formation would probably slow this process down in reality.

Most of the assumptions described above are considered conservative, and this is taken into consideration when making conclusions.

6.2.1.2 Criteria for successful well control

The criteria used here defining a successful well control procedure are not very strict, but are merely criteria for avoiding a blow-out. They have been chosen deliberately to give more room for the DGD features to be shown. If simulating DGD operations using success criteria as those used for the MPD tests described in section 5.3.10, only unrealistically high pump rates and narrow annuli would give results that are anything close to approvable.

6.2.2 Case 1 – Base Case

With the well design depicted in the base case, the pressure drop situation was not controllable, and the formation fluid would have filled the well, probably causing a blow-out. This is in no way acceptable, as it would lead to severe environmental damages and possibly human injuries.

6.2.3 Case 2 – Higher booster pump rate

Even with a booster pump rate of 13550 LPM is a high influx volume avoided. When well pressure overbalance is re-established, the bottom 608m in the wellbore is filled with formation fluid. Not only is the required booster pump rate around double of the best subsea pump currently available for DGD, but in addition is high amount of formation fluid in the wellbore unacceptable in practice.

6.2.4 Case 3 and Case 4 – Narrower riser

A narrower riser clearly increases the velocity of the fluid interface when pumping to change the mud level. The ability to re-establish well control increase drastically with the narrower riser.

The calculated 171% increase in pressure changing speed shows this, along with the simulated results that show that start pressure was regained in 8.1 minutes using the narrower riser; 49% of the time spent with the doubled pump pressure rate in Case 2. This decreased the total influx volume by $\frac{15201-4425}{15201} = 71\%$ from Case 2 to Case 3, which has to be regarded as a massive improvement.

The improvement was so great that a 75 second delay could be added from the rig pump stop to the start of the booster pump to control the well, but still eventual pressure overbalance could be achieved. The delay could be caused by human misinterpretation or a control system malfunction, and adds an extra safety margin.

The results achieved when using the narrower riser, are distinctively much better than those achieved from doubling the pump rates. When using a narrower marine riser the required mud volume is also reduced. It is therefore believed that continuing the development of the 12¼" ID riser as described in section 2.1.2.2 should be a priority.

6.2.5 Case 5 – Higher Pressure margin

To maximize ROP, the wellbore pressure when drilling should not be too high. Therefore, an increase in the BHP when drilling, could lead to a slower drilling process, and hence increased rig costs. By increasing the hydrostatic pressure when circulating with 12 bar, to 17 bar, the BHP would not fall as far below the pore pressure margin when the rig pump stops as in the Case 1. This might stand as the most obvious change in parameters to when wanting to increase safety, but the safety is instead decreasing if the pressure is moving closer to the fracture pressure. As discussed in section 3.1.3.3, lost circulation is important to avoid, and as seen from Figure 52, the pressure when circulating lies closer to the fracture pressure than to the pore pressure, which is not optimal. The 17 bar margin from the pore pressure margin level, is both the least margin to give acceptable well control results, and closed to the maximum pressure with regards to the fracture pressure.

Still, increasing the hydrostatic pressure to increase the safety margin toward the pore pressure, greatly reduces the total influx, and makes it possible to re-establish control of the well. The total influx volume declines by $\frac{15201-4044}{15201} = 73\%$ from Case 2, which is about as good as the results obtained in Case 3.

However, the time spent to regain control is drastically increased compared to Case 2; with a factor of $\frac{21.7}{8.1} = 2.7$. This increases well cost, and is highly unwanted, because time exposed to an unstable well should clearly be minimized.

6.2.6 Case 6 – optimal well design

This is the only example that could come close to fulfilling future regulations for pressure boundaries in open-to-atmosphere high-pressure handling. The influx volume is minimized by $\frac{15201-739}{15201} = 95\%$ compared to Case 2. Worth noticing is that this is obtained by technological solutions available on the market today, not by higher pump rates than those currently available, as in Case 2.

Again, it is not optimal with regard to ROP to have a pressure as high as this when drilling, and the risk of fracturing the well is also increased. Still, this case demonstrates the quickest well control simulated here. A 40 bar friction pressure loss is recaptured in less than 7 minutes under continuous formation influx.

6.2.7 Case 7- Self-Balancing well

The self-balancing well design with the drill pipe width of $OD_{pipe} = 11.18in$ as described in section 5.3.7 is included more or less as a theoretical example to show the possible features in DGD. $OD_{pipe} = 11.18in$ is also the absolute minimum acceptable OD of the drillpipe. To increase the pressure safety margin, keeping the D_{fi} deeper into the well when at pressure balance, an even greater OD is needed to minimize the riser annulus even more.

The drillstring weight increase of 288% cannot be considered as anything other than impossible to handle. If possible, the weight for the heavy pipe should be decreased, but a thinner pipe wall would mean a lower resistance towards fatigue and buckling. To draw a definite conclusion regarding the required weight increase, a more detailed analysis should be conducted to see how large the $ID_{pipe,heavy}$ could be, with still being functional. The pipe would probably also be too heavy for fast rotation of the drillstring. A rotation speed of up to 120-130 RPM is required for optimal ROP and hole cleaning, which also would mean the same rotation speed for the very heavy drill pipe.

Because well circulation with DGD goes through the subsea pump, and not in the riser annulus, increased ECD due to the narrow annulus in the riser would not be a problem.

The example discussed above show that it is possible to achieve a self-balancing well design with regards to formation fluid influx. Another great feature is that the BHP_{hyd} can only build up to the magnitude of the P_{pore}, simply because it is driven by the P_{pore}. This reduces the probability of fracturing the well, because the well pressure is kept at an absolute minimum.

6.2.8 Trapping pressure with MPD

Test results from Houston demonstrate that a 38 bar friction pressure loss can be sustained, when still keeping the BHP within a ±5 bar margin. Results from Gullfaks show that a 13 bar friction pressure loss can be trapped in the well, having the BHP fluctuate a maximum of ±5bar.

These results are superior to any of the above discussed results from the DGD simulations. Using MPD, it is actually possible to "*trap*" the friction pressure, because of the quickness of the MPD choke; not only create a new pressure after the friction pressure has been lost, as done with DGD.

To have this supreme accuracy and agility, the choke position has to be controlled extremely well. Results show that this is possible, either with an automatic control system, or by having trained crew member manually control it. Still, it has to be pointed out that DGD could give a wider acceptance range for delays, as shown in section 0, where the well could be re-controlled after a 75 seconds delay. The choke in an MPD system, has to be closed within few seconds, otherwise, the friction pressure is lost. Use of a backpressure pump (BPP) will make it possible to re-pressurize the wellbore at any time, still after the friction pressure has escaped.

Because MPD can change literally instantly, the assumption of an instantaneous pressure reduction done in the DGD simulations is an advantage for the MPD argument. By including a realistic slower reduction in pumprate, the influx would not have been so severe right at once, and DGD would have been given more time to increase the pressure, and to mitigate the influx.

6.2.9 Pressure handling by BOP

Because the fastest current available closing time for a BOP in ultra-deep water is too long for capturing the friction pressure, even with after-flow in the well, this is not seen as a way of keeping the BHP constant when losing the friction pressure.

6.2.10 General discussion

In reality, the BOP would have been closed, and an alarm on the rig would have sounded long before the amount of formation fluid in the well reached the levels presented in Table 3. This is because an uncontrolled underbalanced well is a very dangerous situation and must be put under control immediately.

6.2.10.1 Influx in the wellbore

In all of the cases presented in Table 3, a formation influx is initiated, but still classified as 'Acceptable'. In an open-to-air wellbore, it is highly unlikely that this would ever be classified as OK in the field. Only a few seconds separates the situation from going from 'risky' to a catastrophe.

Drilling with the well in underbalance, called Underbalanced Drilling (UBD), is an unconventional way of drilling. This is drilling, with acknowledged continuous influx from the formation. There are variants in utilization of UBD, but the important difference from DGD to UBD is that UBD is done with an RBOP, which controls the pressure much more strictly and enables quick pressure changes. This is the only acceptable way of having an underbalanced well. Open DGD is by far

not quick enough to increase the pressure in case of a sudden underbalanced situation. Only case 6 presented in section 5.3.7 is within the range of being acceptable; with an influx volume of 0.7m^3. Other tests in similar

6.3 Summary of the discussion

It is not safe to circulate in a DGD well with the hydrostatic pressure below the pore pressure level. It is shown that well control is rapidly lost if influx is first allowed into the well.

Increased pump rates will increase the agility of the pressure control, but the way of improving it the most is by making the riser slimmer.

6.3.1 Is pressure control using DGD good enough?

The extra added dimension of two fluid gradients is a clear advantage, because of the increased flexibility. Compared to conventional drilling, features offered by DGD are in a new dimension regarding pressure control. However, DGD does not come close to the quickness and accuracy achieved when using a hydraulically sealed annulus, as is done when using MPD. DGD pressure control makes for a pale comparison to MPD, when comparing the 38 bar friction pressure loss that still could not fluctuate BHP any more than 5 bar when using MPD; with the whole of the 40 bar friction pressure being lost in the DGD wellbore in a similar simulation.

On the basis of this, DGD is not good enough. This can also be reasoned for by comparing the thousands of kilograms of heavy weight fluid that has to be moved to change the DGD pressure, with the small choke opening size that has to be changed to alter the MPD pressure. Newton's laws of motion just don't allow DGD to be quicker than MPD. A hydraulically open system cannot keep the BHP sufficiently constant during sudden pressure drops, as experienced when the rig pump stops, but MPD can.

6.4 Recommendations for future work

6.4.1 Tripping

Integrate tripping simulations with a surge and swab model that is more accurate, dynamic and takes more parameters into account, and preferably is calibrated especially for one particular well for optimal accuracy. Parameters included could be fluid, steel and wellbore compressibility, roughness in the wellbore creating singularity friction losses and mud gelling effects.

6.4.2 Trapping

Simulations should be run with gas considered as the formation fluid. The gas expansion due to the lower pressure in the higher part of the annulus should be modelled.

Evaluation of how large the OD of the drill pipe in the riser could be in practice, when still being able to perform drilling, tripping, circulation, etc. This could produce a more definitive conclusion if the self-balancing well is possible to engineer.

7. Conclusions

The well on the Macondo prospect

- Even though the accident on the Macondo prospect was partly caused by human errors and misinterpretations of well signals, it is likely that the incidents evolving into the accident would have been discovered at an earlier state if using DGD when drilling the well. This could have mitigated the consequences of the accident.

Dual Gradient Drilling

- Pressure surges caused by tripping into a hole cannot be totally neutralized using DGD technology. However, by predicting the magnitude of the pressure surges from the coming pipe motions, the hydrostatic pressure can be adjusted to the ideal position in the well, for minimum damage.
- MPD is far superior to a hydraulically open DGD in keeping the BHP constant during sudden pressure drops in the well. MPD can keep the BHP within a change of ±5bar, when a 38bar friction pressure drop is suddenly lost, while DGD will lose the whole magnitude of the friction pressure.
- The hydrostatic well pressure should not be lowered below the pore pressure when using DGD to compensate for the friction pressure when circulating. This involves a high risk of having formation fluid influx in the case of an emergency rig circulation pump stop.
- Reduction of the cross section area in the drillpipe is recognized as the clearly most efficient way of increasing the agility of hydrostatic pressure control with DGD. This can be done both by utilizing drillpipes with a larger OD, or by using a marine riser with a smaller ID.
- Higher pump rates for the subsea and booster pump able quicker pressure control in a DGD system.

8. Bibliography

Aasebø, Trond Erling (AGR). 2012. *AGR EC-Drill.* [interv.] Tarald Gaup. 25 May 2012.

add wellflow as. 2010. *Dynamic Simulations Deepwater Horizon Incident BP.* s.l. : BP, 2010. Investigation Report. Appendix W of the Deepwater Horizon Investigation Report by BP.

—. 2010. *Dynamic Simulations Deepwater Horizon Incident BP.* s.l. : BP, 2010. Investigation Report. Appendix W of the Deepwater Horizon Investigation Report.

AGR Drilling. 2008. *RMR - moves into deepwater with our JIP Partners.* s.l. : AGR Drilling, 2008. Product Specification Sheet.

AGR Drilling Services AS. 2010. AGR moves forward with Chevron to Develop Dual Gradient Drilling System. [Online] March 15, 2010. [Cited: November 5, 201.] http://www.agr.com/News/Press-releases-and-News/AGR-Drilling-Services-Celebrates-100-Wells-Drilled-with-the-Riser-less-Mud-Return-System-RMR/.

AGR. 2012. Enhanced Drilling Solutions. [Online] 2012. [Cited: 15 May 2012.] http://www.agr.com/technology/enhanced-drilling-solutions.

AGR-Group. 2011. Riserless Mud Recovery. [Online] January 1, 2011. [Cited: November 5, 2011.] http://www3.agr.com/our-services/enhanced-drilling-solutions/our-technology/.

API. 2004. *API Spec 16D - Specification for Control Systems for Drilling Well Control Equipment and Control Systems for Diverter Equipment Second Edition.* Houston : American Petroleum Institute, 2004.

Bourgoyne, Adam T. Jr, et al. 1986. *Applied Drilling Engineering.* Richardson, TX : SPE, 1986.

BP. 2010. *Deepwater Horizon Accident Investigation Report.* s.l. : BP, 2010. Accident Investigation.

Burkhardt, J.A. 1961. *Wellbore Pressure Surges Produced by Pipe Movement.* Houston, Texas : Society of Petroleum Engineers, 1961. pp. 595-605. 1546-G.

Cannon, George Humble Oil and Refining Co. 1934. *Changes in Hydrostatic Pressure Due to Withdrawing Dril Pipe from the Hole.* Houston, Texas : American Petroleum Institute, 1934. pp. 42-47. 34-041.

Clark, R.K. and Fontenot, J.E. 1974. *Field Measurements of the Effects of Drillstring Velocity, Pump Speed, and Lost Circulation Material on Downhole.* Houston, Texas : Society of Petroleum Engineers, 1974. ISBN 978-1-55563-763-7.

Close, Frank, McCavitt, Bob and Smith, Brian. 2008. *Deepwater Gulf of Mexico Development Challenges Overview - SPE 113011.* Marrakech, Morocco : Society of Petroleum Engineers, 2008. SPE Paper.

Cohen, John, et al. 2008. Dual-Gradient Drilling. [book auth.] Bill Rehm, et al. *Managed Pressure Drilling.* s.l. : Gulf Publishing Company, 2008, pp. 181-226.

Crespo, Freddy and Ramadan, Ahmed. 2010. *Surge and swab pressure predictions for yield-power-law drilling fluids. [SPE 138938].* Lima, Peru : Society of Petroleum Engineers, 2010. SPE paper.

Crespo, Freddy, Ahmed, Ramadan and Saasen, Arild. 2010. *Surge and Swab Pressure Predictions for Yield-Power-Law Drilling Fluids.* Lima, Peru : Society of Petroleum Engineers, 2010. 138938-MS.

Durkee, Todd, et al. What is the Future Direction of MPD? *A look at Dual Gradient Drilling Concepts.* s.l. : Anadarko, Transocean, Chevron, Signa.

Evaluating New Automatic Well Control Procedure.. **Zhou, Jing, Nygaard, Gerhard and Vefring, Erlend. 2010.** Aberdeen, UK : IADC, 2010. Well Control Europe, Conference & Exhibition 13-14 April 2010. p. 11.

Fossil, Børre and Sangesland, Sigbjørn. 2004. *SPE/IADC 91633: Managed Pressure Drilling for Subsea Applications; Well Control Challenges in Deep Waters.* s.l. : Society of Petrolem Engineers, 2004. SPE/IADC Paper.

Gaup, Tarald. 2012. *MPD-Figures.* NTNU, Trondheim : 2012.

—. 2011. *Pump control simulations for Dual Gradient Drilling.* Trondheim : Norges teknisk-naturvitenskapelige universitet, Fakultet for ingeniørvitenskap og teknologi, Institutt for petroleumsteknologi og anvendt geofysikk, 2011. Specialization Project.

Godhavn/Statoil, John-Morten and Knudsen/Halliburton, Kjetil Arne. 2010. *High Performance and Reliability for MPD Control System Ensured by Extensie Testing.* New Orleans : IADC/SPE, 2010. IADC/SPE 128222.

Goins, W. G, et al. 1951. *Down-the-hole Pressure Surges and Their Effect on Loss of Circulation.* Gulf Oil Company, Houston, Texas : American Petroleum Institute, 1951. 51-125.

Hussain, Quazi E. and Sharif, Muhammad A. R. 1997. *Viscoplastic fluid flow in irregular eccentric annuli due to axial motion of the inner pipe.* 1997. pp. 1038–1045.

Inflation Data. 2012. Historical Crude Oil Prices. [Online] 19 January 2012. [Cited: 27 May 2012.] http://inflationdata.com/inflation/inflation_rate/historical_oil_prices_table.asp.

Lal, Manohar. 1983. *Surge and Swab Modeling for Dynamic Pressures and Safe Trip Velocities.* New Orleans, Louisiana : Society of Petroleum Engineers, 1983. Conference Paper. ISBN 978-1-55563-662-3.

Lundestad, Hans. 2011. *Mud on Stena Don.* [interv.] Tarald Gaup. 16 December 2011.

Malloy, Kenneth P. 2007. Managed Pressure Drilling. *World Oil Online.* March 2007, Vol. 228, 3.

Mitchell, R.F. 1988. *Dynamic Surge/Swab Pressure Predictions.* s.l. : Society of Petroleum Engineers, 1988. pp. 325-333. 16156-PA.

MPD Simulations. **Godhavn, John-Morten. 2010: 03.11 & 05.11.** Trondheim : NTNU, 2010: 03.11 & 05.11. Lecture in a class TPG4215.

NORSOK. 2004. *Well integrity in drilling and well operations - D-010.* Oslo : Standards Norway, 2004.

Ocean Riser Systems. 2008. The LRRS Concept. [Online] 2008. [Cited: December 6, 2011.] http://www.oceanriser.no/?page=4.

Oceaneering International, Inc. 2011. Oceaneering News and media Menu. [Online] 1 February 2011. [Cited: 30 May 2012.] http://www.oceaneering.com/4902/bop-ram-closed-at-depth-in-less-than-25-seconds/.

ORS website. 2012. THE LRRS CONCEPT. [Online] Ocean Riser Systems, 2012. [Cited: 10 May 2012.] http://www.oceanriser.no/?page=4.

Redden, Jim. 2010. Dual-gradient drilling promises to change the face of deepwater. *Offshore.* 5 May 2010, Vol. 70, 50.

—. 2010. Offshore Mag. [Online] May 1, 2010. [Cited: October 20, 2011.] http://www.offshore-mag.com/index/article-display/1931523476/articles/offshore/volume-70/issue-50/drilling-__completion/dual-gradient-drilling.html.

Refinery News. 2012. Chevron has Unveiled New Ship to Perform Dual Gradient Drilling. [Online] May 11, 2012. [Cited: May 26, 2012.] http://refinerynews.com/chevron-has-unveiled-new-ship-to-perform-dual-gradient-drilling/.

Rommetveit, R, et al. 2005. *Ultradeepwater Hydraulics and Well-Control Tests With Extensive Instrumentation: Field Tests and Data Analysis.* Denver, US : Society of Petroleum Engineers, 2005. pp. 251-257. 84316-PA.

Rødland, Arild. 2012. *Student asking questions to a professor.* [interv.] Tarald Gaup. 2 April 2012. Details from a conversation at Rødland's office at PTS, NTNU.

Samuel, G. Robello, et al. 2003. *Field Validation of Transient Swab-Surge Response With Real-Time Downhole Pressure Data.* Amsterdam : Society of Petroleum Engineers, 2003. pp. 280-283. 85109-PA.

Sangesland, Sigbjørn. 2012. *Questions from a student to a professor.* [interv.] Tarald Gaup. 30 March 2012. Questions related to technical drilling sent via E-Mails.

Siem WIS AS. 2010. Siem Offshore. [Online] August 2010. [Cited: October 20, 2011.] http://www.siemoffshore.com/Admin/Public/DWSDownload.aspx?File=%2FFiles%2FFiler%2FPresentations%2FSiemWIS-Presentation-August+2010.pdf.

SIEM WIS. 2012. SiemWIS - Products & Concept. [Online] 1 January 2012. [Cited: 15 May 2012.] http://www.siemwis.com/page/356/concept.

Sigbjørn Sangesland, Olve Sunde Rasmussen. 2007. *Evaluation of MPD methods for compensation of surge-and-swab pressures in floating drilling operations.* Texas, US : IADC/SPE, 2007. 108346.

Skalle, Pål. 2010. *Drilling Fluid Engineering.* s.l. : Ventus Publishing ApS, 2010.

—. 2009. *Pressure Control During Oil Well Drilling.* Trondheim : Ventus Publishing ApS, 2009. pp. 44-59.

Srivastav, R., et al. 2012. *Surge and Swab Pressures in Horizontal and Inclined Wells.* University of Oklahoma; Det norske oljeselskap ASA. Mexico City, Mexico : Society of Petroleum Engineers, 2012. SPE 152662.

Tonning, Anders. 2011. *Evaluation of Well Control Procedure for Managed Pressure Drilling.* Trondheim : Norges teknisk-naturvitenskapelige universitet, Fakultet for ingeniørvitenskap og teknologi, Institutt for petroleumsteknologi og anvendt geofysikk, 2011. MSc Thesis.

Transocean. 2011. *MACONDO WELL INCIDENT. Transocean Investigation Report. Volume I.* s.l. : Transocean, 2011. p. 40, Accident investigation report.

Wagner, R.R., Halal, A.S. and Goodman, M.A. 1993. *Surge Field Tests Highlight Dynamic Fluid Response.* Amsterdam : SPE, 1993. 25771-MS.

White, Frank M. 2006. *Fluid Mechanics 6.ed.* s.l. : The McGraw-Hill Companies, 2006.

Wood, Sir Ian. 2000. World Oil Online. [Online] August 2000. [Cited: September 30, 2011.] http://www.worldoil.com/August-2000-Service-and-operating-companies-join-forces-to-meet-deepwater-challenges.html.

Økland, John. 2010. Offshore.no. [Online] June 28, 2010. [Cited: December 2, 2011.] http://www.offshore.no/nyheter/sak.aspx?id=29623.

9. Nomenclature

Abbrevations and Subscripts

BHA	-	Bottom Hole Assembly	BHP	-	Bottom Hole Pressure
$BHST$	-	Bottom Hole Static Temperature	BPP	-	Back pressure Pump
BOP	-	Blow-out Preventer	$BP\ \&\ bp$	-	Booster pump
CCS	-	Continuous Circulation System	cs	-	Cross-sectional
DGD	-	Dual Gradient Drilling	DP	-	Drillpipe
ECD	-	Equivalent Circulation Density	ETP	-	Engineering Technical Practice
fi	-	fluid interface	GoM	-	Gulf of Mexico
GBS	-	Gravity Based Structure	$HPHT$	-	High pressure & High temperature
hyd	-	Hydrostatic	ID	-	Inner Diameter
LPM	-	Liters per minute	$LRRS$	-	Low Riser Return System
mMD	-	meter Measured Depth	$MODU$	-	Mobile Offshore Drilling Unit
MPD	-	Managed Pressure Drilling	$mTVD$	-	meter True Vertical Depth
MWD	-	Measure While Drilling	OBM	-	Oil Based Mud
OD	-	Outer Diameter	OH	-	Open Hole
PI	-	Productivity index	PL	-	Power Law
$RBOP$	-	Rotary Blow-out Preventer	RCD	-	Rotating Control Device
req	-	required	RIH	-	Run In Hole
RKB	-	Rotary Kelly Bushing	RMR	-	Riserless Mud Recovery
SMO	-	Subsea suction Module	SPM	-	Subsea Pump Module
$SP\ \&\ sp$	-	Subsea Pump	sw	-	Sea water

TVD	-	Total Vertical Depth	UBD	-	Underbalanced Drilling
YPL	-	Yield Power Law	WBM	-	Water Based Mud

Greek letters

ρ	-	Fluid or material density	ϕ	-	Dimensionless constant
Δ	-	Incremental change	τ	-	Fluid Shear Rate

Latin letters

A	-	Area	a	-	acceleration
D	-	Depth	d	-	diameter
F	-	Correction factor	g	-	Gravity constant
H	-	Height	k	-	Fluid consistency Index
L	-	Length	n	-	Fluid behavior Index
P & p	-	Pressure	Q	-	Pump rate
T & t	-	Time	V	-	Volume
V_p	-	Velocity of pipe	W	-	Weight
Z	-	Depth reference			

10. Appendix

10.1 In data from the Excel sheet

The in data excel sheet is included in the digital posting. It can be acquired from the author of the report or possibly from NTNU. It has therefore not been considered necessary to copy-paste the Excel-sheet here.

10.2 Program code from the simulations

The MATLAB files (*.m-format) can be achieved on request from the author or possibly from NTNU. The program code is not included here. This has been considered unnecessary because the files are submitted digitally along with the thesis.